2011

An OFDM Based Aeronautical Communication System

Jamal Haque
University of South Florida, jamal_haq@yahoo.com

An OFDM Based Aeronautical Communication System

by

Jamal Haque

A dissertation submitted in partial fulfillment
of the requirements for the degree of
Doctor of Philosophy
Department of Electrical Engineering
College of Engineering
University of South Florida

Major Professor: Wilfrido Moreno, Ph.D.
Salvatore Morgera, Ph.D.
Paris Wiley, Ph.D.
Miguel A. Labrador, Ph.D.
John Samson, Ph.D.

Date of Approval:
November 4, 2011

Keywords: Cognitive radio, Intercarrier interference, Doppler estimation, Parametric frequency estimation, Smart antenna, Beam forming, Software Defined Radio

DEDICATION

To my wife's undeterred love and support.

To my young boys' love, patience and sacrifice.

To my siblings' support and constant encouragement.

Finally, the upbringing, inspiration, dedication and sacrifice of my Mother, Afser J. Haque and my late Father, M. Manazirul Haque. It is he who instilled the dream of education.

I dedicate this accomplishment to my Father.

May He Rest in Peace.

ACKNOWLEDGEMENTS

The completion of this dissertation was a monumental task and one of my life-long dreams. I could not have completed this without the support of my family (especially my wife), and friends at work and school. My wife's steadfast support and patience were the pillar behind the completion of this endeavor. I would like to express my deepest gratitude and thanks to all of them.

My sincere thanks and regards to my advisers, Dr. Wilfrido Moreno and Dr. Hüseyin Arslan. Their guidance was instrumental in accomplishing this long term endeavor. I am very grateful for their support, guidance, encouragement and personal commitment. Special thanks to Dr. Moreno for his encouragement, mentorship and leadership.

I wish to thank Dr. Miguel A. Labrador, Dr. Paris Wiley, Dr. Salvatore Morgera, and Dr. John Samson for serving on my committee and for offering their valuable feedback. I owe much to my friends Mustafa Cenk Ertürk, Murat Karabacak, Dr. Sabih Guzelgoz, Dr. Mustafa E. Sahin, Alphan Sahin, Keith Souders and Arivind Solanki for their help and encouragement. Thanks to my niece, Zeesha Hyder, who throughout the process helped proofread my dissertation.

TABLE OF CONTENTS

LIST OF TABLES

LIST OF FIGURES

LIST OF ACRONYMS

3G	3rd Generation
3GPP	3rd Generation Partnership Project
4G	4th Generation
ATCRBS	Air Traffic Control Radar Beacon System
ADN	Aeronautical Data Network
ADS-B	Automatic Dependent Surveillance-Broadcast
ADSL	Asymmetric Digital Subscriber Line
AR	Auto Regressive
ARMA	Auto Regressive Moving Average
ASDR	Aeronautical Software Defined Radio
AS	Aircraft Station
ATC	Air Traffic Control
ATM	Air Traffic Management
AWGN	Additive White Gaussian Noise
BER	Bit Error Rate
BPSK	Binary Phase Shift Keying
BS	Base Station
CASDR	Cognitive Aeronautical Software Defined Radio
CCI	Co-Channel Interference
CE	Cognitive Engine
CDMA	Code Division Multiple Access
CDR	Critical Design Reviews
CFO	Carrier Frequency Offset

CP	Cyclic Prefix
CR	Cognitive Radio
DAC	Digital to Analog Converter
DAB	Digital Audio Broadcast
DFT	Discrete Fourier Transform
DOA	Direction of Arrival
DSP	Digital Signal Processor
DL	Downlink
DME	Distance Measuring Equipment
DSSS	Direct-Sequence Spread Spectrum
EV	EigenVector
FAA	Federal Aviation Administration
FCC	Federal Communications Commission
FDMA	Frequency Division Multiple Access
FFT	Fast Fourier Transform
FPGA	Field Programmable Gate Arrays
GPP	General Purpose Processor
GPS	Global Positioning System
GS	Ground Station
ICI	Intercarrier Interference
IEEE	Institute of Electrical and Electronics Engineers
IF	Intermediate Frequency
ITU	International Telecommunication Union
JTRS	Joint Tactical Radio System
LMS	Least Mean Square
LTE	Long Term Evolution
MA	Moving Average

MC	Multi-Carrier
MIMO	Multiple-Input Multiple-Output
MP	Multipath
Mpbs	Mega Bit Per Second
MRC	Maximal Ratio Combining
MS	Mobile Station
MUSIC	MUltiple Signal Classification
NB	Narrow Band
NBI	Narrow-Band Interference
NLOS	Non-Line of Sight
OFDM	Orthogonal Frequency Division Multiplexing
OFDMA	Orthogonal Frequency Division Multiple Access
OSI	Open Systems Interconnection
PAPR	Peak-to-Average-Power Ratio
PDA	Personal Digital Assistant
PHY	Physical Layer
PN	Pseudo Noise
QAM	Quadrature Amplitude Modulation
QPSK	Quadrature Phase Shift Keying
RF	Radio Frequency
RMS	Root Mean Square
SC-FDMA	Single Carrier Frequency Division Multiple Access
SC	Selective Combining
SER	Symbol Error Rate
SNR	Signal-to-Noise Ratio
SPW	Signal Processing Workstation
SRR	System Requirements Review

TCAS	Traffic Alert and Collision Avoidance System
TDMA	Time Division Multiple Access
UMTS	Universal Mobile Telecommunications System
VHF	Very High Frequency
VOIP	Voice Over Internet Protocol
VOR	Very High Frequency Omnidirectional Range
W-CDMA	Wideband Code Division Multiple Access
WiMAX	Worldwide Interoperability for Microwave Access
WLAN	Wireless Local Area Network
WRC	World Radio Communication Conference
WSSUS	Wide-Sense Stationary Uncorrelated Signal

ABSTRACT

Wireless connectivity is becoming an integral part of our society. A new paradigm for aeronautical data services is beginning to take shape. The advances in signal processing, rapid prototyping, an insatiable consumer demand for Internet services, increase in aircraft traffic, aircraft safety, etc., are driving the demand for high speed data services. Programs led by the National Aeronautics and Space Administration (NASA), the Federal Aviation Administration (FAA), EUROCONTROL and Networking the Sky for Civil Aeronautical Communications (NEWSKY) are all looking into aeronautical platforms as part of their Aeronautical Data Network (ADN). The desire is to provide low delay, cost effective and high speed data connectivity for aeronautical platforms. The platforms can also be used as a relay for ground and airborne nodes. Such a capability could potentially provide data connectivity to remote areas. Most of the current high altitude platforms, i.e., aircraft, provide data connectivity through a satellite. However, satellite resources are limited and expensive, and they offer limited data throughput as compared to a terrestrial network. A potential solution is connectivity to ground stations that can provide high speed physical layers. Since the frequency spectrum is a valuable estate and needs to be used efficiently, the use of spectrum efficient techniques are evaluated. This dissertation discusses issues and challenges for developing a high speed ground based physical layer for aircraft and proposes a novel solution. A detailed analytical analysis is presented to show the issues related to aeronautical channel and its impacts to aeronautical communication system. Specifically, the impact of Doppler shifts that limit the use of efficient modulation schemes, such as Orthogonal Frequency Division Multiplexing (OFDM), is presented. OFDM is sensitive to Doppler shifts. In addition, Doppler spread and shifts in aeronautical channels depict different characteristics compared to terrestrial networks, i.e., multiple Doppler shifts

and delays. Parametric techniques are investigated to accurately estimate the Doppler shifts. The results of parametric methods for estimating the Doppler shifts are presented. The simulation results of MUltiple Signal Classification (MUSIC), Eigenvector (EV) and Minimum norm methods are considered for an aeronautical channel and their performances is presented.

OFDM, in combination with dense encoding, offers a robust communication and spectrum compression. Its use is limited to the terrestrial domain due to its sensitivity to Doppler shifts. OFDM sensitivity to frequency shifts results in Intercarrier Interference (ICI) and degrades spectral efficiency. High mobility platforms, i.e., trains and aircraft, are challenging environments for OFDM performance. OFDM ICI, caused by the high mobility of the platforms, is investigated and potential methods are proposed. A high speed aeronautical physical layer will allow ADNs to provide a critical service for various situations, such as public safety communication, Denial of Service (DoS), disaster situations, in-flight Internet, etc.

An aeronautical channel imposes a challenging environment for an OFDM based physical layer. This environment, two ray channel, consists of dual Doppler shifts impacting the received signal. A novel approach based on smart antenna processing is proposed, not only to mitigate the problem, but also to take advantage of the dual Doppler shifts. The Doppler shifts in the aeronautical environment can be mitigated and taken advantage of to improve the system performance. The received corrupted signal is first separated by the use of beam forming antenna processing and then combined using diversity combining techniques.

This research concludes with feasibility analysis that explores the system and architecture requirements for a cognitively driven and reconfigurable hardware for aeronautical platforms. The scope of such a system is to provide an intelligent configurable radio system, radio connectivity for the changing geographical locations, and political and regulatory policies with which an aircraft must comply. Such an industry could take advantage of opportunistic services available today and in the future. The global movement of the aeronautical industry can take advantage of emerging wireless services and standards to provide

high speed seamless data connectivity. Advances in components and processing hardware can provide the configurable hardware required for such a capability. Therefore, a Cognitive Aeronautical Software Defined Radio (CASDR) system will provide an intelligent, self-configurable software and hardware solutions for the aeronautical system.

CHAPTER 1

INTRODUCTION

Aeronautical Data Networks (ADN), in which aeronautical platforms are potentially part of a multi-tier network, is researched for future wireless communication systems. The three leading reasons for developing an ADN system are:

- The growth in air transportation is driving the data communication demand for Air Traffic Control (ATC) and Air Traffic Management (ATM) [5].
- The need for low delay, low cost and high speed in-flight multimedia services [6].
- Potential use of ADNs as a backbone for terrestrial communication networks [7–9].

In addition, such a system could provide services for ground networks, public safety, military communication and high data rate in-flight connectivity. To provide high speed connectivity, an increase in bandwidth or an increase in bits per hertz is required. The desire is to use the available bandwidth for the increase in throughput. As the number of bits per hertz increases, the receiver is more sensitive to channel impairments and thus susceptible to bit errors. This sensitivity is exacerbated in a wireless channel, where multipath, path loss and Doppler shifts cause performance degradation. OFDM offers efficient channel encoding and robustness against frequency selective channel conditions. OFDM breaks the bandwidth into smaller bandwidths, which can then be encoded by denser bits/hertz coding, such as Quadrature Amplitude Modulation (QAM).

OFDM based systems have been adopted and proposed for several current and future communication systems globally, i.e., Asymmetric Digital Subscriber Line (ADSL) services, IEEE 802.11a/g/n, IEEE 802.16, IEEE 802.20, Digital Audio Broadcast (DAB) and digital

terrestrial television broadcast. The performance of the OFDM system will depend on its performance under the aeronautical channel conditions. The aeronautical channel can be broken into three segments: takeoff/landing, en route and taxiing/parked. Since an aircraft spends most of its time in the en route segment, this dissertation will focus on the en route channel. For the en route environment, most of the current research assumes a two ray model [10, 11]. The remaining two segments fall within the scope of the Non-Line of Sight (NLOS) dispersive channel. A two ray channel in an aeronautical environment will experience a narrow sparsely populated Doppler spread bandwidth and shifts, i.e., less than 360^o [1]. Each ray in the two ray channel will experience significantly different Doppler shifts. Also, the en route channel experiences a different condition between air to ground and ground-to-air.

Onboard commercial airline communication has evolved over the last few decades. The connectivity, either through ground link or through satellite, provides voice and data communication. However, such services have limited bandwidth for data connectivity. The growth of the cellular phone, data connectivity, low cost Personal Digital Assistant (PDA) and low cost data services has changed the consumer appetite for Internet connectivity. The Internet has driven accessibility for various services, e.g., banking, stocks, and bill payments, which are driving the data demand. The global workforce and remote working culture has revolutionized global corporations and human interactions, independent of location. Consumers are carrying PDAs, laptops, cell phones, etc., that can support high speed connectivity. Therefore, there is a need to provide high bandwidth for in-flight data connectivity.

To provide wireless connectivity in the aircraft, first and foremost, the threat of wireless RF emissions to aircraft communication and navigation systems needs to be considered. Flight safety is a priority before any such system is implemented. Table 1.1 shows critical navigation frequencies used in flight navigation and communication systems. These frequencies provide cockpit to ground voice communication, instrument landing capability, situational awareness, etc., that are critical to the safety of flight operations [12].

The Traffic Alert and Collision Avoidance System (TCAS), operating at 1090 MHz, is an on-board aircraft conflict detection and resolution system used by all carrier aircraft that carry more than ten passengers in the United States. TCASs allow individual aircraft to monitor other aircraft within its vicinity, without ground control or any third party in the loop. Pilots are constantly aware of their neighbors in the sky [13]. The Very High Frequency Omnidirectional Range (VOR) transmits in the very high frequency range of 108.1 through 117.95 MHz. This system consists of several hundred ground stations that transmit navigational track guidance signals used by aircraft. The navigation signal allows the airborne receiving equipment to determine a magnetic bearing from the station to the aircraft. This line of position is called the 'radial' from the VOR. The intersection of the two radials, from different VOR stations, on the chart provides the position of the aircraft [14]. The Distance Measuring Equipment (DME), operates at 962 - 1213 MHz. It is a transponder-based radio navigation technology that measures distance by timing the propagation delay of very high frequency radio signals [15]. The Global Positioning System (GPS) operates at 1227.60 and 1176.45 MHz. GPS is a space based global navigation satellite system created by the Department of Defense (DOD). It operates with 24 satellites that provide location and time information under all conditions, on and near Earth. An unobstructed line of sight to four or more GPS satellites allows an accurate estimation of the aircraft location [16]. The Very High Frequency (VHF) band of 118 - 188 MHz, also known as aircraft band, is allocated for voice communication and navigation purposes. Air Traffic Control Radar Beacon System (ATCRBS), operates at 1030 MHz and is critical to flight navigation.

There are multiple papers on potential RF interference with the critical frequencies shown in Table 1.1 [17–19]. The test results were taken with a nominal PDA's transmit power. However, an increase in transmit power may be required, if the device in the aircraft was to talk directly to the ground terminal. In addition, given the number of passengers in the aircraft, RF coupling of these devices with flight critical systems is a safety concern. Also, aircraft navigation systems are becoming more and more dependent on RF signaling.

Table 1.1 Critical Navigation Frequencies.

Frequency Range(MHz)	Aircraft Systems	Spectrum (MHz)
105-140	LOS	108.1-111.95
	VOR	108-117.95
	VHF	118-188
325-340	GS	328.6-335.4
960 - 1250	TCAS	1090
	ATCRBS	1030
	DME	962-1213
	GPS L2	1227.60
	GPS L5	1176.45
1565 - 1585	L1	1575.42 +/-2

Following are some of the critical issues, if individual phones, PDAs or laptops are allowed to connect to ground networks.

- For aircraft flying at 33,000 ft (10.1 km or 6.25 miles) and 550 Mph, the increased LOS distance will require increased transmit power. This would increase the possibility of interference with critical flight systems. The number of passengers concentrated in the small area will exacerbate the interference problem.

- At high altitudes, a cell phone or any wireless enabled device could engage with many base stations. The mere reason for frequency re-use is to increase the capacity of cellular providers. A cell phone having a bird's eye view will be able to engage with multiple base stations. This is counterproductive to the frequency re-use methodology.

- Current systems are designed to manage Doppler shifts and the capability to hand over calls within base stations for mobiles traveling on the average of 60 Mph. The flight dynamics with average speeds of 550 Mph will force a redesign of these critical system parameters.

There are multiple issues with the use of PDAs during flight, especially connecting them to ground networks directly. Also, with increased wireless activity, a mobile phone or any wireless enabled device could prove to be hazardous to flight systems. Therefore,

the simplest approach is to manage transmit power from individual users by connecting the radios to a pico-base station within the cabin [20–22] to reduce transmitted power. The system and safety issues mentioned above, are driving system designers for a very short range base station that can service the on-board passengers. Thus, a system is taking shape around a pico-base station inside an aircraft, where the frequency re-use of a ground cellular system is used, with a power control feature to reduce interference. The short proximity to the user allows limited power emissions and therefore lowers the probability of RF interference [23]. This pico-base station will then communicate through a backbone wireless link directly to the ground or via a satellite.

The following sections cover the wireless connectivity technologies that are currently being developed or are under development, and their limitations.

1.1 Satellite Services

Satellite systems such as INAMREST provide capability for voice and data links [24]. However, the use of satellites for data connectivity is expensive, and their capacity and throughput is limited. Companies such as Connexion and Iridium have similar capabilities, and Iridium Next is working on developing the next generation of satellite systems with increased throughput.

The data and voice services by Inmarsat P, Globalstar and Iridium are in effect today [25–28]. Their available data rates and services are shown in Table 1.2. The chronic problem with these services is low bandwidth. Also, communication through a satellite generally means a higher latency, which limits the performance of Voice-over-IP (VoIP) calls.

1.2 Air-to-Ground Broadband Services

The Airvana Air-to-Ground (ATG) radio access network infrastructure enables service providers to allow communication links to aircraft [29]. Airlines and general aviation operators can use this ATG link to deliver data and voice-over-IP services to passengers.

Table 1.2 Satellite Services.

Service/Systems	Inmarsat P	Globalstar	Iridium
Voice	2.4 kbps vocoder	0.6-9.6 kbps CELP	2.4-4.8 kbps VSELF
Data	V22	2.4kbps(18kbps-fixed)	2.4kbps
fax	Group3	-	Group3
Paging	Alphanumeric	Alphanumeric	Alphanumeric

The Airvana ATG system uses the air interface for air-to-ground communication. It delivers an average throughput of 1 Mbits/s to 2 Mbits/s to aircraft. Inside an aircraft cabin, this broadband connection can be shared using WiFi or pico-cellular, enabling wireless connectivity to passengers. The Airvana solutions are limited to flights over land and do not offer solutions for oceanic flights. The Airvana base station operates in the 800 MHz spectrum that has been especially allocated by the US Federal Communications Commission (FCC) and includes special filters that meet the stringent specifications required for operation in this spectrum. It delivers peak data rates of 3.1 Mbits/s and 1.8 Mbits/s for ground-to-air and air-to-ground communication respectively, in the 1.25 MHz spectrum. A single Airvana SkyBTS base station provides more data throughput than a satellite transponder. Hundreds of Airvana SkyBTS base stations can be deployed at a fraction of the cost compared to launching a single satellite. While round trip latency on a satellite based system exceeds 300 ms and makes the satellite based system unusable for VoIP, round-trip delays for an Airvana ATG system are less than 100 ms.

1.3 Wireless Technology Growth

Due to stringent safety requirements, deployment cost and training, technology insertion is slow. Traditionally, custom communication solutions were designed for aircraft systems. However, due to the low cost of PDAs and the desire for compatibility with current wireless standards, there is a growing need to develop systems and architectures that provide seamless wireless connectivity.

As aircraft density increases with travel increase, the limited satellite bandwidth will not be able to keep up with the increase in data demand. A data link to/from the ground is a viable solution for the future. The cell phone technology was initially targeted for voice communication. However, with increased usage and demand, the desire is to build a network capable of supporting multimedia data transmissions. Network connectivity is becoming more data centric.

The broadband wireless industry, which provides high data rate terrestrial network connections to stationary sites, has matured to the point where it can look into a wireless metropolitan area network, instead of local area networks for small offices. IEEE Standard 802.16, with its WirelessMAN air interface, sets the stage for widespread and effective wireless connectivity deployment worldwide [30]. Even as Third Generation (3G) wireless equipment continues to grow, Fourth Generation (4G) systems are being implemented. 3G systems, such as High Speed Packet Access (HSPA), provide up to around 15-20 Mbits/s downlink and about 5-10 Mbits/s uplink. 4G systems are being designed to support 5 to 10 times those rates with greater than 100 Mbits/s or more in the downlink and over 50 Mbits/s in the uplink. See Table 1.3 for different wireless standards, rates and range of coverage [31].

3G/4G wireless communications have successfully increased the bandwidth available for new applications through the use of Code Division Multiple Access (CDMA) for physical layer transmission. Unlike older schemes that multiplex data for individual channels through frequency or time divisions, CDMA spreads data using the constructive interference properties of the codes associated with each channel to perform the multiplexing. CDMA has proven itself effective in the packet switched voice wireless world. Spread spectrum techniques have allowed a more efficient and flexible use of bandwidth than previous systems.

Regarding 4G standards, 3G standards (3rd Generation Partnership Project (3GPP) and 3rd Generation Partnership Project 2), have indicated that Orthogonal Frequency Division Multiple Access (OFDMA) is their choice for the physical layer transmission tech-

Table 1.3 Wireless Standard Comparison.

Standard	Family	Radio Tech	Down (Mbps)	Up (Mbps)	Notes
802.16e	WiMAX	MIMO-SOFDMA	70	70	10 Mbps at 10 km.
802.11a	WLAN	OFDM	54	54	Range 100 Meters
802.11b	WLAN	DSSS	11	11	Range 120 Meters
802.11g	WLAN	OFDM	54	54	Range 140 Meters
802.11n (09)	WLAN	MIMO	248	248	Range 250 Meters
HIPERMAN	HIPERMAN	OFDM	56.9	56.9	
WiBro	WiBro	OFDMA	50	50	Mobile Range (900 m)
iBurst	iBurst 802.20	HC-SDMA	64	64	3-12 km
UMTS W-CDMA	UMTS/3GSM	CDMA/FDD	0.384/14.4	0.384/5.76	1-2Mbps, 200kbps, 28.8kpbs.
UMTS-TDD	UMTS/3GSM	CDMA/TDD	16	16	
LTE UMTS	UMTS/4GSM	OFDMA	100	50	Still in Development
1xRTT	CDMA2000	CDMA	0.144	0.144	Obsoleted by EV-DO
EV-DO,Rev.	CDMA2000	CDMA/FDD	2.45/3.1	0.15/1.8	

nology. However, the first standard to be deployed using the new multiplexing technique is IEEE 802.16e, or WiMAX (Worldwide Interoperability for Microwave Access). An earlier version of WiMAX, known as 802.16d, is already online in some areas for fixed access wide area data networks. The main difference between the two standards is that 802.16e provides features for mobility. Therefore, an ADN network could potentially establish connectivity by adopting these standards and provide data connectivity for in-flight services.

Figure 1.1 Congested Airspace Forecaster (Source [2]).

This requires that the issues related to aeronautical channels are resolved. In addition to keeping up with changing and evolving industry standards, a software centric processing architecture for aircraft is required, i.e., software defined radio. This allows aircraft radio hardware to keep up with the changes.

1.4 Air Traffic and Forecast

Ever increasing air travel combined with the appetite for global business is increasing air traffic. Passengers increasingly want to travel for either business or personal needs [32]. International air travel continues to increase at a rapid pace. The US Federal Aviation Administration (FAA) forecasts continuing growth rates of 3.9 percent or more through 2030, for flights to and from the United States [33, 34]. Air traffic across oceanic airspace in regions of the world may grow even more rapidly. With global air traffic increase, the current available data connectivity may not be able to keep pace with this demand while employing communication technologies developed over 50 years ago.

Figure 1.1 depicts current air traffic over North America, Europe and Asia. In addition to providing ground communication, the increase in flights and potential reduction in flight separation requirements, this would be ideal for an ad-hoc or combined mesh network for future aeronautical Internet communication solutions. Figure 1.2 shows Boeing's estimate of growth in air travel, which shows the increase in air traffic [2]. The FAA's system of controlling and monitoring airspace is increasingly coming under pressure because of the increased aircraft congestion. The FAA and other companies are working on advanced

technologies capable of real time monitoring of aircraft separation in a 3D (three dimensional) airspace, such as the FAA's Next Generation Air Transportation System (NextGen). NextGen is a comprehensive system overhaul of the National Airspace System to make air travel safe and efficient, while supporting increased air traffic [35].

1.4.1 Air Traffic Routes and Separation

The clustering of the routes is indicative of the increase in air travel due to increase in population, global business and leisure. Figure 1.3 shows the international continental airline flight routes. The flow of various aircraft will form regional clusters that could communicate with each other, (see Figure 1.4). This clustering is being considered to create a mesh of aircraft networks. The clusters in essence could communicate through ground

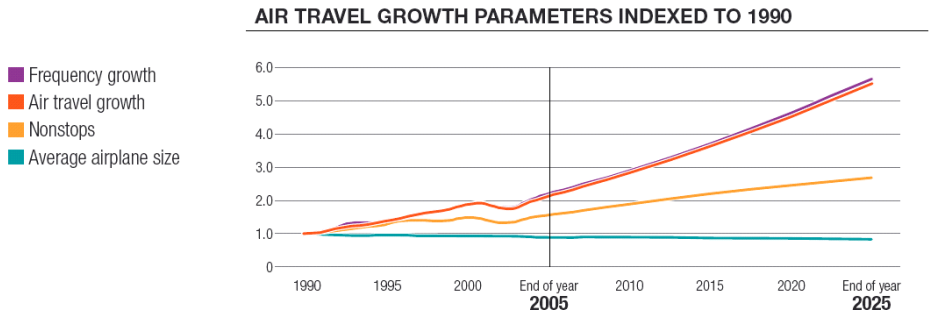

Figure 1.2 Boeing Estimate of Air Travel Growth (Source [2]).

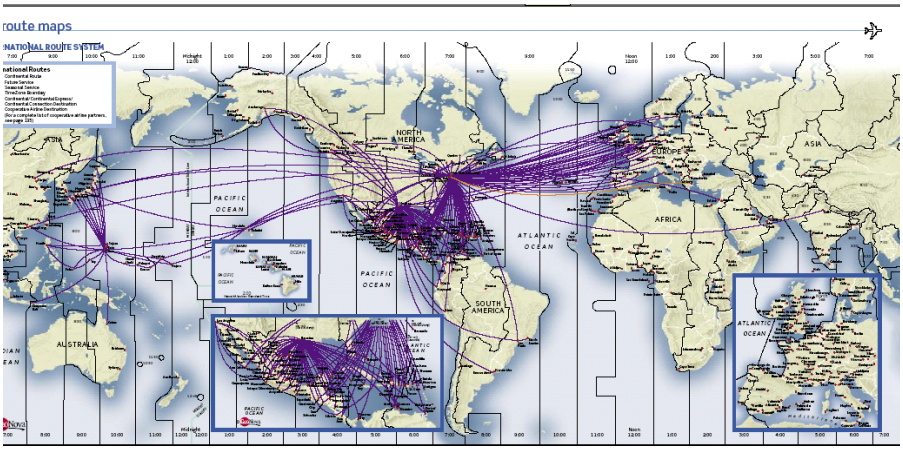

Figure 1.3 Continental Airline Traffic Routes (Source [3]).

links and back to airspace clusters of interest [6]. Hence, the aircraft closest to a ground station could support a high data rate physical layer link and could serve as the server or hotspot for other aircrafts in the vicinity. This would require a developing technology that can support a high data rate backbone to the ground stations.

Air traffic control and operation is a service provided by ground based controllers who direct aircraft on the ground and in the air. A controller's task is to separate certain aircraft and prevent them from coming too close to each other by use of lateral, vertical and longitudinal separation. Secondary tasks include safe, orderly and expeditious flow of traffic and providing information, such as about weather and navigation, to pilots.

In air traffic control, separation between aircraft is the driving requirement for safety. Air traffic controllers apply rules, known as separation minima, to maintain safe flying skies [36]. All these systems are being revamped with technology, such as ADS-B and TCAS, that would allow visibility to pilots and air traffic controllers. The technologies slated for deployment will allow closer proximity of flights and could also help form clusters of communications. Hence, mesh networked aircraft will require a high speed ground physical layer to provide connectivity for aircrafts who are not close to a ground tower. Figure 1.5 and Figure 1.6 [4] shows aircraft traffic activity at the Tampa International airport.

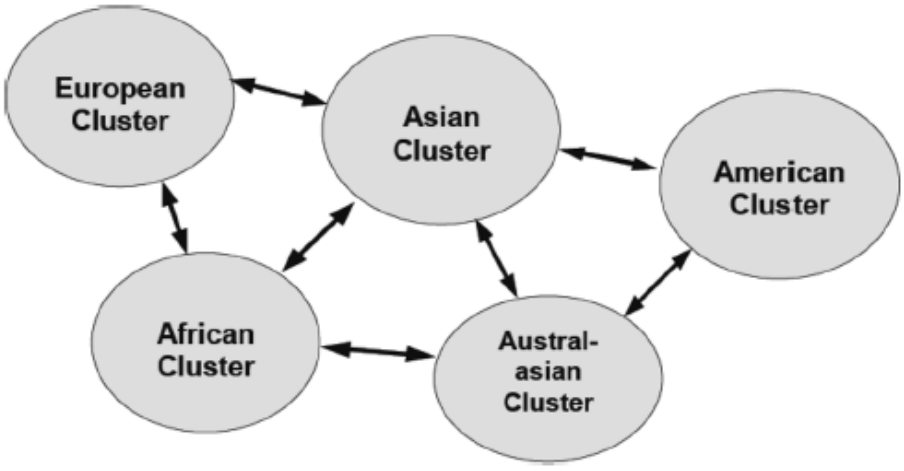

Figure 1.4 Continental Traffic Clusters.

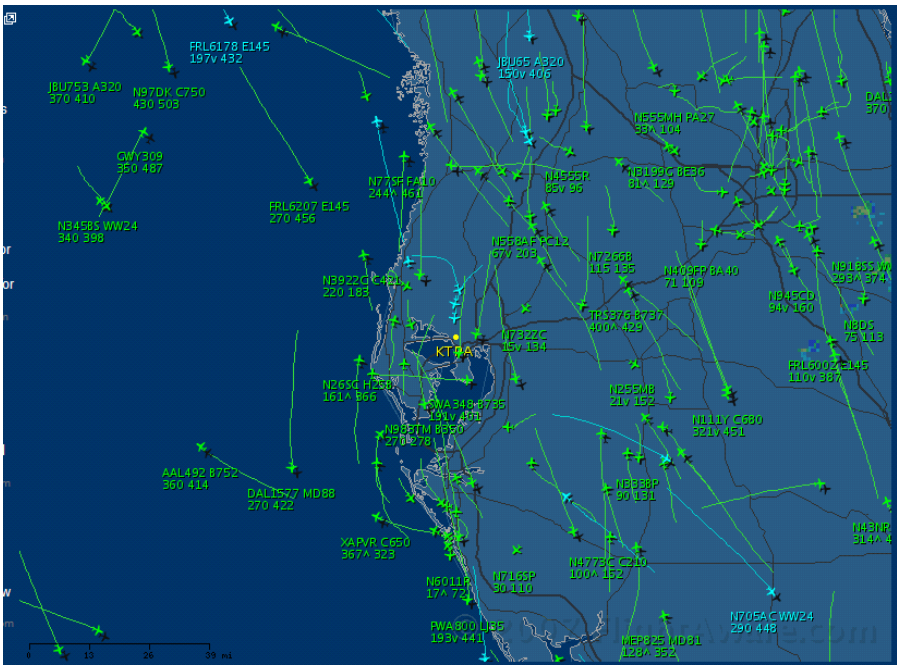

Figure 1.5 Aircraft in Tampa Airspace (Source [4]).

1.5 Orthogonal Frequency Division Multiplexing (OFDM)

OFDMA is based on Orthogonal Frequency Division Multiplexing (OFDM). This technology has been successfully used in ADSL, Wi-Fi (802.11a/g), DVB-H and other high speed digital transmission systems. It is not surprising that the first foray of OFDM into

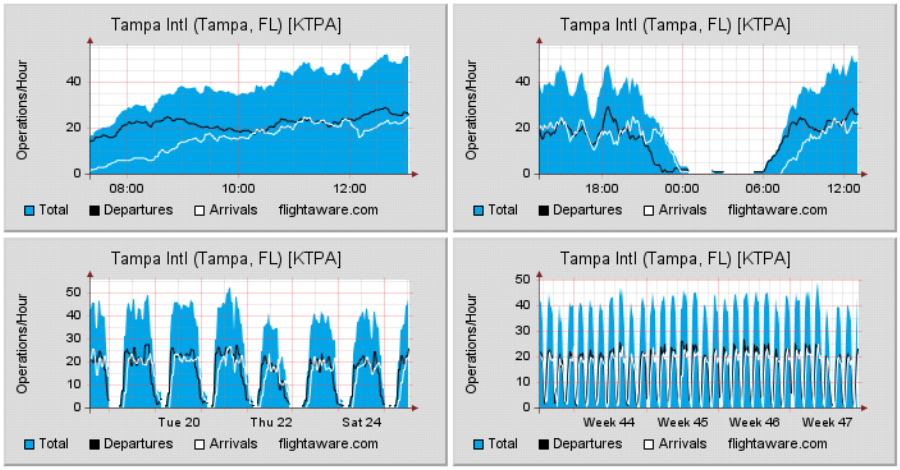

Figure 1.6 Periodicity of Aircraft Traffic in Tampa Airspace (Source [4]).

the cellular wireless world was fixed-access WiMAX 802.16d. This wireless standard has been used to provide high speed Internet access either as a replacement for other access technologies like ADSL or cable, or to provide service in regions where the other access technologies have not been deployed.

In OFDM, usable bandwidth is divided into a large number of smaller bandwidths that are mathematically orthogonal using Fast Fourier Transforms (FFTs). Reconstruction of the band is performed by the Inverse Fast Fourier Transform (IFFT). FFTs and IFFTs are well defined algorithms that can be implemented efficiently when sized as powers of two. One beneficial feature of this technique is the ease of adaptation to different bandwidths. The smaller bandwidth unit can remain fixed, even as the total bandwidth utilization is changed. For example, a 10 MHz bandwidth allocation may be divided into 1,024 smaller bands, whereas a 5 MHz allocation would be divided into 512 smaller bands. These smaller bands are referred to as subcarriers. The smaller bands act as individual communication links and can be encoded with different encoding densities. Also, while the larger bandwidth experiences fading, the subcarrier will experience flat fading.

1.5.1 Benefits of OFDM

One of the challenges of today's wireless systems is multipath. Multipath results from reflections between a transmitter and receiver, whereby the reflections arrive at the receiver at different times. The time span separating the reflection is referred to as delay spread. This type of interference tends to be problematic when the delay spread is on the order of the transmitted symbol time. Typical delay spreads are microseconds in length, which is close to CDMA symbol times. OFDM symbol times tend to be on the order of 100 microseconds, making multipath less of a problem. In order to mitigate the effect of multipath, a guard band of about 10 microseconds, called the cyclic prefix, is inserted after each symbol.

Achieving higher data rates with OFDM systems is more efficient than CDMA systems. The number of bits per unit hertz is referred to as the spectral efficiency. One method of achieving this higher efficiency is through the use of higher order modulation. Modulation

refers to the number of bits that each subcarrier transmits. For example, in a four point quaternary amplitude modulation (QAM), there are two bits transmitted per subcarrier. In 16 QAM, there are 4 bits and 64 QAM yields 6 bits per subcarrier.

1.5.2 OFDM Bandwidth Flexibility

OFDM allows systems to easily adapt to the available spectrum. The stated goal of both Long Term Evolution of 3GPP (LTE) and WiMAX is to support bandwidth allocations from 1.25 to 20 MHz. In addition, the systems can support either time division or frequency division multiplexing. All of this flexibility allows service providers to roll out 4G systems in different ways for different areas depending on the needs of the markets. As the early stages of 4G wireless networking unfold, system developers are beginning to consider what solutions might be best suited for WiMAX and other OFDM based equipment.

New expectations of migration to 4G networks will bring a new level of expectations to wireless communications. Just as the digital wireless revolution in the 1990s made mobile phones available for everyone, the higher speeds and packet delivery of 4G networks will make high-quality multimedia available everywhere. The key to achieving this higher level of service delivery is a new air interface, OFDMA, which is in turn enabled by the high level of performance offered by a new generation of advanced DSPs. Carriers will benefit from greater flexibility by using OFDMA, since in the same spectrum they will be able to offer more channels, including higher-bandwidth channels, with diverse services.

With wireless technology maturity and air traffic growth, there is a growing demand for high speed data connectivity. This same demand is also true for in-flight data communication. This dissertation focuses on a design of advanced physical layer capability to provide a high speed in-flight data connectivity. Thus, the OFDM based physical layer for the aeronautical environment is researched. The critical parameters impacting the performance of OFDM are researched and a novel solution is proposed. The higher layer Open Systems Interconnection (OSI) layers are beyond the scope of this dissertation and shall be left for future studies, researchers and system designers.

1.6 Research Platform

Signal modeling and simulations have become a critical element of research and development, especially in the area of communication and signal processing. This is due to the advancement in high speed analog to digital converters and available processing capability, which has paved the way to process most of the complex signal processing in the digital domain. Most of today's advanced signal processing is implemented on Digital Signal Processors (DSP), General Purpose Processors (GPP) or in Field Programmable Gate Arrays (FPGA). Therefore modeling in software allows the verification of algorithms that can be implemented in the above mentioned processing solutions. There are multiple leading software modeling tools, such as MATLAB, MATHCad, Signal Processing Worksystem (SPW), Synopsis, etc. [37–39]. In this research, MATLAB was chosen as the tool of research. MATLAB (matrix laboratory) is a numerical computing system developed by MathWorks. MATLAB allows single line matrix operations: plotting capabilities, easy implementation of algorithms, development of user interface and interfaces to other programming languages, such as C and C++. In this dissertation, MATLAB was used to develop an aeronautical specific channel model, analyze the impact of ICI on OFDM performance, and develop algorithms.

1.7 Research and Technology Development Process

Research, technology or product development can be structured in a systematic process, where research allows formulation and validation of the concept before any investment in hardware development is committed. This high level systematic process is shown as a flow of major functions in Figure 1.7. The first step is to identify the problem. This could be a new problem or a desire to improve the performance of an existing system. The next step is to perform a detailed literature search of current research activities in the area of interest. This is a critical and iterative step, since a detailed search and review of published papers brings the student and the professor up-to-date in the area of their interest. This iterative

process creates new ideas and leads to novel research. Concepts and ideas formulated are analyzed theoretically for possible solutions. This process results in iterative literature surveys for novel ideas or concepts implemented in other applications that may be applicable for the problem at hand. Finally, this iterative process helps develop a possible solution that needs further research and validation. For signal processing, software modeling serves to validate these proposed concepts. The environments in which the algorithms are supposed to perform are modeled in software, i.e., MATLAB. For example, in communication systems, the MATLAB channel model is developed. MATLAB models of the algorithms are developed and run against channel environments. Monte Carlo simulations with varying parameters are run to understand and validate the performance. Results of literature study, evaluation of proposed solutions and simulation is evaluated for possible publications. The next step is to start identifying conferences and journals to publish the research. The research paper for publication is prepared by first clearly identifying and explaining the problem at hand, followed by the current state of the art, proposed solution, modeling and

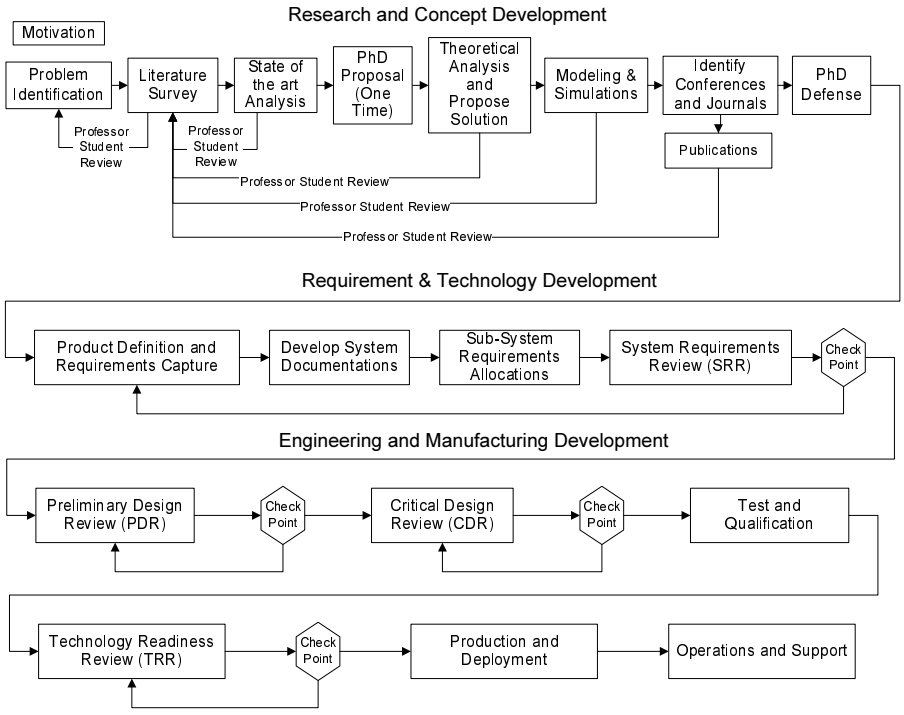

Figure 1.7 Research and Product Development Process.

analysis. This is also the point that if, a product were to be developed based on research, then the next step would be to start capturing the algorithm performance requirements. The requirements development stage includes trading processing architecture, identifying board, interface definition, requirements documentation, hardware trades and sub-system allocation. A critical checkpoint is a System Requirements Review (SRR), where customer, senior management, chief engineer, designers, test, etc. are invited to review the proposed design and an approval to move forward is solicited. The preliminary and Critical Design Reviews (CDR) are similar checkpoints during the hardware design cycle without the procurement of hardware. After a successful CDR, hardware procurement is approved. This is followed by system testing and qualification. Finally, the product is shipped.

1.8 Dissertation Outline

This dissertation focuses on analysis and impact of high speed data communication in an aeronautical environment using OFDM. The limiting cases were evaluated, researched and a solution enabling the use of OFDM in aeronautical communication was proposed. A novel method to correct the corrupted signal due to aeronautical channel impairment is proposed. A MATLAB model was developed for aeronautical two ray channel, algorithm performance for Doppler estimation and novel beam forming method to mitigate the impact of aeronautical channel. Finally a novel, intelligent and configurable hardware is proposed, where the proposed OFDM system can be one of the implementation. The major contributions are shown in Figure 1.8. Introduction, literature study, algorithm development and performance results with summary are presented in the following chapters.

1.8.1 Chapter 1: Introduction

This chapter sets up the motivation and the stage of this dissertation. It explores the possibility of an aeronautical data system. It provides insight into the current capabilities, limitations and evolution of current wireless technology and standards. Finally, it presents the problem, challenges and limitation of developing the capability.

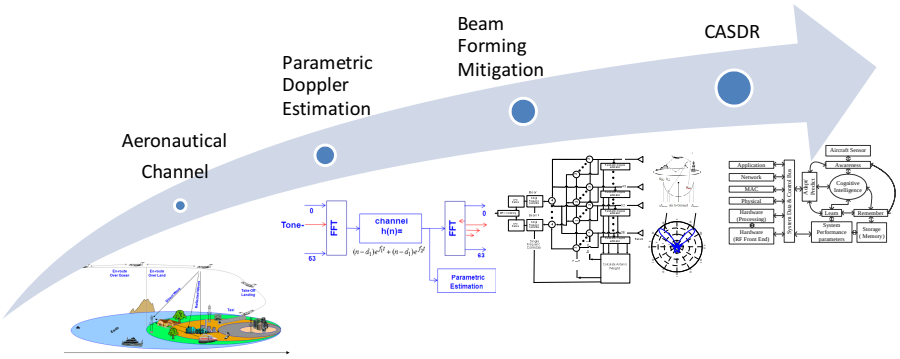

Figure 1.8 Research Contributions.

1.8.2 Chapter 2: Aeronautical Channel

In any communication system the transmitter and receiver are designed to mitigate the impact of the channel. Therefore, understanding and accurately modeling the channel is the key to the development of encoding and decoding algorithms. This chapter introduces the channel parameters critical to the aeronautical channel and their impact on OFDM. The aeronautical channel conditions are modeled and presented with a MATLAB model developed for this dissertation. The contents of this chapter in part or in whole are published in reference [40].

1.8.3 Chapter 3: Aeronautical Intercarrier Interference Analysis for OFDM

Application of OFDM based channel encoding provides increased spectral efficiency and frequency selective robustness. However, OFDM is sensitive to Doppler shifts. This chapter provides the analytical analysis of the two ray aeronautical channel and its impact on the OFDM based system. The contents of this chapter in part or in whole are published in reference [41].

1.8.4 Chapter 4: Parametric Doppler Shifts Estimation in Aeronautical Environments

The impairment of aeronautical channel caused by the dual Doppler shifts needs to be estimated accurately for compensation. This chapter presents the parametric based Doppler

estimation algorithms to accurately estimate the Doppler shifts. Simulations of parametric algorithms and their results are presented. The contents of this chapter in part or in whole are published in reference [42].

1.8.5 Chapter 5: Doppler Shift and ICI Mitigation Using Smart Antenna Processing

This chapter presents the novel beam forming method to mitigate the dual Doppler shifts caused by an aeronautical channel. The critical issues of combined multipaths arriving at the receiver with different Doppler shifts are presented. Analyses with MATLAB simulation results are presented to show the viability of the beam forming methods and its ability to separate the two signals for the aeronautical case. The contents of this chapter in part or in whole are submitted for publication.

1.8.6 Chapter 6: Cognitive Aeronautical Communication System

The dynamic nature of an aircraft and its global traveling requirement opens the concept of a smart radio system that would learn the available services, channel conditions, and user demand, and dynamically configure the radio parameters. The chapter presents the notional concept of Cognitive Aeronautical Software Defined Radio (CASDR). The contents of this chapter in part or in whole are published in references [43, 44]. As an example, the OFDM based system in this dissertation and its beam forming based compensation can be implemented in CASDR.

1.8.7 Chapter 7: Conclusion and Future Studies

Dissertation accomplishments are summarized, with concluding remarks and future studies pertinent to this dissertation outlined and encouraged.

CHAPTER 2

AERONAUTICAL CHANNEL

The understanding of the channel is important in the development of a communication system. As the signal travels from one point to another, it experiences changes that need to be compensated by the receiver. The changes experienced by the signal depend on the location of the transmitter, receiver and the environment. A signal traveling between an earth station and a satellite must pass through the earth's atmosphere, including the ionosphere, and experiences attenuation, signal depolarization, refraction, reflection and delays. The signal transmission on the earth's surface also interacts with the atmosphere, where, depending on the frequency, a reflection or refraction of the signal could come from the earth atmosphere. Surface communication is broken down into large and small scale, differentiating between path loss and multipath [45]. Figure 2.1 shows the different environments of signal propagation for different aircraft communication links. Signal propagation from ground to 10 km is referred to as surface communication. The region of earth atmosphere between 10 km to 60 km is called the troposphere. Beyond 60 km to 600 km is the ionosphere region.

Satellite services such as Inmarsat at 37,786 km and Iridium at 781 km require increased proportional transmit power due to their altitude. They require Line of Sight (LOS) and have delays associated with signal propagation time. Signal propagation in a non-line of sight cases is limited and experiences rapid performance degradation. Relative to Inmarsat, Iridium is in lower orbit and has lower delays. Satellite services provide large coverage; however, they are prone to rapid signal attenuation and require line of sight at all times. Earth surface communication due to shorter distances will experience less signal attenuation, but they are prone to signal blocking and multipath. In general, electromagnetic propagations

are combinations of direct path, reflection, diffraction, and scattering. The distance between the transmitter and receiver lends to direct path signal loss. The presence of reflecting objects and scatters in the channel results in attenuation in the received signal and amplitude fluctuation, due to incoherent adding of the transmitted signals. This summation of the reflected waves leads to multipath fading. The multipath delay spread is essentially the duration of the channel impulse response. Hence, it causes the smearing of signal in the frequency domain. A transmitted tone would appear with some positive/negative change of transmitted frequency. The characteristics of multipath delay spread are critical parameters in selecting various equalizing techniques for optimum performance. The inverse of multipath delay spread is called coherence bandwidth, which is a measure of a channel's frequency selectivity. The coherence bandwidth expresses the width of frequency bandwidth, where the channel equally affects the transmitted signal. The effect of these on signal ampli-

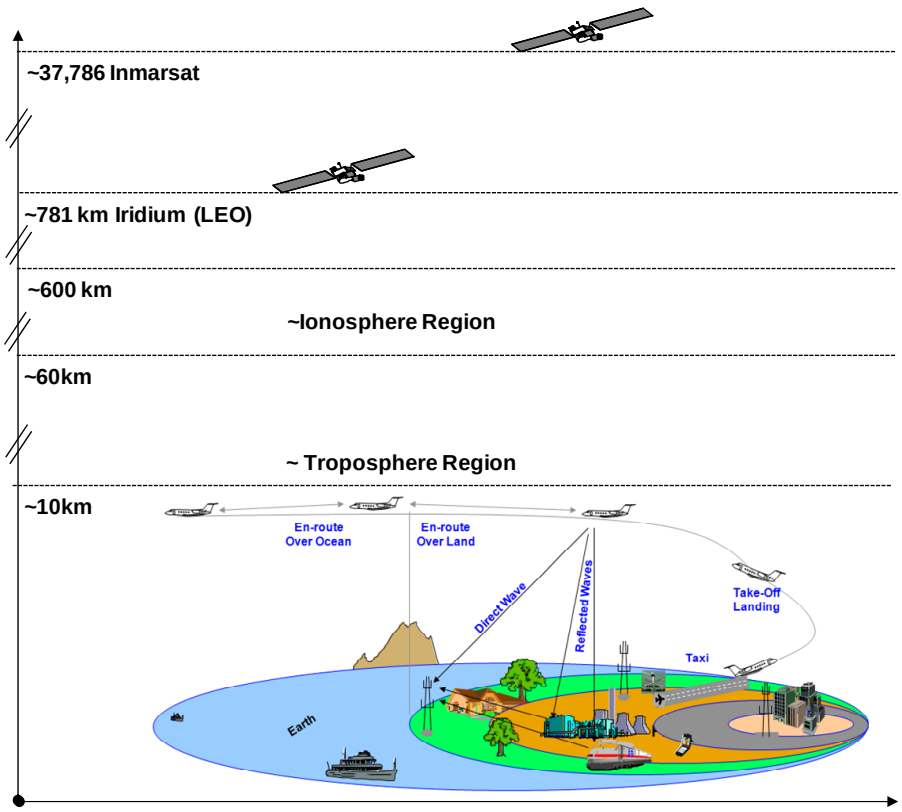

Figure 2.1 Radio Propagation.

tude is of primary interest. The physical movement of the transmitter and receiver toward each other, results in the compression or expansion of frequency known as Doppler shift. This also shows up as the spread of frequency over the transmitted carrier. The inverse of Doppler spread is expressed as coherence time, which is a measure of the rate of channel variations.

The modeling can be divided into two types of fading effects that characterize mobile communications: large scale and small scale fading effects. Propagation models that determine the mean signal strength for an arbitrary transmitter-receiver separation over larger distances are useful in estimating the radio coverage area of a transmitter and are called large scale propagation models. Aircraft experience both large and small channel conditions due to their changing altitude and speed; therefore, Doppler shifts play a dominant role in aircraft channel modeling [46].

2.1 Ionospheric Waves

The collection of ionized particles and electrons in the region 60 km above earth is called the ionosphere. This is formed due to the interaction of solar wind. Frequencies between 30 and 300 MHz are reflected by the ionosphere and travel much further than ground waves by bouncing back and forth between the edge of the ionosphere and earth (see Figure 2.2). Commercial FM broadcasting, VHF, TV signals and short wave radio take advantage of this

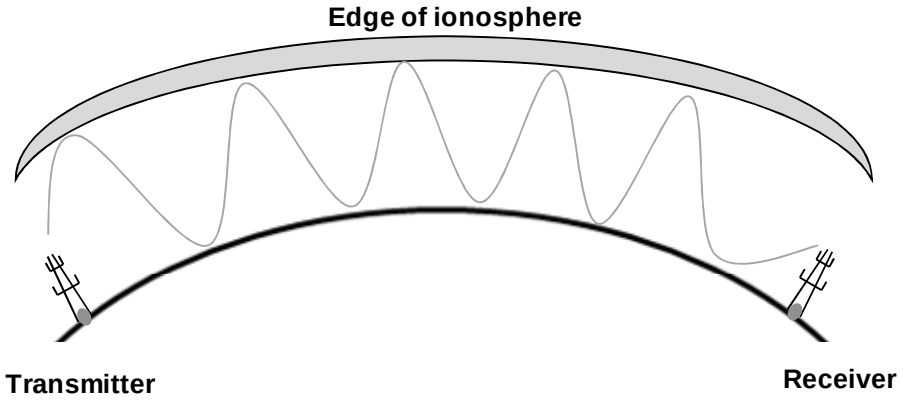

Figure 2.2 Ionospheric Waves.

propagation [47, 48]. The ionosphere generally impacts satellite and aircraft communication through satellite. Surface communication is only affected if the frequency of operation is between 30 and 300 Mhz.

2.2 Tropospheric Waves

In the range of frequencies above 300 MHz and less than 3 GHz, a phenomenon occurs where the signals cannot cross the troposphere and are scattered by it. The scattered waves, which are much weaker, can be received and demodulated. This mode of media behavior is called troposphere scattering (see Figure 2.3) [49, 50].

2.3 Earth Surface Channel Characteristics

In any communication system design, understanding the impairment of the channel is key to designing the transmitter and receiver algorithm.

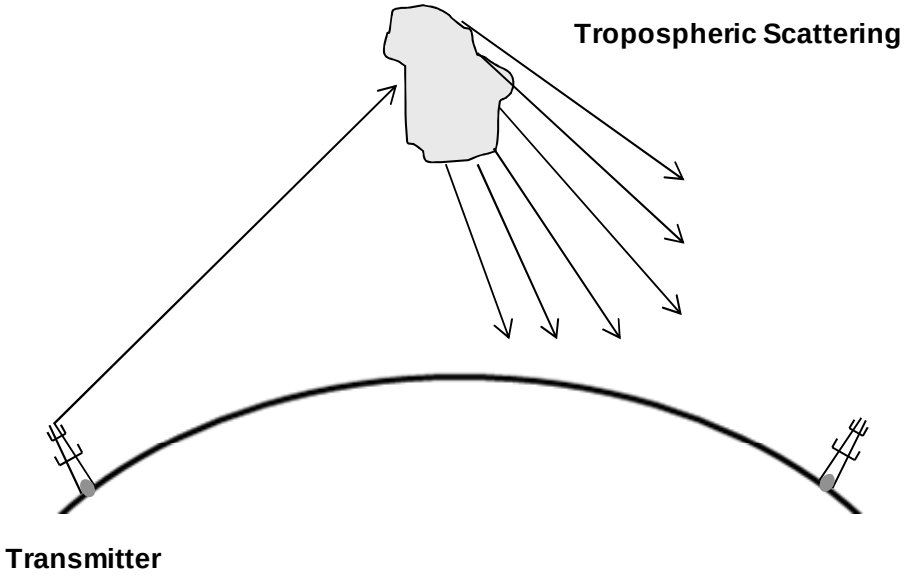

Figure 2.3 Tropospheric Waves.

2.3.1 Large Scale Model: Path Loss

The path loss is the ratio between the received signal power and transmitted signal power that decreases as the distance between the transmitter and receiver increases. The path loss model also depends on the channel frequency, Smulders *et al.* compared the path loss model for 1.7 GHz and 60 GHz [51]. They showed that the difference is higher than 45 dB. The following simple path loss model is generally used. Figure 2.4 shows the aircraft line of sight links; while moving from one base station to another, one will experience loss and the other will experience gain [52–54]. The radio path loss between a transmitter and receiver $FSPL$, is essentially free space loss given by the equation

$$\begin{aligned} FSPL &= (\frac{4\pi}{\lambda}d)^2 \\ &= (\frac{4\pi}{c}df)^2, \end{aligned} \tag{2.1}$$

where d is the path distance between the transmitter and receiver in meters, λ is the wavelength of the transmitting signal in meters, f is the frequency of the signal in hertz and c is the speed of light. Eq. (2.1) only accounts for the direct LOS paths and neglects atmospheric absorption [55]. For L band (960 - 1164 MHz), depending on the range of operation, Figure 2.5 shows the signal attenuation for various distances. This is the critical

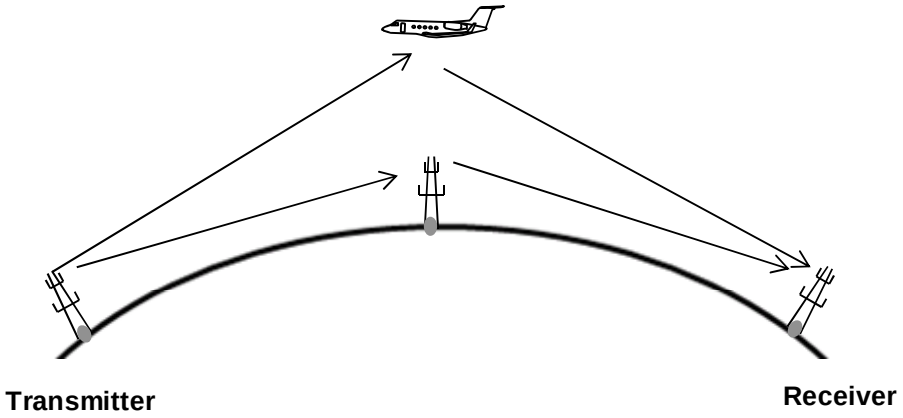

Figure 2.4 Aeronautical LOS Scenario.

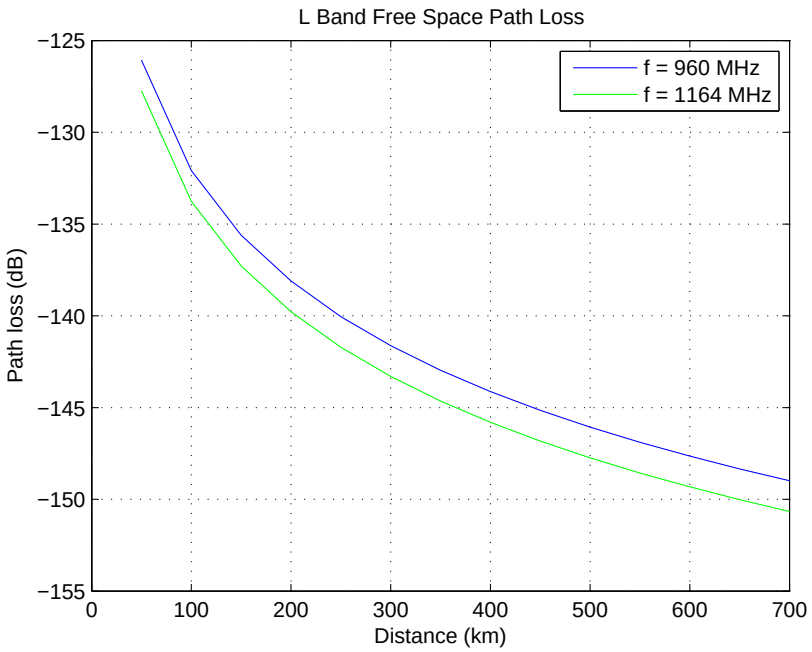

Figure 2.5 L Band Signal Path Loss.

part of link budget, as this derives the transmit power, antenna gains and receiver sensitivity requirement. Based on link margin and aircraft LOS, a minimum number of ground stations will have to be installed to provide continuous connectivity.

2.3.1.1 Rain

Signal attenuation due to rain is the second most significant after free space loss. Rainfall is a natural earthly phenomena consisting of H_2O. It varies with time, duration, and density of H_2O from location to location. At certain frequencies, the impact of rainfall on received signal strength becomes a constraint on the performance of the LOS terrestrial communication link. In a temperate climate, most of this impact is at frequencies above 10 GHz, while in the tropical climates, including the equatorial climate, the frequency as low as about 7 GHz is impacted. This is due to the fact that the raindrops are larger in the temperate climate. For example, the attenuation can vary from 0.1 dB in California to 12 dB in Seattle.

Accommodations for rain can be made by adaptive systems that can increase transmit power, the use of forward error correction and ground diversity. Adaptive transmit power control requires available link margin and an ability to communicate in both directions to command the transmitter to increase power. The forward error correction helps reduce error caused by the received signal strength fluctuation. Ground diversity, such as having another ground station located a few miles away in a rainy region, can improve the rain attenuation by more than half.

There are many popular rain models that are used to estimate the rain loss, such as the NASA Rain Attenuation Model, Crane Rain Attenuation Model and CCIR Rain Attenuation Model [56, 57].

Rain attenuation is more of a challenge for frequencies above 10 GHz, especially the operation of aeronautical communication in the L-band region, which will be least affected. A system designer establishing the worst and best case link budget needs to take into account potential attenuation due to rain, since an aircraft will be traveling in different climate conditions.

2.3.2 Small Scale Model: Multipath

The cause of fading is dependent on the relation between the signal parameters, such as bandwidth, symbol period, etc., and the channel parameters, such as Root Mean Spread (RMS) delay spread and Doppler spread. Time dispersion due to multipath effects causes the transmitted signal to undergo either flat or frequency selective fading. If the mobile channel has a constant gain and linear phase response over a bandwidth that is greater than the bandwidth of the transmitted signal, then the received signal will undergo flat fading. In contrast, the channel creates frequency selective fading. Depending on how rapidly the transmitted baseband signal changes as compared to the rate change of the channel, the channel can be classified either as a fast fading or slow fading channel.

A multipath signal is a combination of multiple rays, and each ray is a delayed and attenuated copy of the original signal. Rays arrive at the receiver at various times and are

combined in an additive manner. In general, the received signal is composed of a direct LOS component and multipath components.

If mobile communication systems operate in urban areas where there is no direct LOS path between the transmitter and the receiver, the fading components have a Raleigh distribution. In rural areas, the probability of the existence of LOS is relatively higher and the resultant signal which combines the LOS component and multipath fading has a Rician distribution. The long-term variation in the mean level is known as slow fading, which has a log-normal probability density function. Slow fading is caused by movement over distances large enough to produce gross variations in the overall path between the ground tower and the mobile aircraft.

2.3.2.1 Time Dispersion and Delay Spread

Channel parameters are characterized by the time dispersion parameters whose main components are mean excess delay and Root Mean Square (RMS) delay spread. These parameters give a clear indication of the expected performance of the wireless system. The RMS delay spread is the square root of the second central moment of the power delay profile:

$$\tau_{rms} = \left[\frac{\int_{-\infty}^{\infty} (t - \tau_m) \left| h(t) \right|^2 dt}{\left| h(t) \right|^2 dt} \right]^{1/2} . \tag{2.2}$$

where,

$$\tau_m = \frac{\int_{\infty}^{\infty} t \left| h(t)^2) \right| dt}{\int_{\infty}^{\infty} \left| h(t)^2) \right| dt}, \tag{2.3}$$

τ_m is the mean excess delay spread of the channel and $h(t)$ is the channel impulse response. RMS delay spread indicates the dispersion of the radio channel, and consequently, inter-symbol interference. It can also be used to estimate the maximum reliable data rate, $R_{\max}$, without any equalization and diversity combining [58]. As the antenna distances increase, the RMS delay spread also increases [54]. This characteristic is expected, since the longer the distance between the transmitter and receiver, the bigger the delay of the multipath

components.

$$R_{\max} = \frac{1}{4\tau_{rms}}. \tag{2.4}$$

2.3.2.2 Coherence Bandwidth

Coherence bandwidth is the statistical average bandwidth of the channel, over which signal propagation characteristics are correlated. It is defined on the basis of the complex autocorrelation $R(\Delta f)$ of the frequency response $H(f)$. $R(\Delta f)$ is defined as

$$R(\Delta f) = \int_{\infty}^{\infty} H(f)H^*(f)df. \tag{2.5}$$

The coherence bandwidth is declared for value of Δf, where $R(\Delta f)$ decreases by 3 dB. Coherence bandwidth is inversely proportional to the RMS delay spread.

2.3.3 Doppler Shift

The Doppler effect is the perceived change in frequency resulting from the relative movement of the transmitter and receiver. As the aircraft approaches a ground station or an aircraft, the frequency received by the instruments on board the aircraft will be higher than the transmitted frequency f_c, whereas frequencies lower than f_c will be received by an aircraft as it moves away from the ground station or an aircraft.

The line of sight will experience the Doppler shift that is the cosine of the angle looking down toward the ground station. The reflected signal will have a different angle. This reflected signal will experience multipath and the received ground station will also experience multiple copies of this reflected signal. Each of the multiple copies will experience different Doppler shifts, thus causing the Doppler spread around the main Doppler shift.

$$f_d = \frac{v}{\lambda} cos(\theta), \tag{2.6}$$

where f_d is the Doppler shift frequency, v is the speed of the aircraft in the communication system, c is the speed of light and θ is the angle between the direction of the traveling

aircraft and the receiver. Doppler shift due to aircraft speed is far larger than currently designed in cellular and wireless LAN communications.

2.4 Aeronautical Channel Scenarios and Characteristics

The aeronautical channel, due to the dynamic nature of an aircraft, experiences a constantly changing environment. A literature search reveals numerous citing in regards to various aeronautical channel segments. Particularly, papers by Hass, Bella and Elnoubi have a wealth of information on ground-to-air channel characteristics from theoretical and empirical data [1, 10, 11]. Studies done by Elnoubi show with empirical data that during an en route scenario, there is a dominant signal most of the time. Analysis and channel measurement for narrow and wide band Aeronautical channels was done by Rice *et al.* [59–61].

Elnoubi *et al.* participated in flight test analysis to characterize the air-to-ground channel fading. An ad-hoc group formed by the Airlines Electronic Engineering Committee's (AEEC) data radio subcommittee conducted tests at Midway Airport in Chicago and another at St. Paul Airport in Minneapolis. Each test included transmitting an unmodulated continuous wave (CW) from the aircraft radio and recording the received signal from the ground radio after the down conversion to a center frequency of 3 KHz. The transmitted frequency in both tests was in the 118-136 MHz band. The transmission took place during taxi, takeoff, flying in the airport vicinity, and landing at the terminal. The recorded signals were sampled and analyzed to extract channel statistics. Channel statistics were extracted and analyzed from the recorded signals. The results showed Rician fading with a strong line of sight component most of the time [62, 63]. However, severe fading was recorded during takeoff and landing. This is understandable, since as the plane lowers its altitude and approaches the airport or large city, its Rician fading will progressively turn into Raleigh fading [64].

The dynamic nature of aircraft motion will generate different scenarios for channel characteristics. These scenarios will be characterized by a different type of fading, the Doppler

shifts and the delays in the system. The air-to-ground or air-to-air channel links will experience varying conditions, depending on the state of the aircraft journey. While taxiing and parked at the airport terminal, wireless activity can simply be based on small scale models, with no LOS (see Figures 2.6 and 2.7). Hence, a Raleigh channel model currently used for WLAN development will suffice. The dynamics of the aircraft geographical movement can be broken down into the following categories for channel characterization [65–67]:

- Taxi/ Parked at the Airport. Channel condition as defined by local area network for current WLAN is considered sufficient. In this scenario, either the passengers are waiting or disembarking from the plane. The vicinity of the aircraft to the terminal means it is within the means of accessing airport WLAN or WIMAX services. The conditions where multiple objects block the LOS RF signal propagation means an Non-Line Of Sight (NLOS) multipath environment. This would be a situation in which if the aircraft was equipped with CASDR capability, it would change its hardware configuration to accommodate for the available terrestrial services.

- Take Off or Landing. Table 2.1 shows different characteristics for this scenario. This would be the transitioning from static ground channel conditions to dynamic conditions where multipath will gradually decrease, and path loss and Doppler shift will start changing until the aircraft reaches a steady state of airspeed and altitude. Due to the short duration of this event and combined with the safety concerns of take off and landing, this dissertation does not focus in this area. Instead, this dissertation focuses on primarily the en route part of the flight, where there is more demand for high bandwidth data connectivity.

- En route (Cruising Altitude and Speed). Over land, the altitude of less than 10 km is well within the WiMax and MAN networks radio range. Aircraft altitude and speed will introduce variables that would have to be compensated in the receiver. Ideally, the changes required to support such a data link should remain within the aircraft radio. This would allow the ground transceiver to maintain its interoperability and

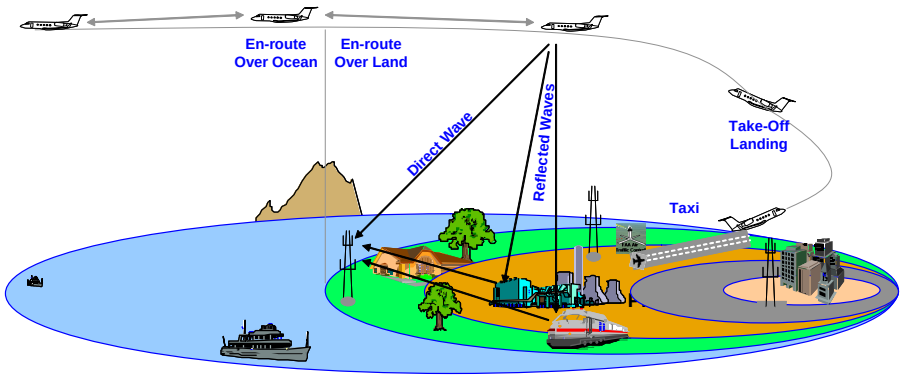

Figure 2.6 Aeronautical Channel Scenario.

control cost. Having clear access to the ground will require least dependence on the aeronautical mesh networks. The distance between aircraft flying in congested routes, such as North America, Europe, South Asia, and Australia, can be used to create an aeronautical mesh network. In this scenario, the plane closer to the ground terminal will provide the link to the Internet portal. Table 2.1 shows channel characteristics for the above mentioned scenarios.

2.5 Problem Statement

In a wireless system design, understanding the limits and bounds of channel impairment theoretically is the first step, which establishes a means to understand performance. Theo-

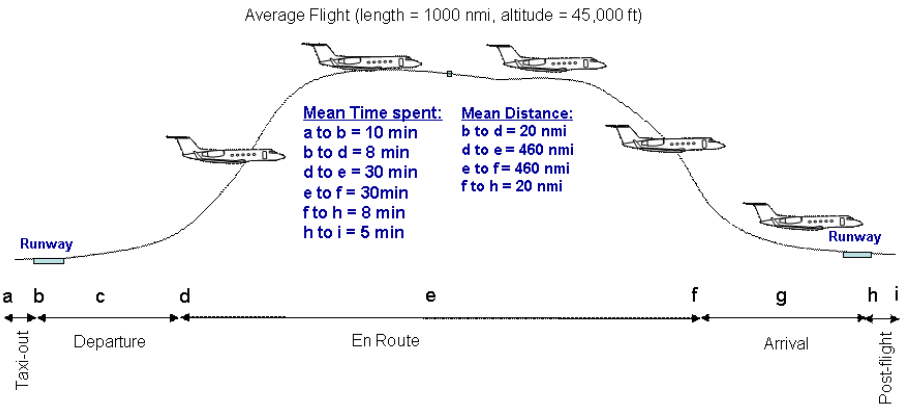

Figure 2.7 Aeronautical Flight Scenario.

Table 2.1 Aeronautical Channel Characteristics (Source [1]).

Parameters	**Parking Scenario**	**Taxi Scenario**	**Arrival Scenario**	**En-Route (Air-Air)**	**En-Route (Air-Gnd)**
Aircraft Velocity v(mph)	0-5.5	0-15	25- 150 typ. 85	440 17 - 440 typ 250	620
Maximum Delay t_{max}(s) Worst Case	$7.0x10^{-6}$	$7.0x10^{-6}$	$7.0x10^{-6}$	$66x10^{-6}$ – $200x10^{-6}$	$33x10^{-6}$ – $1x10^{-3}$
Number of echo paths	20	20	20	20	20
f_{dLOS}/f_{dmax}	-	0.7	1	1	1
Rice Factor K_{Rice} (dB)	-	6.9	15(mean). $9-20$	15(mean). $2-20$	15(mean). $2-20$
Start angle of beam(deg)	0.0	0.0	-90	178.25.0	178.25.0
End angle of beam	360	360	90	181.75	181.75
Exp or Two Ray	Exp.	Exp.	Two Ray	Two Ray	Two Ray

retically developed parameters and equations are then statistically modeled in a simulation environment such as MATLAB. Finally, the simulated model is calibrated through actual measurements, if possible. Unlike the local area network, which are in offices and home environments, and can be modeled and easily calibrated by a sample of actual channel impulse responses, the aeronautical environment poses a daunting task, since it is a huge area for any system designer to try to measure for calibration. In Chapter 6, a novel concept is presented with the CASDR system to be able to measure this large area with the use of aircraft traffic. In the long run, CASDR will facilitate capturing the channel response of the travelled route. Due to this problem, a LOS model for most aeronautical conditions is considered. Radio parameters are set for the least common denominator of the channel conditions for all areas traversed by the aircraft.

Let $h(l,n)$ be the channel equation.

$$h(l,n) = \sum_{l=0}^{L} h_l e^{\frac{j2\pi f_d(n-\tau_l)}{N}} \delta(n-\tau_l), \tag{2.7}$$

where h_l, f_d and τ_l are amplitude, Doppler shift and delay for each path respectively. $l = 1, 2, 3...L$ are number of paths. In the aeronautical case, the limiting case of $L = 2$, which is what the system will experience in the en route scenario, will be used. In this case, the LOS will experience Doppler shift, which is a function of elevation angle, θ, and maximum Doppler frequency, as shown in eq. 2.6. For the diffused path, according to Bello, the Wide Sense Stationary Uncorrelated Signal (WSSUS) channel emulates a small area characterization for a multipath channel [10]. Doppler spread for aeronautical communications depicts a Doppler bandwidth less than 360^o, compared to a wireless LAN environment. For each channel condition, a progressive increase and decrease of multipath and received angle spread of stations is discussed, as it moves from a flat surface terrain/rural area to mountainous (rough) terrain/urban area. Most of the current research assumes a two ray model, as the channel model for flat surface areas. In an extremely rough environment the channel model results in an intermittent loss of LOS along with increasing angle spread to match the Jakes Doppler spread [68].

In order to increase spectral efficiency, an OFDM system is evaluated for aeronautical environments. OFDM based systems have been adopted and proposed for several current and future communication systems globally, i.e., Asymmetric Digital Subscriber Line (ADSL) services, IEEE 802.11a/g/n, IEEE 802.16, IEEE 802.20, Digital Audio Broadcast (DAB), and digital terrestrial television broadcast. For the aeronautical channel, most of the current research assumes a two ray model [11]. In an extremely rough environment the en route channel experiences an intermittent loss of LOS signal with increasing Doppler spread to match the Jakes Doppler spread. Hence, the Doppler spread along with intermittent loss of LOS will depict either a two ray model or NLOS Jakes spectrum.

In this dissertation, an OFDM system is evaluated for the challenging aeronautical channel. The en route channel condition, which is modeled as a two ray channel model and experiences a dual Doppler shift [1] is studied. A two ray aeronautical channel model will have a narrow sparsely populated Doppler spread bandwidth i.e., less than 360^o [10]. Therefore, a modified Doppler model for ADN can be developed as follows. The use of D_f

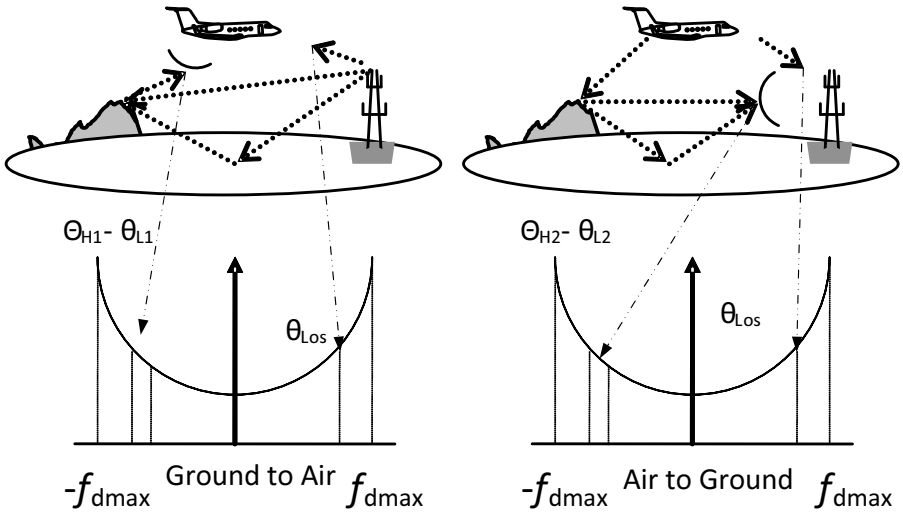

Figure 2.8 Doppler Power Spectrum for ADNs.

factor i.e., $D_{\mathrm{f}} = \frac{\Theta_{\mathrm{H}} - \Theta_{\mathrm{L}}}{2\pi}$, $(\Theta_{\mathrm{H}} - \Theta_{\mathrm{L}}) \leq 2\pi$, $D_{\mathrm{f}} \in \{0, 1\}$, represents going from flat to rough terrain environments (D_{f} from $0 \rightarrow 1$):

$$D = \begin{Bmatrix} 2D_f, & \Theta_H \geq \Theta \geq \Theta_L \\ \infty, & else \end{Bmatrix}, \tag{2.8}$$

where $\Theta = \cos^{-1}\left(\frac{f_d \lambda}{v}\right)$, and $|f_d| \leq \mathrm{f_{d,max}}$. Therefore, Doppler density can be given as:

$$p_{f_d}(f_d) = \begin{Bmatrix} \frac{1}{\pi D \mathrm{f_{d,max}} \sqrt{1 - \left(\frac{f_d}{\mathrm{f_{d,max}}}\right)^2}}, & \text{if } |f_d| \leq \mathrm{f_{d,max}} \\ 0, & else \end{Bmatrix}, \tag{2.9}$$

Figure 2.8 depicts two different Doppler shifts in an aeronautical two ray channel model. Since $f_{d,max}$ for an aircraft can be significantly high, the two rays will have different Doppler shifts. It can be assumed that the LOS Doppler shift will represent a deterministic Doppler shift that can be tracked and corrected by traditional frequency shift algorithms [69]. The reflected path will depict a random Doppler, which can span anywhere between $f_{d,max}$ to $-f_{d,max}$ with a narrow Doppler spread. As a worst case, if the direction of the LOS path

coincides with the heading of the aircraft resulting in a carrier shift equal to maximum Doppler shifts i.e., $f_{d,Los} = f_{d,max}$. The worst case would be when the reflected signal comes from behind, that is when $f_{d,Ref} = -f_{d,max}$. The angle of spread or Doppler spread of the reflected signal, $\Theta_H - \Theta_L$ for a flight en route is less than a few degrees and as an aircraft approaches, lands, and taxis to park, it will go up to 360^o, with decreasing $f_{d,max}$. In addition, due to distances between the transmitter and receiver, the two rays have significant delay relative to each other's arrival time. For the en route case, assuming a typical 10 km altitude, then a typical echo delay could be as much as 33 μs for ground-to-air links and 66 μs for air-to-air links (see Table 2.1 for details). Therefore, for the aeronautical propagation environment, the OFDM receiver needs to estimate the dual Doppler shifts and correct them to reduce the effects of orthogonality deterioration between subcarriers which results in ICI [70].

2.6 MATLAB Model

A MATLAB model was developed to emulate the dual Doppler shifts, as shown in Figure 2.8, with equation 2.9. Figure 2.9 shows the two ray MATLAB model, where signal $x(n)$ experiencing delays, τ, based on the path it travels and goes through two different Doppler shifts. The LOS path experiences a single Doppler shift f_{d1}, with associated gain a_1. The reflected path, having N smaller rays, causes the Doppler spread. This NLOS path signal will experience multipath. While it will have a center f_{d2}, each of the multipaths will have a random Doppler shift causing the Doppler spread. This is modeled with single Doppler shifts, f_{d2} and Doppler spread bandwidth, D_{bw}. The Doppler spread bandwidth is the phase change of the Doppler shifts frequency and less than 360^o,

The results of the MATLAB model are shown in Figures 2.10 and 2.11. Figure 2.10 shows the case where there are two significant Doppler shifts in the channel with no Doppler spread around the reflected path Doppler shift. Figure 2.11 shows the case where the reflected path has a Doppler spread around the center or Doppler shift.

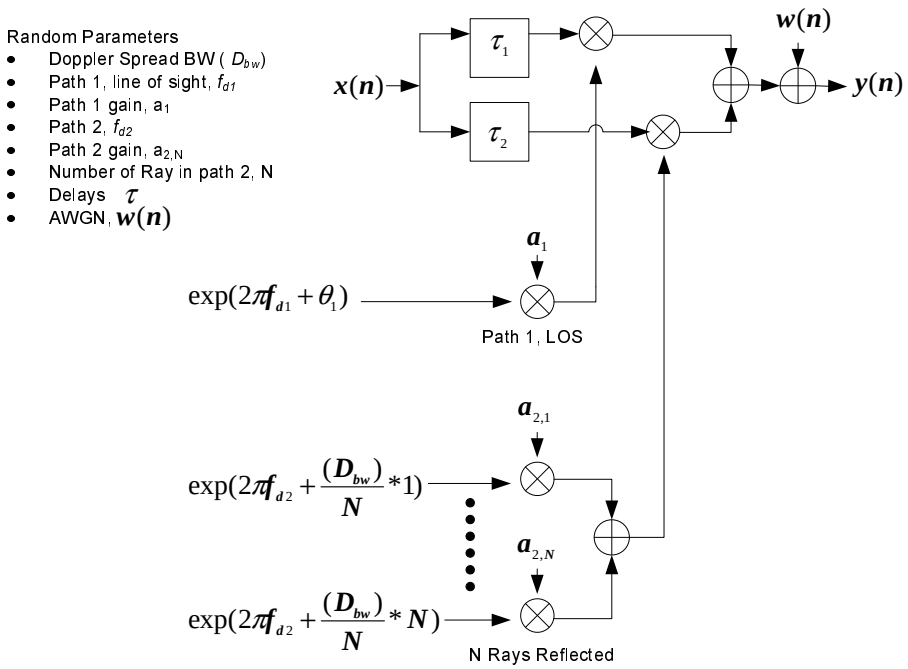

Figure 2.9 Two Ray MATLAB Aeronautical Channel Model Diagram.

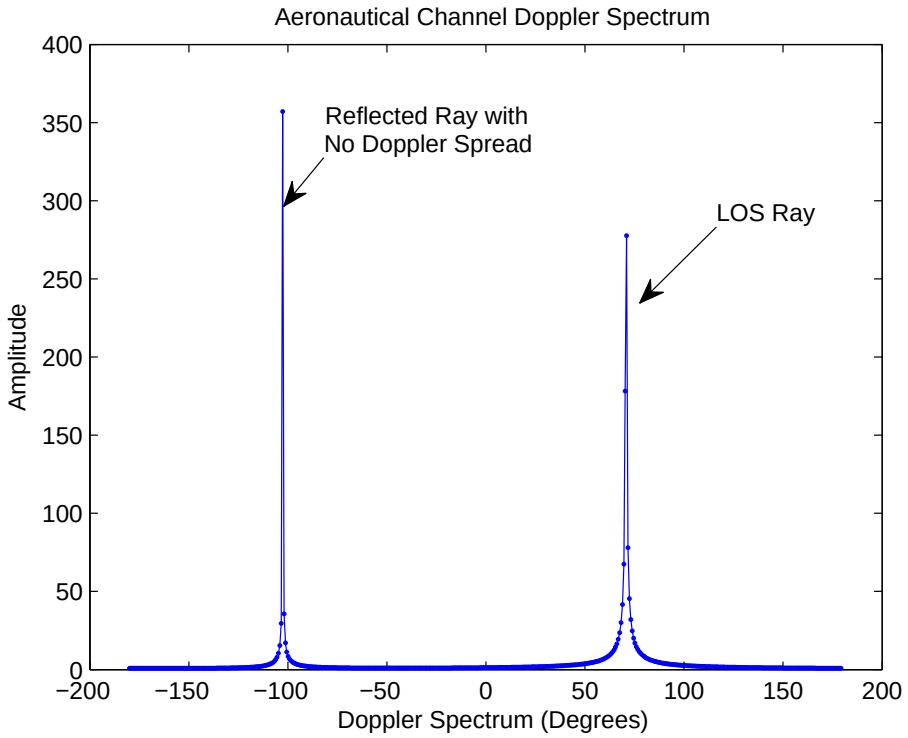

Figure 2.10 Two Ray MATLAB Aeronautical Channel Spectrum with No Doppler Spread.

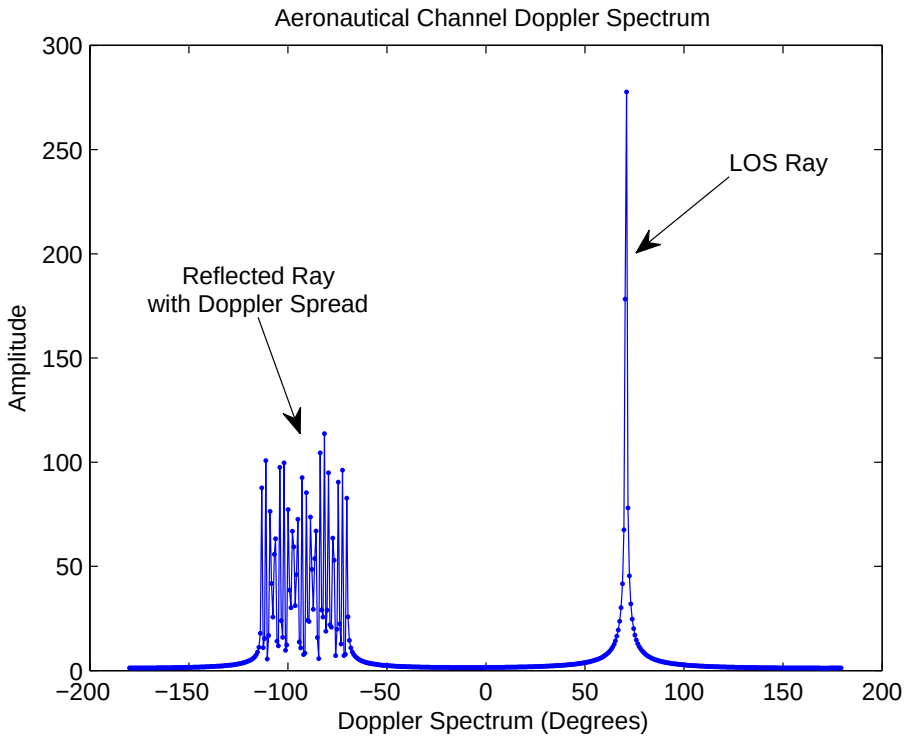

Figure 2.11 Two Ray MATLAB Aeronautical Channel Spectrum with Doppler Spread.

2.7 Conclusion

In this chapter, a review of channel parameters and their impact were discussed. In particular, the aeronautical channel identified as a two ray channel with a strong LOS component with a reflected signal consisting of Doppler spread. The two signals of different Doppler shifts with Doppler spread was identified as the source of main OFDM performance degradation.

CHAPTER 3

AERONAUTICAL INTERCARRIER INTERFERENCE ANALYSIS FOR OFDM

3.1 Introduction and Motivation

The exponential growth in wireless communication, driven particularly due to the desire for mobility is forcing an efficient use of spectrum in multipath environments. Among the different techniques used for spectral efficient encoding, OFDM is one of the leading techniques. In addition to spectral efficiency, OFDM offers robustness against multipath channel impairment. If the channel maximum delay spread is longer than the transmitted symbol duration, the received signal suffers from Inter-symbol Interference (ISI). OFDM takes a set of narrow band signals and encodes it into the desired or available bandwidth. The set of narrow band signals thus delivers a parallel data transmission. The receiver converts it back to the set of narrow band signals. Therefore, relative to the coherence bandwidth, each narrow band experiences flat fading. This reduces the equalizer requirement on the receiver end to mostly a single tap to compensate for channel distortion. Thus, if severe amplitude due to channel is compensated, then amplitude modulated signal encoding can be used, such as Quadrature Amplitude Modulation (QAM).

OFDM channel encoding was proposed in the 1960's [71]. The concept of Multi-Carrier (MC) transmission was first proposed in detail by Chang [72] in 1966. An in depth description of MC can be found in [73] and [74]. Before Chang, Doelz *et al.* [75] had implemented a special MC system for a single-sideband voice channel in 1957. Weinstein and Ebert proposed the time-limited MC transmission in 1971, which is what is known as OFDM. OFDM was not proposed for wireless application until the 1980's [76], mostly due to the

limitations in processing hardware. Since then, there has been a rapid deployment of major OFDM based systems, such as digital audio [77], digital video broadcasting (DVB-T) [78], the IEEE 802.11a local-area network standard [79], and the IEEE 802.16a Metropolitan Area Network Standard (WMAN) [80]. OFDM allows for data rates of up to 75 Mb/s in the IEEE 802.16e Wireless Metropolitan Area Network standard [81], and is in the process of being deployed in the fourth-generation mobile wireless systems [82, 83]. In terms of satellite services, OFDM has been successfully deployed in Sirius satellite radio, which is now part of SiriusXM satellite radio service [84–86].

OFDM was evaluted to increase spectral efficiency in the aeronautical environment. However, as discussed in Chapter 2, the aeronautical channel imposes a debilitating Doppler shifts characteristic that renders the use of OFDM inept for the application. The result of Doppler shifts is an Intercarrier Interference (ICI) in the OFDM demodulation [87]. Figure 3.1 shows how a single tone when sent over a Doppler shifted channel is seen by the receiver. If there was no Doppler shift, the tone would show up intact on the same subcarrier; however, due to the Doppler shift the energy bleeds into the neighboring subcarrier, as shown in the figure. OFDM is sensitive to carrier frequency offset, Doppler shifts, and spread, since these parameters result in loss of subcarrier orthogonality [88, 89]. Therefore, for an aeronautical OFDM application, the ICI caused by multiple Doppler shifts needs to be analyzed and mitigated for OFDM channel encoding. While there has been considerable research done in the application of OFDM and ICI mitigation techniques, previous research has focused on OFDM system design over time-invariant frequency-selective channels.

A two ray channel in an aeronautical model will show a narrow, sparsely populated Doppler spread bandwidth, i.e., less than 360^o [1]. Hence, the two rays may have signifi-

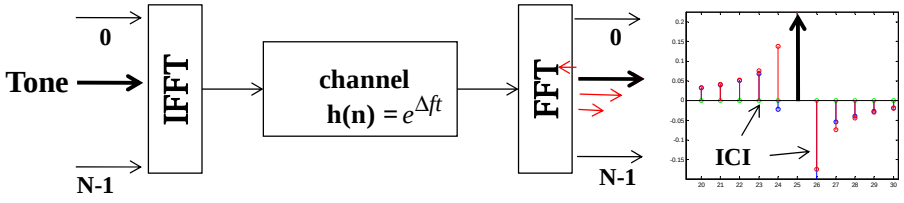

Figure 3.1 Energy Bleeding in OFDM Symbol Due to Doppler Shift.

cantly different Doppler shifts. The ICI analysis will show the impact of these dual Doppler shifts and how they cause ICI in the OFDM symbols.

3.2 Aeronautical OFDM ICI Analysis

ICI is one of the key issues to evaluate the performance of an OFDM system. The analysis follows a general sample-spaced multipath fading channel model for analytical traceability.

In Figure 3.2, $x(n)$ is the discrete time sample of the transmitted OFDM signal, which can be given as

$$x(n) = \text{IDFT}\{X(k)\} = \sum_{k=0}^{N} X(k) e^{\frac{j2\pi kn}{N}}, \quad 0 \leq n \leq N-1, \tag{3.1}$$

where $X(k)$ is the symbol transmitted on the k^{th} subcarrier and N is the number of subcarriers. The channel is modeled as

$$h(l,n) = \sum_{l=0}^{L} h_l(n) e^{\frac{j2\pi\epsilon_l(n-\tau_l)}{N}} \delta(n-\tau_l) \ , \ l = 0, 1, ..., L-1 \ , \tag{3.2}$$

where Δf is the OFDM subcarrier frequency, $\epsilon_l = \frac{f_{Dl}}{\Delta f}$ are the normalized Doppler shifts, $h_l(n)$s are the path gains which are zero-mean stochastic processes with normalized overall power, so that $E\left[(h_l(n))\right] = 0$ and $\sum_{l=0}^{L-1} E\left[(h_l(n))^2\right] = 1$. However, since Doppler shifts are modeled with exponentials as in [70], path gains are assumed to be constant (i.e., $h_l(n) = h_l$) over large time intervals due to the large propagation environment (note that path loss values change slowly due to large distances of communications [6]) while the aeronautical node is moving. Therefore, for the aeronautical two ray channel, ϵ_0 and ϵ_1,

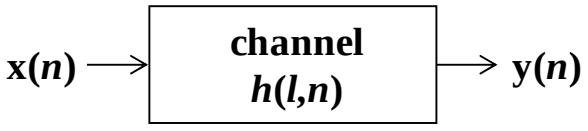

Figure 3.2 Channel Input and Output.

there will be two normalized Doppler shifts for the first and the second ray respectively, i.e., $\epsilon_0 = \frac{f_{D0}}{\Delta f}$ and $\epsilon_1 = \frac{f_{D1}}{\Delta f}$, where f_{D0} and f_{D1} are the Doppler shifts due to two paths. Assuming that the receiver is synchronized to the first path $\tau_0 = 0$ and $\tau_1 = \tau$, i.e., τ being integer, the received signal $y(n)$ is the combination of eq. (3.1) and eq. (3.2),

$$y(n) = h_0 e^{\frac{j2\pi\epsilon_0 n}{N}} x(n) + h_1 e^{\frac{j2\pi\epsilon_1(n-\tau)}{N}} x(n-\tau) + w(n), \tag{3.3}$$

where $0 \leq n \leq N-1$. To help simplify notation, the derivation of eq. (3.3) can be separated into two parts, i.e., first ray $A(n)$ and second ray $B(n)$,

$$y(n) = \underbrace{h_0 e^{\frac{j2\pi\epsilon_0 n}{N}} x(n)}_{A(n)} + \underbrace{h_1 e^{\frac{j2\pi\epsilon_1(n-\tau)}{N}} x(n-\tau)}_{B(n)} + w(n). \tag{3.4}$$

Since the received signal is a linear combination of the two ray model $y(n) = A(n) + B(n) + w(n)$, the Fourier Transform of (3.4) is written as

$$Y(k) = \mathrm{DFT}\{A(n)\} + \mathrm{DFT}\{B(n)\} + W(k). \tag{3.5}$$

Let us begin by first analyzing $B(n)$,

$$\begin{aligned} B(n) &= h_1 e^{\frac{j2\pi\epsilon_1(n-\tau)}{N}} x(n-\tau) \\ &= h_1 \sum_{k=0}^{N-1} X(k) e^{\frac{j2\pi(n-\tau)(k+\epsilon_1)}{N}}, \end{aligned} \tag{3.6}$$

replacing the variable k with m in eq. (3.6) and applying DFT,

$$
\begin{aligned}
B(k) &= \frac{1}{N}\sum_{n=0}^{N-1}\left\{h_1\sum_{m=0}^{N-1}X(m)e^{\frac{j2\pi(n-\tau)(m+\epsilon_1)}{N}}\right\}e^{\frac{-j2\pi n}{N}} \\
&= \frac{h_1}{N}\sum_{n=0}^{N-1}\sum_{m=0}^{N-1}X(m)e^{\frac{j2\pi}{N}(-\tau(m+\epsilon_1)+n(m-k+\epsilon_0))} \\
&= \frac{h_1}{N}\sum_{m=0}^{N-1}X(m)e^{\frac{-j2\pi\tau(m+\epsilon_1)}{N}}\underbrace{\sum_{n=0}^{N-1}e^{\frac{j2\pi n}{N}(m-k+\epsilon_1)}}_{\text{Geometric Series Expansion}}. \qquad (3.7)
\end{aligned}
$$

The term shown within the curly bracket can be calculated via geometric series expansion, i.e., $S_n = \sum_{k=0}^{n} r^k = \frac{1-r^{n+1}}{1-r}$ where $r = e^{\frac{j2\pi n}{N}(m-k+\epsilon_1)}$. Then eq. (3.7) can be written as

$$
B(k) = \frac{h_1}{N}\sum_{m=0}^{N-1}X(m)e^{\frac{-j2\pi\tau(m+\epsilon_1)}{N}}\left[\frac{1-e^{j2\pi(m-k+\epsilon_1)}}{1-e^{\frac{j2\pi}{N}(m-k+\epsilon_1)}}\right]. \qquad (3.8)
$$

Re-arranging terms by taking $e^{j2\pi(m-k+\epsilon_1)}$ and $e^{\frac{j2\pi}{N}(m-k+\epsilon_1)}$ outside the parenthesis to take advantage of trigonometric identity.

$$
= \frac{h_1}{N}\sum_{m=0}^{N-1}X(m)e^{\frac{-j2\pi\tau(m+\epsilon_1)}{N}}e^{j\pi(m-k+\epsilon_1)(\frac{N-1}{N})}\ldots
$$

$$
\left[\frac{e^{-j\pi(m-k+\epsilon_1)}-e^{j\pi(m-k+\epsilon_1)}}{e^{\frac{-j\pi}{N}(m-k+\epsilon_1)}-e^{\frac{j\pi}{N}(m-k+\epsilon_1)}}\right]. \qquad (3.9)
$$

By using trigonometric identity $\sin(x) = \frac{1}{2j}[e^{jx} - e^{jx}]$, eq. (3.9) can be re-written as:

$$
B(k) = \sum_{m=0}^{N-1}X(m)\frac{h_1\sin\left(\pi(m-k+\epsilon_1)\right)}{\pi(m-k+\epsilon_1)}e^{j\pi(m-k+\epsilon_1)}\underbrace{e^{\frac{-j2\pi\tau(m+\epsilon_1)}{N}}}_{\text{Due to Delay}}, \qquad (3.10)
$$

Let $S_1(m,k)$ be

$$
S_1(m,k) = \frac{h_1\sin\left(\pi(m-k+\epsilon_1)\right)}{\pi(m-k+\epsilon_1)}e^{j\pi(m-k+\epsilon_1)}\underbrace{e^{\frac{-j2\pi\tau(m+\epsilon_1)}{N}}}_{\text{Due to Delay}}. \qquad (3.11)
$$

Eq. (3.10) can be written as

$$B(k) = \sum_{m=0}^{N-1} X(m) S_1(m,k). \tag{3.12}$$

Similarly, assuming $\tau = 0$ in eq. (3.12), $A(k)$ can be calculated as

$$A(k) = \sum_{m=0}^{N-1} X(m) S_0(m,k), \tag{3.13}$$

where

$$S_0(m,k) = \frac{h_0 \sin\left(\pi(m-k+\epsilon_0)\right)}{\pi(m-k+\epsilon_0)} e^{j\pi(m-k+\epsilon_0)}. \tag{3.14}$$

Therefore, combining $A(k)$ and $B(k)$,

$$Y(k) = A(k) + B(k). \tag{3.15}$$

$$Y(k) = \sum_{m=0}^{N-1} X(m) S_0(m,k) + \sum_{m=0}^{N-1} X(m) S_1(m,k), \tag{3.16}$$

where $S_0(m,k)$ and $S_1(m,k)$ are defined in eq. (3.14) and eq. (3.11) respectively. Then factoring out $X(m)$,

$$Y(k) = \sum_{m=0}^{N-1} X(m) \underbrace{[S_0(m,k) + S_1(m,k)]}_{\mathrm{S(m,k)}}, \tag{3.17}$$

For simplification, let $S(m,k) = S_0(m,k) + S_1(m,k)$. The transmitted symbol is related to the transmitted symbol in the interested subcarrier with coefficient $S(k,k)$ and also related

to the other subcarriers symbols with $S(m,k)$, as in eq. (3.18),

$$S(m,k) = \underbrace{\frac{h_0 \sin\left(\pi(m-k+\epsilon_0)\right)}{N\sin(\pi(m-k+\epsilon_0)/N)}\; e^{j\pi(1-1/N)(m-k+\epsilon_0)}}_{\text{First Ray}} + \underbrace{\frac{h_1 \sin\left(\pi(m-k+\epsilon_1)\right)}{N\sin(\pi(m-k+\epsilon_1)/N)}\; e^{j\pi(1-1/N)(m-k+\epsilon_1)}\; e^{\frac{-j2\pi\tau(m+\epsilon_1)}{N}}}_{\text{Second Ray}}. \quad (3.18)$$

Note that eq. (3.18) is the linear combination $S_0(m,k)$ and $S_1(m,k)$. Therefore, the final relation of the received signal with energy from neighboring subcarrier can be written as:

$$Y(k) = X(k)S(k,k) + \underbrace{\sum_{m=0,\ m\neq k}^{N-1} X(m)S(m,k)}_{\text{ICI}} + \underbrace{W(k)}_{\text{Noise}}, \quad (3.19)$$

where the received symbol is related to the transmitted symbol in interested the subcarrier with coefficient $S(k,k)$ and also related to the other subcarrier symbols with $S(m,k)$ which can be given as

$$S(m,k) = \frac{1}{N}\sum_{l=0}^{L-1}\sum_{n=0}^{N-1} h(l,n) e^{\frac{j2\pi n(m-k)}{N}} e^{\frac{-j2\pi ml}{N}}. \quad (3.20)$$

Note that if time variation of the channel is negligible, then there will be no ICI.

$$S(m,k) = \begin{cases} H(k) & m = k \\ 0 & m \neq k \end{cases} \quad (3.21)$$

The ICI caused by an aeronautical channel is illustrated in Figure 3.3. Note that ICI power is high even for very small NDFs in the dual Doppler shifts aeronautical channel scenario, compared to the terrestrial two path channel model given in [90].

The exact ICI power (P_{ICI}) in terms of the Doppler spectral density is given as [90]

$$P_{\text{ICI}} = 1 - \int_{-f_{\text{d}}}^{f_{\text{d}}} p_{f_d}(f_d)\text{sinc}^2(\frac{f}{\Delta f})df. \quad (3.22)$$

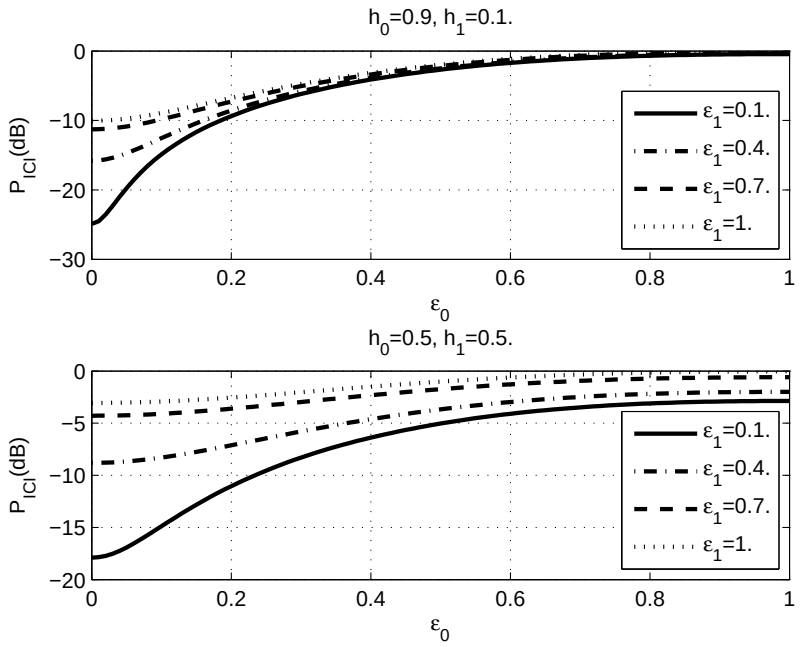

Figure 3.3 ICI Power for Various ϵ_0 and ϵ_1 Values.

Therefore, using (2.9) in (3.22) for the two ray dual shift model, with the modifications described in [70], the ICI power can be given as

$$P_{\text{ICI}} = 1 - \left[(h_0)^2 \text{sinc}^2(\epsilon_0) + (h_1)^2 \text{sinc}^2(\epsilon_1)\right]. \tag{3.23}$$

3.3 Conclusion

In this chapter analytical analysis was done on the effect of a two ray aeronautical channel on the performance of OFDM. The additional energy as shown in Figure 3.1 and Figure 3.3 shows ICI energy bleeding into the neighbor subcarrier due to the Doppler shifts. Therefore, for an OFDM system to function in an aeronautical environment, the impact of the dual Doppler shifts needs to mitigated.

CHAPTER 4

PARAMETRIC DOPPLER ESTIMATION IN AERONAUTICAL ENVIRONMENTS

4.1 Introduction and Motivation

Frequency estimation is broken into two major methods, parametric and non-parametric spectrum estimation. For the OFDM system operating in the aeronautical environment, Doppler frequencies that are fractions of OFDM subcarriers need to be estimated in order to compensate for the effects of ICI. Non-parametric methods, Fourier Transforms (FT), would require a much higher FT size compared to OFDM size in order to estimate dual Doppler shifts smaller than subcarrier spacings. The non-parametric or classical technique estimation starts with estimating the autocorrelation $r_x(k)$ of the signal of interest. The power spectrum is then calculated by taking the Fourier Transform of $r_x(k)$.

$$r_x(k) = \frac{1}{2N+1} \sum_{n=-N}^{N} x(n+k)x^*(n). \tag{4.1}$$

$$P_{\text{NonParametric}}(e^{jw}) = \sum_{k=-N+1}^{N} r_x(k)e^{-jkw}. \tag{4.2}$$

The second technique of non-classical or parametric frequency estimation is based on using the model of the process to estimate the power spectrum or frequency of the signal of interest.

In this chapter, parametric methods to estimate Doppler shifts are used. A parametric method tries to understand the process and extracts the coefficient of the process for spectrum estimation. Typically, parametric models are categorized as autoregressive (AR),

Moving Average (MA), Autoregressive Moving Average (ARMA) and harmonic. In the parametric method, knowing the process of the signal is the key to improving performance. For example, if the signal $x(n)$ is known to be a pth order autoregressive process, then the signal data can be used to estimate the coefficient of the following all-pole model [91].

$$P_{\text{Parametric}}(e^{jw}) = \frac{1}{\left|\sum_{k=0}^{p} a_p(k) e^{-jkw}\right|^2}. \tag{4.3}$$

While one technique relies on the number of sample points, the other relies on the prior knowledge of the signal process for increased estimation and performance. In aeronautical communication, the desire is to estimate the Doppler shifts within the smallest number of OFDM symbols with the resolution required to correct for the OFDM ICI. Transmission of pilot tones, preamble or a tone is ideal for parametric Doppler frequency estimation, since the signal process is known. Thus an appropriate model can be used to estimate the Doppler shifts in the aeronautical channel.

As discussed in prior chapters, the challenge is to estimate the multi-Doppler shifts in the aeronautical channel, particularly the two ray shifts. The combination of the speed and carrier frequency, $f_{d,max}$ for an aircraft can be significantly high and dynamic compared to terrestrial systems. Based on the channel characteristics, the two rays will have different Dopplers. It can be assumed that the LOS Doppler shift will represent a deterministic Doppler shift, that can be tracked and corrected by traditional frequency shift algorithms [69]. The reflected path will depict a random Doppler shift, which can span anywhere between $f_{d,max} to - f_{d,max}$ with a narrow Doppler spread. This will be a second and different Doppler shift. As a worst case, if the direction of the LOS path coincides with the heading of the aircraft resulting in a carrier shift of the LOS path of $f_{d,Los} = f_{d,max}$, the reflected component could come from behind and have the worst case of $f_{d,Ref} = -f_{d,max}$.

For estimation of single Doppler or carrier frequency offset, extensive research has been done in the past. Existing techniques often require transmission of reference OFDM symbols or pilots such that the phase shifts in those symbols can be exploited in a data-aided approach [92]. Various non-data aided or blind approaches, which are in general more effi-

cient in spectrum utilization, have been applied, e.g., exploiting the redundancy in OFDM guard intervals [93]. More recently, another approach to non-data aided blind estimation has been proposed utilizing null carriers and are used in typical OFDM systems [94].

The aeronautical multipath fading channel can be characterized as a linear, time-varying system model [95]. Multipath propagation causes delay spread and time variation of multipath components and cause the Doppler spread in which angle of arrival depicts a different model compared to Jakes model. Time variation and Doppler shift of the channel over the duration of the OFDM symbol will cause intercarrier interference (ICI) in OFDM systems, which degrades the performance, since ICI can be seen as additional near-Gaussian noise [96] [97].

4.2 Parametric Spectral Estimation for Aeronautical Doppler

In OFDM systems, the knowledge of pilot tone or known preamble provide a priori knowledge of the process. Hence, a representative harmonic process based parametric estimation is chosen. In the harmonic parametric model, the frequencies of interest are extracted through a method known as eigendecomposition of the autocorrelation matrix. The autocorrelation matrix is decomposed into two subspaces, the signal subspace and the noise subspace. Assuming a training tone is generated by encoding only one subcarrier with a Binary Phase Shift Keying (BPSK) modulation in a 64 point FFT OFDM system to evaluate the channel characteristics, i.e., $X(k) = 1$ for $k = \rho$ and $X(k) = 0$ for all other k, then,

$$\begin{aligned} x(n) &= IDFT\{X(k)\} \\ &= e^{\frac{j2\pi\rho n}{N}} \quad . \end{aligned} \tag{4.4}$$

This tone is generated to characterize the two ray channel model, given the two ray channel represented by eq. (3.3). Thus the received signal will be

$$\begin{aligned} y(n) &= h_0 e^{\frac{j2\pi n(\epsilon_0+\rho)}{N}} + h_1 e^{\frac{j2\pi(n-\tau)(\epsilon_0+\rho)}{N}} + w(n) \\ &= h_0 e^{jn\omega_0} + h_1 e^{j(n-\tau)\omega_1} + w(n). \end{aligned} \tag{4.5}$$

If the variance of $w(n)$ is σ_w^2, then the autocorrelation function of $y(n)$ will be

$$r_y(k) = |h_0|^2 e^{jk\omega_0} + |h_1|^2 e^{jk\omega_1} + \sigma_\omega^2 \delta(k), \tag{4.6}$$

where ω_i are the Doppler shifted pilot tone frequencies in radians for $i = 1, 2$ and $\omega_i = \frac{2\pi(\epsilon_i+\rho)}{N}$ (details of eq. 4.6 can be found in appendix A). For two ray aeronautical channel, $\omega_1 \neq \omega_2$, their phases are independent, uniformly distributed random variables. Therefore, the expectations of all cross products are zero. The size (MXM) of autocorrelation matrix for $y(n)$ is the sum of the autocorrelation matrix due to the signal $\mathbf{R}_s = (\mathbf{R}_0 + \mathbf{R}_1)$ and the autocorrelation matrix due to noise, $\mathbf{R}_n$. The autocorrelation matrix may be written as $\mathbf{R}_y = \mathbf{R}_0 + \mathbf{R}_1 + \mathbf{R}_n$. Note that if $\mathbf{e}_0$ and $\mathbf{e}_1$ are defined as the eigenvectors i.e., $\mathbf{e}_i = [1,\ e^{j\omega_i},\ e^{j2\omega_i}, \cdots,\ e^{j(M-1)\omega_i}]^T$ then,

$$\mathbf{R}_y = \underbrace{|h_0|^2 \mathbf{e}_0 \mathbf{e}_0^H}_{\mathbf{R}_0} + \underbrace{|h_1|^2 \mathbf{e}_1 \mathbf{e}_1^H}_{\mathbf{R}_1} + \underbrace{\sigma_w^2 \mathbf{I}}_{\mathbf{R}_n}, \tag{4.7}$$

where $\mathbf{R}_s = |h_0|^2 \mathbf{e}_0 \mathbf{e}_0^H + |h_1|^2 \mathbf{e}_1 \mathbf{e}_1^H$ is a rank two matrix representing the component of $\mathbf{R}_y$ that is due to the signal and $\mathbf{R}_n = \sigma_w^2 \mathbf{I}$ is a diagonal matrix that is due to the noise. A more concise way to express this decomposition is to write $\mathbf{R}_y$ as follows:

$$\mathbf{R}_y = \mathbf{E}\mathbf{H}\mathbf{E}^H + \sigma_w^2 \mathbf{I}, \tag{4.8}$$

where $\mathbf{E} = [\mathbf{e}_0 \mathbf{e}_1]$, is an Mx2 matrix containing two signal vectors $\mathbf{e}_0$ and $\mathbf{e}_1$ and $H = \text{diag}\{|h_0|^2, |h_1|^2\}$. Let $\mathbf{v}_i$ and λ_i be the eigenvectors and eigenvalues of $\mathbf{R}_y$ respectively,

with eigenvalues arranged in decreasing order, $\lambda_1 \geq \lambda_2 \geq \ldots \geq \lambda_i$ Since $\mathbf{R}_y = \mathbf{R}_s + \sigma_w^2\mathbf{I}$, then,

$$\lambda_i = \lambda_i^s + \sigma_w^2, \tag{4.9}$$

where λ_i^s are the eigenvalues of $\mathbf{R}_s$. Since the rank of $\mathbf{R}_s$ is equal to two, then $\mathbf{R}_s$ has only two nonzero eigenvalues and both are greater than zero. Therefore, the first two eigenvalues of $\mathbf{R}_y$ are greater than σ_w^2 and the remaining eigenvalues are equal to σ_w^2.

Thus, the eigenvalues and eigenvectors of $\mathbf{R}_y$ may be divided into two groups. The first group has eigenvectors with their respective eigenvalues greater than σ_w^2, i.e., $\mathbf{V}_s = [V_1, V_2, \ldots V_p]$. This set is referred to as signal of interest containing eigenvectors and are in the signal subspace. The second group consists of eigenvectors that have their eigenvalues equal to σ_w^2 and hence the associated vectors are $\mathbf{V}_n = [V_{p+1}, V_{p+2} \ldots V_M]$. They are referred to as noise containing eigenvectors and span the noise subspace. Another way of writing the decomposition $\mathbf{R}_y$ is

$$\mathbf{R}_y = \mathbf{V}_s\mathbf{V}_s^H + \mathbf{V}_n\mathbf{V}_n^H. \tag{4.10}$$

Projecting a vector into either signal or noise subspace can be done by multiplying $\mathbf{V}_s\mathbf{V}_s^H$ and $\mathbf{V}_n\mathbf{V}_n^H$ respectively. In addition, since $\mathbf{R}_y$ is Hermitian, the eigenvectors $\mathbf{v}_i$ form an orthonormal set. Therefore, the signal and noise subspaces are orthogonal. It is possible to extract all the parameters of interest about the transmitted signal from the eigenvalues and eigenvectors of $\mathbf{R}_y$.

In the following sections, three eigendecompensation methods are discussed, with variations in how the signal and noise space vectors are separated and how the ω_i are extracted from the signal. The three methods are: MUltiple Signal Classification (MUSIC), Eigen-Vector method EV and Min Norm (Min Norm) algorithms [98].

4.2.1 MUSIC Method

The MUSIC algorithm assumes white noise of variance σ_w^2. Let $\mathbf{R}_x$ be MxM autocorrelation matrix of x(n) with $M > P + 1$. Then the eigenvalues are arranged in decreasing

order with their corresponding eigenvectors. The eigenvectors are divided into two groups, the p signal eigenvector with the largest eigenvalue, and $M-p$ noise vectors that mostly have eigenvalues equal to σ_w^2. The eigenvector of $\mathbf{R}_x$ will have a length of M, each of the noise subspace eigenfilters will have $M-1$ roots [99].

$$V_i(z) = \frac{1}{\sum_{k=0}^{M-1} v_i(k) z^{-k}}; i = p+1, ..., M. \tag{4.11}$$

P of the roots will lie on the unit circle at the frequencies of the complex exponentials and the eigenspectrum associated with the noise eigenvector $\mathbf{v}_i$ will exhibit sharp peaks at the frequencies of interest. The remaining $(M-p-1)$ roots may lie anywhere and some may cause spurious peaks in the eigenspectrum. However, the MUSIC algorithm takes care of these spurious peaks by means of averaging, as presented in the following equation:

$$P_{MU}(e^{jw}) = \frac{1}{\sum_{i=p+1}^{M} |e^H v_i|^2}. \tag{4.12}$$

For the two ray model, the roots of the MUSIC algorithm can be taken to extract the frequency of interest. The z-transform equivalent of eq.(4.12) is

$$P_{MU}(z) = \frac{1}{\sum_{i=p+1}^{M} V_i(z) V_i^*(\frac{1}{z^*})}. \tag{4.13}$$

Thus, finding the angles of the roots of $P_{\mathrm{MU}}(z)$ will consist of ω_i containing the Doppler shift ϵ_i due to each ray. Finally, subtracting the known transmitted tone, the ϵ_i can be extracted as:

$$\epsilon_i = \frac{N\omega_i}{2\pi} - \rho \ . \tag{4.14}$$

4.2.2 Eigenvector Method

The Eigenvector method estimates the exponential frequencies from the peaks of the eigenspectrum. The Eigenvector method differs from the MUSIC algorithm in that it is based on compensation of each eigenvector with its associated eignevalue and appears to

produce less spurious peaks.

$$P_{EV}(e^{jw}) = \frac{1}{\sum_{i=p+1}^{M} \frac{1}{\lambda_i} |e^H v_i|^2}, \tag{4.15}$$

where λ_i is the eigenvalue associated with each eigenvector $\mathbf{v}_i$. Therefore, the roots of $\mathbf{P}_{EV}$ will help find the Doppler shifts.

4.2.3 Minimum Norm Method

Instead of forming an eigenspectrum that uses all of the noise eigenvectors, the Min Norm algorithm uses a single vector $\mathbf{a}$ that is constrained to lie in the noise subspace.

$$P_{MN}(e^{jw}) = \frac{1}{|e^H a|^2}, \tag{4.16}$$

where $\mathbf{a} = \mathbf{V}_n \mathbf{V}_n \mathbf{v}$ is the projection matrix that projects an arbitrary vector $\mathbf{v}$ onto the subspace. In eq. (4.10), $\mathbf{R}_y$ can be factored into its respective signal and noise subspace.

The z-transform of the coefficients in $\mathbf{a}$ may be factored as follows:

$$A(z) = \sum_{k=0}^{M-1} a(k) z^{-k} = \prod_{k=1}^{p} (1 - e^{jw_k} z^{-1}) \prod_{k=p+1}^{M-1} (1 - z_k z^{-1}) \tag{4.17}$$

where $\mathbf{z}_k$ for k = p+1, ...,M-1 are the spurious roots that do not lie on the unit circle. The problem then is to determine which vector in noise space minimizes the effects of the spurious roots on the peaks of the eigenspectrum. The approach that is used in the minimum norm algorithm is to find the vector $\mathbf{a}$ that satisfies the following three constraints:

1. Vector $\mathbf{a}$ lies in the noise subspace.

2. Vector $\mathbf{a}$ has minimum norm.

3. First element of $\mathbf{a}$ is unity.

The first constraint ensures that the p roots of A(z) lie on the unit circle. The second constraint requires that the spurious roots of A(z) lie inside the unit circle. The third constraint

demands that the minimum norm solution is not the zero vector. Finally, determining the roots of $\mathbf{P}_{mn}$ will consist of the ω_i containing the Doppler ϵ_i caused by the shifts of the two ray aeronautical channels.

4.2.4 Doppler Calculations from Parametric Equations

Based on the above three methods of calculating the ω_i, a generic systematic process can be identified, the steps of which are as follows:

1. Calculate the eigenvalues and eigenvectors of the autocorrelation matrix.

2. Determine the frequency ω_i from the eigenvector associated with the eigenvalue. MUSIC, EV and Min Norm methods each uses a variation of how to use a combination of the eigenvalues and eigenvectors in determining the frequencies.

3. Finally, determine ω_i by finding the angle of the roots of equations (4.12)(4.15)(4.16).

4. Hence, subtract the known transmitted signal to get the Doppler frequencies of interest.

$$\epsilon_i = \frac{N\omega_i}{2\pi} - \rho. \tag{4.18}$$

4.2.5 Parametric Modeling Sensitivity

The parametric Doppler shift estimation is driven by a priori knowledge of the signal process. Depending on the modeling techniques, each of the AR, ARMA, and MA parametric models incur a different modeling error. For example, in AR, the Burg algorithm finds a set of all-pole model parameters that minimizes the sum of the squares of the forward and backward prediction error. In the analysis of sinusoids, the Burg algorithm is prone to spectral splitting, and peak locations are highly dependent upon the phases of the sinusoids. This splitting of a single spectral peak into two or more occurs when the incoming signal is over modeled, i.e., when the modeling order p is too large. If the signal process is known and an appropriate model with a known modeling order is selected, a higher resolution spectrum estimation can be achieved within a short signal length. For the nominal case,

based on Haas [1], the aeronautical channel is based on two ray model and will most likely experience two Doppler shifts. However, there could be a greater or less than two Doppler shifts in the channel in extreme cases. Therefore, in the event that the model parameter is different than the number of Doppler shifts in the channel, this will result in estimation error. Figure 4.1 shows the performance of the MUSIC algorithm in the event that the modeling order is chosen incorrectly. The incorrect model order results in an average of a four percentage error, which will impact the overall system BER performance. Note that, while over modeling shows an improvement in the frequency estimation, due to increase of roots in the all pole model, e.g., $p = 5$ is showing better performance than $p = 3$. There are more Doppler frequencies estimated than the actual number of Doppler shifts in the channel. In the simulation, an error calculations compares the correct frequencies for its calculation. However, in a system application, the receiver will not have this a priori information. This will result in loss of performance due to additional Doppler shifts. In the next chapter, the impact of this modeling error on system BER performance is shown in Figure

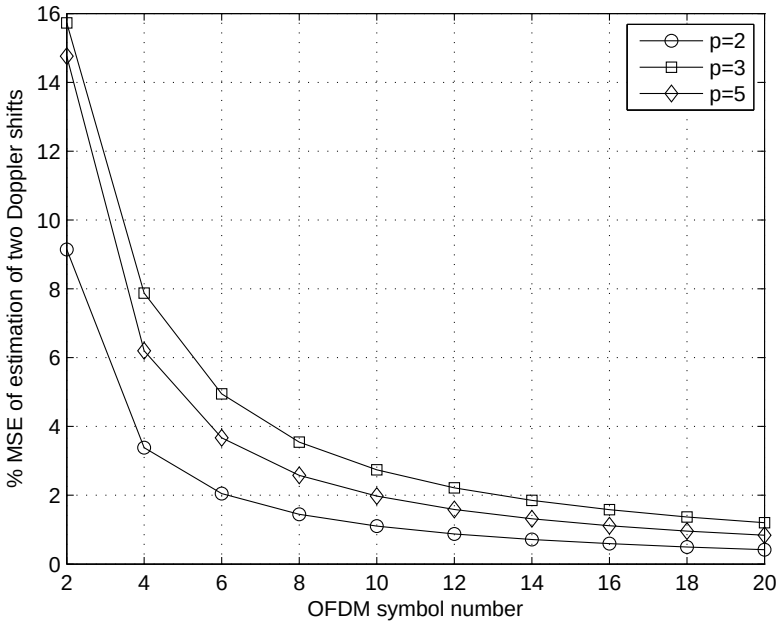

Figure 4.1 Parametric Estimation Modeling Error.

5.7. It is apparent that there is an impact due to incorrect model order selection. Therefore, techniques to estimate modeling parameters, i.e., order, need to be considered [100]. Channel estimation techniques that have the capability to estimate channel multipath or echoes can be used to estimate the model order [101, 102].

4.3 Simulations and Results

MATLAB simulations were performed to evaluate the performance of the three mentioned algorithms (see Table 4.1 for simulation parameters). Simulations were based on a 64-point OFDM symbol with a signal to noise ratio of 20 dB. A dual Doppler shift error ranging from -0.5 to +0.5 subcarrier was randomly introduced to simulate the Doppler caused by the aeronautical channel. An extensive iteration and averaging was done to better estimate the performance. Since parametric algorithms are driven by the size of autocorrelation matrix MxM, a simulation to determine the size of MxM was performed. Figure 4.2 shows the relative performance of the number of OFDM symbols as a function

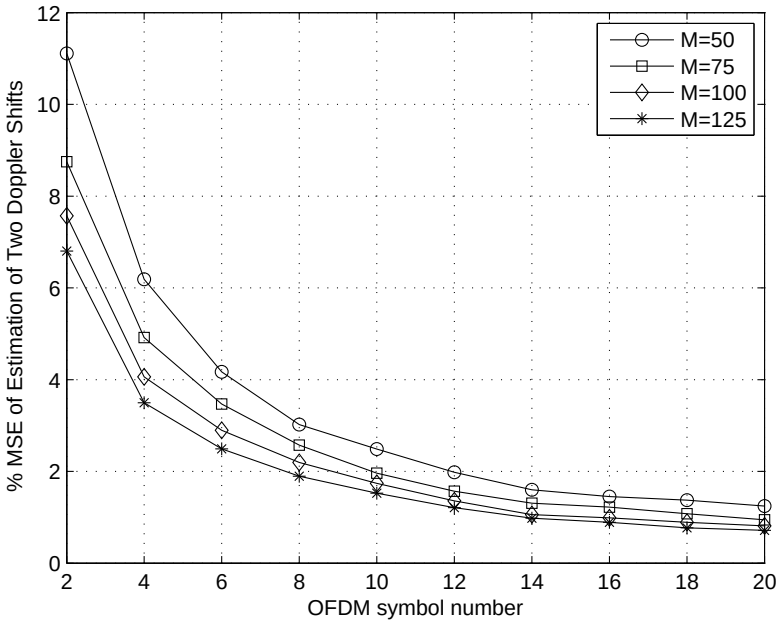

Figure 4.2 Performance of MUSIC Algorithm.

of Mean Square Error (MSE) for different autocorrelation M matrices. The increase in symbols show performance improvement. It also means an increase in delays. However, the increase in autocorrelation matrix M and OFDM symbols is a trade between processing complexity against increasing the delay in the system. Simulation relations clearly show flattening out of performance error at around fourteen OFDM symbols. Hence, between 50 to 125 M, there is only a less than one percent performance improvement.

Next, the MUSIC, EV and Min Norm algorithms were evaluated for relative Doppler shift estimation performance. Figure 4.3 shows the Doppler estimation of the three different parametric algorithms, as a function of OFDM symbols and MSE. Although the performance curve of the three algorithms is relatively close, the Min Norm algorithm shows a slightly better performance based on MSE results.

4.4 Conclusion

In this chapter parametric spectrum estimation was identified as a means to accurately estimate the dual Doppler shifts within the bounds of OFDM ICI improvement. MATLAB simulations using the parametric MUSIC, EV and Min Norm algorithms were evaluated and their performance shows a less than one percent MSE error in estimating the Doppler frequency. The parametric method of Doppler shift estimation exploits the harmonic nature of transmitted OFDM pilot tone or multiple tones to first estimate the harmonic process as a means of autocorrelation matrix. Furthermore, the eigendecompensation of this au-

Table 4.1 Parametric Simulation Parameters.

Parametric Simulation Parameters	
OFDM Symbol (N)	64 Samples in a Symbol
OFDM CP	1/4
Modulation	QPSK
Channel	Two Ray Model
1^{st} and 2^{nd} Ray Angles	Uniform Distr. $\{0, 2\pi\}$
Carrierf_c	1000 Mhz (L-Band)
Parametric Model Order	p
SNR	20 dB
Autocorrelation Matrix	MxM

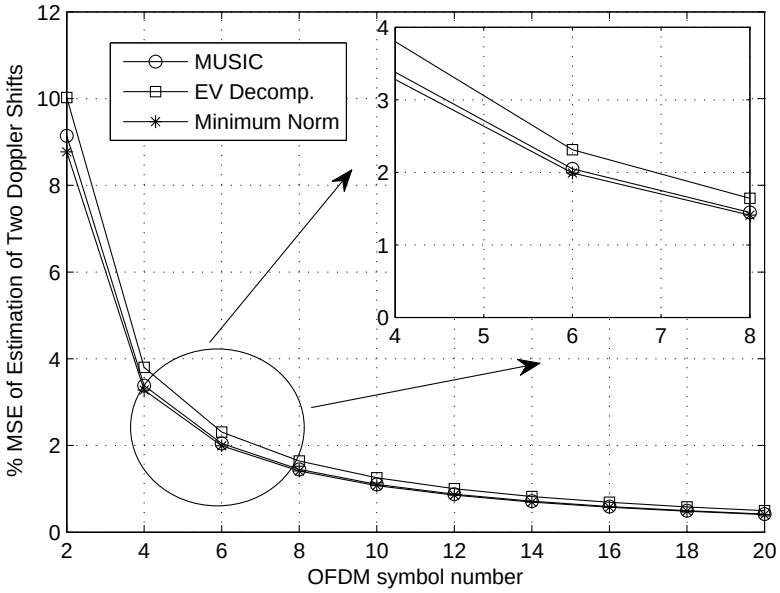

Figure 4.3 Performance of MUSIC, EV and Minimum Norm Algorithms.

tocorrelation is used to estimate the Doppler frequencies. It is evident from simulation results that parametric based dual Doppler shifts can accurately and efficiently estimate the Doppler shifts caused by the aeronautical channel. Further research in the area of exploiting the parametric methodology of learning the process of signals to estimate the Doppler shifts can be expanded to create transmitted signals with a process that is fine tuned to the parametric algorithm at the receiver.

CHAPTER 5

DOPPLER AND ICI MITIGATION USING SMART ANTENNA PROCESSING

5.1 Introduction and Motivation

Spatial filtering, also known as beam forming, is where an array of antenna elements together with signal processing can either block or direct the radiation or reception of signals in the desired signal direction [103]. In essence, relative to an isotropic antenna radiation, which radiates or receives energy in all directions, a smart beam forming focuses the energy or receives the energy in the direction of interest. In the aeronautical channel environment, the direction of arrival can be taken advantage of to mitigate the ICI caused by the dual Doppler shifts in an OFDM based aeronautical system. Chao *et al.* proposed a non-contiguous orthogonal signal division multiplex based technique to mitigate ICI in high speed mobile systems [104]. The focus of this technique was the application of a Non-Contiguous Orthogonal Frequency Division Multiplexing (NC-OFDM) system in a wide band cognitive radio communications, e.g., IEEE 802.22. Jianping *et al.* proposed a delay and Doppler shift joint tracking method based on the extended Kalman filter and zero-force equalization method to cancel ICI [105]. These two techniques were specific in resolving the issues related to the non-uniformed Doppler spread in the wideband aeronautical or high altitude, high speed platforms.

In this chapter, a beam forming method is proposed to separate signals with different Doppler shifts, since in the aeronautical channel environment, even though there is more than one Doppler shift with Doppler spread, they are separate from each other with individual spread. Furthermore, the separated signals can now be combined to improve

the performance. Therefore, diversity techniques are investigated to take advantage of the aeronautical two ray channel for the OFDM system, by first separating the signals, then removing the individual Doppler shifts and finally, combining the two received signals.

Figure 5.1 shows the beam forming concepts that can separate the two signals. Both the direct and the reflected paths have a narrow spread and random Doppler shifts. Assume two Doppler shifts can span anywhere between $f_{d,max}$ to $-f_{d,max}$ [1]. Then the Doppler spectrum for the aeronautical channel can be given as $p_{f_d}(f_d) = \sum_{l=0}^{L-1}(h_l(n))^2\delta(f - f_{Dl})$, where $h_l(n)$, f_{Dl} are defined in eq. (3.2), and $L = 2$. Therefore, in this study the impact of dual Doppler ICI will be investigated as it relates to an aeronautical channel.

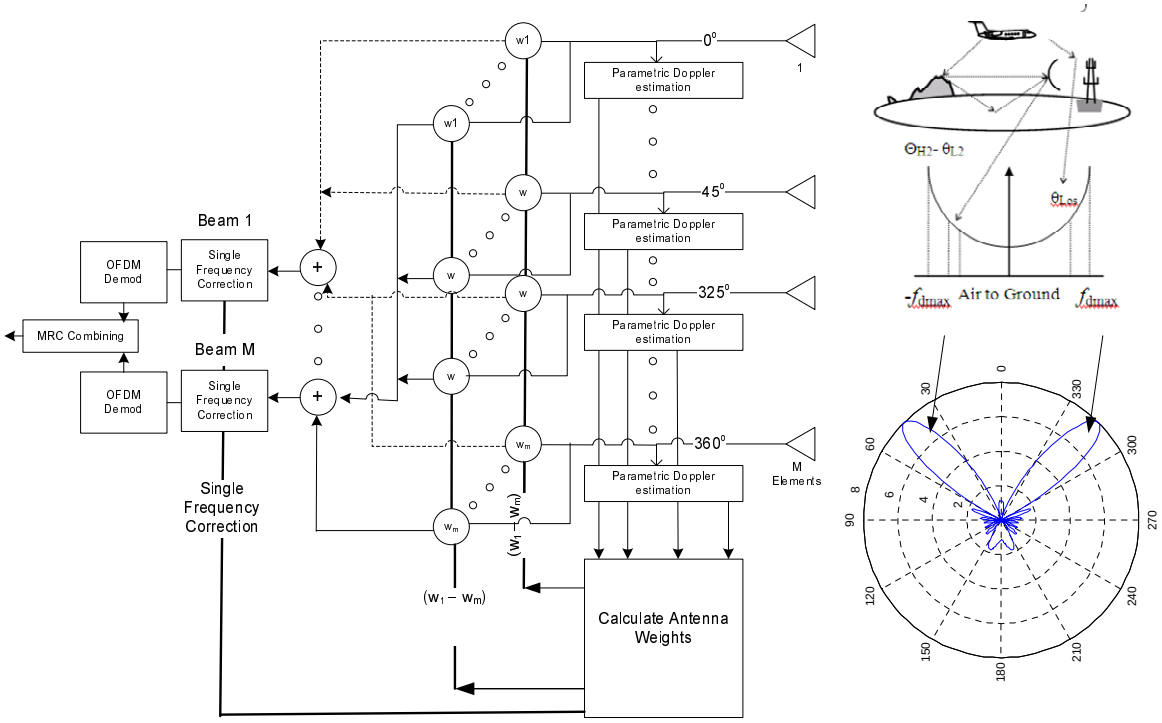

Figure 5.1 Beam Forming Block Diagram.

5.2 Beam Forming Based Signal Separation for Aeronautical Doppler Correction

The ICI of received OFDM signals undergoing dual Doppler shifts or many can be corrected by the use of beam forming to separate the two or multiple arriving signals affected by different Doppler shifts. Once the signals are separated, each signal containing a single Doppler shift can be corrected by conventional means. In the previous chapter, the use of parametric Doppler estimation was shown to estimate the multiple Doppler shifts in an aeronautical channel. By taking advantage of estimated individual shifts, the angle of arrival derives the antenna weight coefficients to separate the signals for individual processing. The received signals are then further combined to improve the receiver performance using diversity combining schemes. Figure 5.2 shows the multi-Doppler receiver block diagram. As shown in Figure 5.2, the received signals are used to estimate the dual Doppler shifts using parametric algorithms, from which an angle of arrival of each signal is estimated. The estimated Doppler shifts are later used to correct for individual Doppler shifts after the signals are separated. This angle of arrival is used to calculate two different sets of antenna beam forming weights, where one set notches out the other signal and allows the signal of interest to pass through and vice versa for the other (see Figure 5.3). Finally, the two received signals are combined using diversity techniques, which improves the performance. Therefore, not only is the impact, due to aeronautical channel, mitigated the received signal performance is improved. Figure 5.3 shows the beam forming under a two ray dual shifts

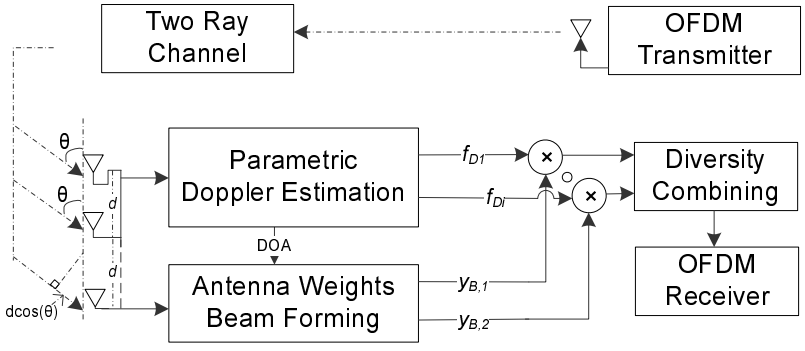

Figure 5.2 Aeronautical Receiver Block Diagram.

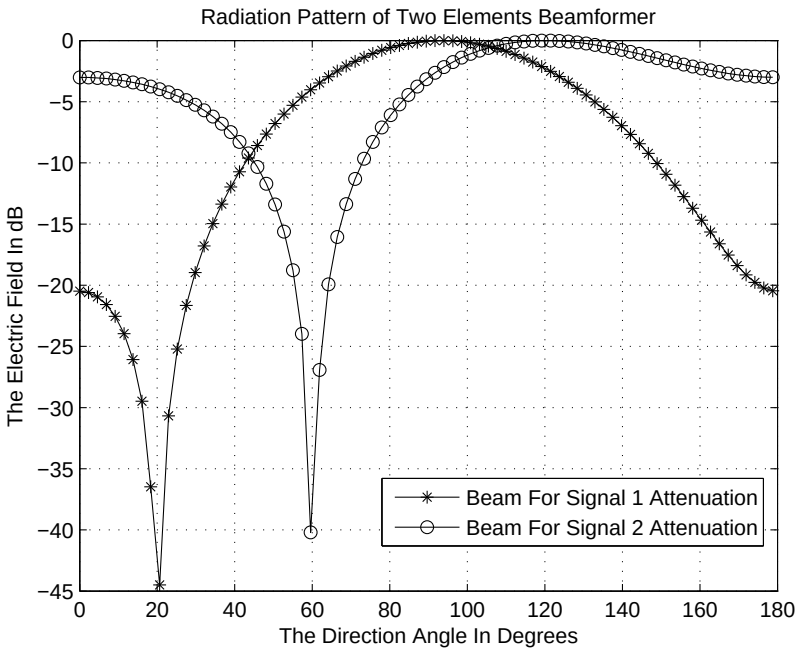

Figure 5.3 Beam Forming Radiation Patterns.

aeronautical channel, where two signals arriving from different angle of arrivals, i.e., 20^o and 60^o, are notched out by using separate beam forming antenna weights. This is due to the aeronautical channel and can be taken advantage of by first separating the signal and then adding them with diversity combining techniques. Figure 5.4 shows the example where a two antenna array is used to separate arriving OFDM signals corrupted by the aeronautical two ray channel condition. The transmitted OFDM constellation, shown in Figure 5.4(a), passes through the aeronautical channel and is corrupted, as shown in Figure 5.4(b). The received signal processed by the antenna array is shown in Figure 5.4(c) and Figure 5.4(d), which are the separated two signals. Figure 5.5 shows the case when the signal is processed by a four array antenna. Hence, by increasing the number of antenna elements, there is an increase in performance, since narrower beams can be created to separate the signals.

In an array of antenna sensors, if the signal arriving at the sensors are θ and each of the M sensors are d distance apart, then the received signal adjacent to the sensor travels a difference of $\frac{f_c}{c} d \cos(\theta)$, where f_c is the signal carrier frequency and c is the propagation

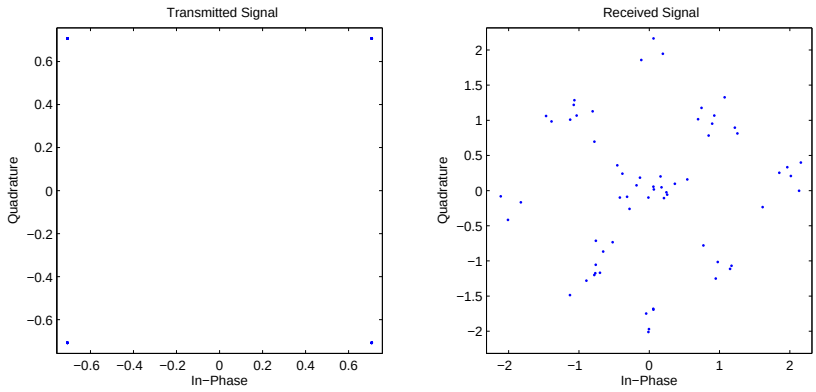

(a) Transmitted OFDM Signal Constellation.

(b) Received OFDM Signal Constellation.

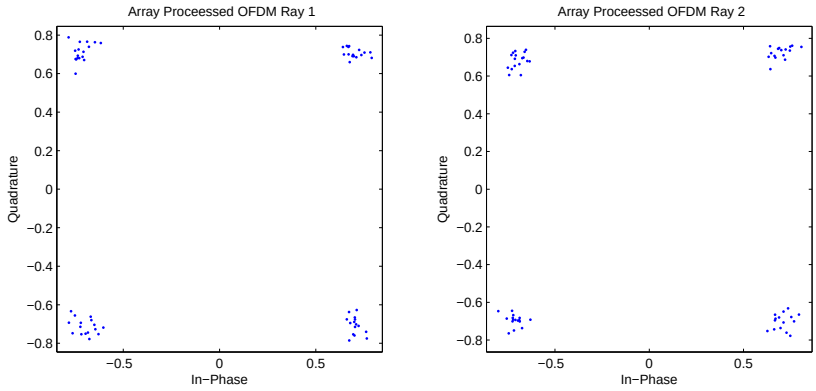

(c) Received Antenna Array Processed OFDM Ray 1 Constellation.

(d) Received Antenna Array Processed OFDM Ray 2 Constellation.

Figure 5.4 Two Antenna Array Signals of Transmitted and Received Constellation.

speed. Therefore, the phase difference between two elements is $-m\frac{f_c}{c}d\ \cos(\theta)$, where md is the distance between the two neighboring sensor elements [106]. For each of the sensor elements, assume it multiplied by a weighting factor, i.e., w_n. Therefore, the received signal $y(n)$ at m^{th} sensor element will be

$$y_m(n) = y(n)e^{jm\frac{fc}{c}d\ \cos(\theta)}\ , \tag{5.1}$$

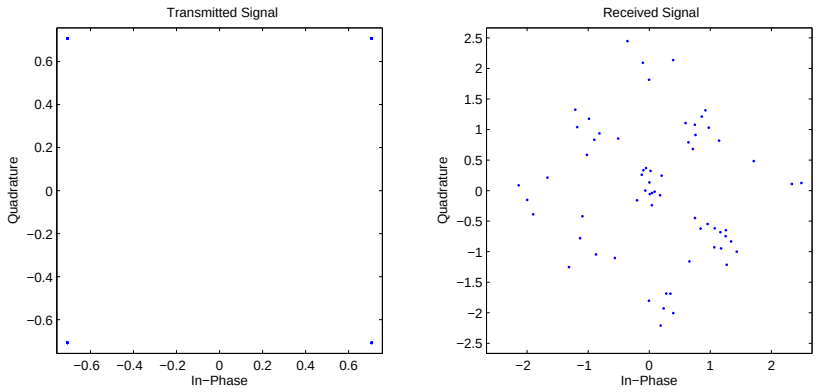

(a) Transmitted OFDM Signal Constellation.

(b) Received OFDM Signal Constellation.

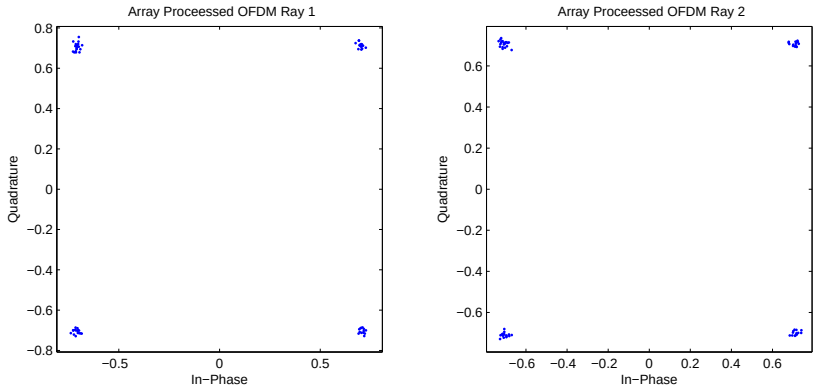

(c) Received Antenna Array Processed OFDM Ray 1 Constellation.

(d) Received Antenna Array Processed OFDM Ray 2 Constellation.

Figure 5.5 Four Antenna Array Signals of Transmitted and Received Constellation.

since the signal $y(n)$ will experience the antenna array factor due to the geometry of the sensors at reception. Hence, the beam formed received signal for l^{th} path will be

$$y_{\text{B},l}(n) = \sum_{m=0}^{M-1} y_m(n) w_{m,l}(n) \ , \ l = 0, 1, ..., L-1 \ , \tag{5.2}$$

where $y_{\text{B},l}(n)$ is the outcome of the signal spatially processed through $w_{m,l}$ weights of M sensor elements for L arriving paths. Therefore, the L rays of signals arriving at the antenna arrays will have unique angles of arrivals θ_l. Hence, if the angles are known, the respective

array weights can be calculated as

$$w_{m,l} = e^{jm\frac{f_c}{c}d\ \cos(\theta_l)}. \tag{5.3}$$

Each l signal will have its associated array weight, $w_{m,l}$, based on the direction of arrival. Given that the various Doppler frequencies are estimated with eq. (4.14), and the knowledge of the speed of the mobile platform known, the arriving angle of different signals can be calculated as

$$\theta_l = \cos^{-1}\left(\frac{f_{\mathrm{D}_l}\lambda}{v}\right). \tag{5.4}$$

For multi-beam forming to separate signals, each arriving angle will be used to generate different array weights using eq. (5.3). For an aeronautical two ray channel there will be two, $L = 2$, arriving signals with different angles of arrival [1]. In one particular case of signals arriving from angle 20^o and 60^o, two beams forming weights were generated. Figure 5.3 shows the radiation pattern for the respective angles of arrival with two antenna elements. Note that the beam for signal one with 20^o will attenuate the signal, allowing the other signal from 60^o to pass through. Similarly, beam two will attenuate the 60^o signal. Thus for the aeronautical two ray channel, there will two such spatially processed signals, $y_{\mathrm{B},0}(n)$ and $y_{\mathrm{B},1}(n)$. The signals are then combined to improve the performance. In this dissertation, Maximal Ratio Combining (MRC) and Selective Combining (SC) [107] were selected for investigation in the upcoming subsection.

5.3 Diversity Combining

Each of the beam formed signals, l, based on the two ray channel fading statistics, will experience fading. This may result in the loss of the transmitted signal. This loss can be reduced by combining the different beams formed from the aeronautical signal. The process of combining these signals, with independent fading statistics, to reduce large attenuation of the desired signal, is referred to as diversity combining. While there are multiple techniques, Selective Combining (SC) and Maximum Ration Combining (MRC) were evaluated. These

two serve as the boundary conditions of diversity combining techniques from simple to complex. All others are variations that fall within this boundary.

5.3.1 Selection Combining

In selection combining, the signal with the highest signal power is selected for further processing [108]

$$Dw_l = \begin{cases} 1 & \text{if } l = l_0 \\ 0 & \text{o/w} \end{cases}, \tag{5.5}$$

where l_0 denotes the selected branch and Dw_l is the weight for each branch. The branch with the highest signal to noise ratio is selected. Thus, for the aeronautical channel the SC equation will be:

$$y_{\text{SC}}(n) = y_{\text{B},0}(n) Dw_0 e^{\frac{j2\pi\epsilon_0 n}{N}} + y_{\text{B},1}(n) Dw_1 e^{\frac{j2\pi\epsilon_1 n}{N}}. \tag{5.6}$$

5.3.2 Maximum Ratio Combining

In maximal ratio combining, the beam formed aeronautical signals are co-phased and the gain on each branch is set equal to the signal amplitude to the mean noise ratio [109]. MRC diversity combining branch weights are given by

$$Dw_l = a_l e^{j\theta_l}, l = 0, 1, ..., L-1. \tag{5.7}$$

With $a_l = \frac{E[y_{\text{B},l}(n)]}{N_0}$, $E[y_{\text{B},l}(n)]$ and N_0 denotes the mean signal in the l^{th} branch and noise power. When the mean noise power in all branches is identical, the gain on each branch becomes proportional to the signal amplitude. Hence, the MRC output can be given as was in eq. (5.6). Figure 5.6 shows the diversity combining BER performance for SC and MRC.

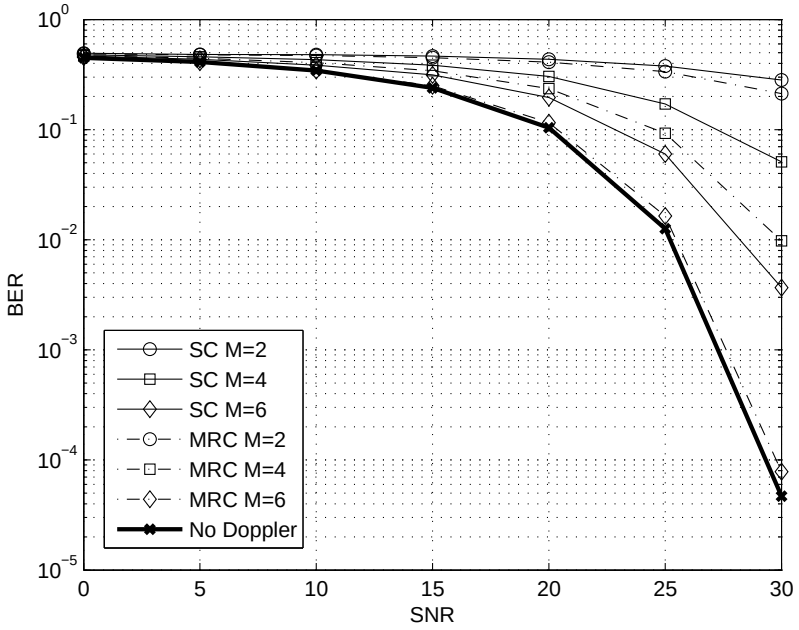

Figure 5.6 BER Performance of Beam Forming Signal Separation and Diversity Combining vs SNR.

5.4 Simulations and Results

Simulations are performed based on a 64-point OFDM system (see Table 5.1 for parameters details). An OFDM signal is transmitted and the receiver sees a corrupted signal due to the addition of two different Doppler shifted signals. Based on the angles, the beam forming coefficients are generated for the spatial processing of the received signals.

Table 5.1 Simulation Parameters.

Simulation Parameters	
OFDM Symbol (N)	64
OFDM CP	1/4
Modulation	QPSK
Channel	Two Ray Model
1^{st} and 2^{nd} Ray Angles	Uniform Distr. $\{0, 2\pi\}$
Carrier f_c	1000 Mhz (L-Band)
Sensor Separation	0.3m

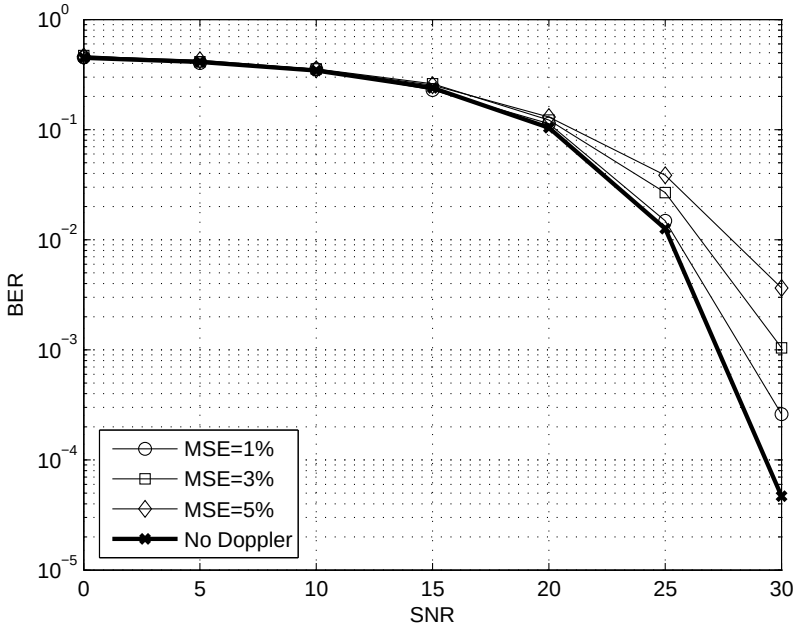

Figure 5.7 BER Performance with DOA Estimation Error vs SNR.

The signals are separated using beam forming for M sensor arrays, as was described earlier. Figure 5.6 shows the Bit Error Rate (BER) performance for a two ray channel condition with random Doppler shifts. There is a significant increase in performance, as the number of antenna elements are increased. In addition, when the separated two signals are combined using MRC and SC, there is an increase in performance using MRC combining. There is a 4 dB performance increase with MRC combining. Another simulation was run to estimate the BER performance with respect to the direction of angle estimation error, as shown in Figure 4.1. Figure 5.7 shows the respective performance for one to five percentage MSE error. Therefore it shows BER performance loss due to estimation error. The problem of OFDM signals impacted due to multiple Doppler shifts can be compensated for by the use of beam forming to separate the arriving signals. The performance loss due to DOA estimation error can easily be improved with diversity combining the multiple signals.

5.5 Conclusions

In this chapter, beam forming method was presented to take advantage of two ray channel characteristics. This novel application is especially useful for the aeronautical case and simulation results show it is an enabling technique to facilitate the use OFDM in high mobile platforms. This technique separates the received corrupted signal based on DOA at the array of antennas. The separated signals are first corrected for single Doppler shifts and then combined using diversity combining SC and MRC techniques to improve the system BER performance. Further study in the area of the joint recursive estimation of dual Doppler frequency shifts, using less sequence information, has potential for future work. In addition, a joint estimation of Doppler shift and correction for the aeronautical system could simplify the receiver algorithm.

CHAPTER 6

COGNITIVE AERONAUTICAL COMMUNICATION SYSTEM

6.1 Introduction

Wireless connectivity has progressed significantly in the last few decades in providing reliable and bandwidth efficient data connectivity. Given the limited resource in multi-dimensional electro-space, i.e. time, frequency, space, polarization, modulation and orthogonal signalization, an increase in data rate can be achieved through multi-dimensional resource efficiency. To achieve higher spectral density, higher signal energy over noise (Eb/No) is required [110, 111]. In the past few decades, the increased time spent in the air by higher numbers of users is creating a demand for data [9, 112]. In addition, the aircraft can be used as a relay. Therefore, aircraft based Aeronautical Data Networks (ADN) for future wireless communication structure is increasingly being discussed by NASA, FAA, EU, etc. A key enabler would be a robust physical layer. From the networking point of view, there are a couple of studies where in-flight Internet with both aeronautical ad-hoc networking and centralized manner strategies are discussed [6, 8]. The global movement of the aeronautical system can take advantage of emerging wireless services and standards. This chapter explores the concept for a Cognitive Aeronautical Software Defined Radio (CASDR).

6.2 Motivation and Challenges

The ever-changing geographical environments of an aircraft and an increasing availability of different wireless services makes one wonder, what if such services can be accessed in real time. This motivation has led to the development of a concept system and hardware that would accommodate to rapid changes, from not just aircraft location, but also from

the growth of services and industry evolution. Figure 6.1 depicts the notional framework of opportunistic wireless data service that may be available for an aircraft. At higher altitudes, the services may be more traditional and fixed; however, on the ground, the growing WiMAX and local area network services may be available to the aircraft. The high speed mobility of an aircraft adds additional challenges to the design of a system physical layer, such as path loss and multi-Doppler spread and shifts [40].

6.3 Literature Review

The desire for a universal and a reconfigurable terminal first appeared in military publications. The need for mobility and accessibility has been the driving requirement. One of the early concepts was a reconfigurable system called "SPEAKeasy" [113]. The Software Communications Architecture (SCA) developed by the Joint Tactical Radio System (JTRS) program of the U.S. Department of Defense (DoD) further fueled the growth of SDR [114]. JTRS aims to provide a family of digital, programmable, multiband, multimode, modular

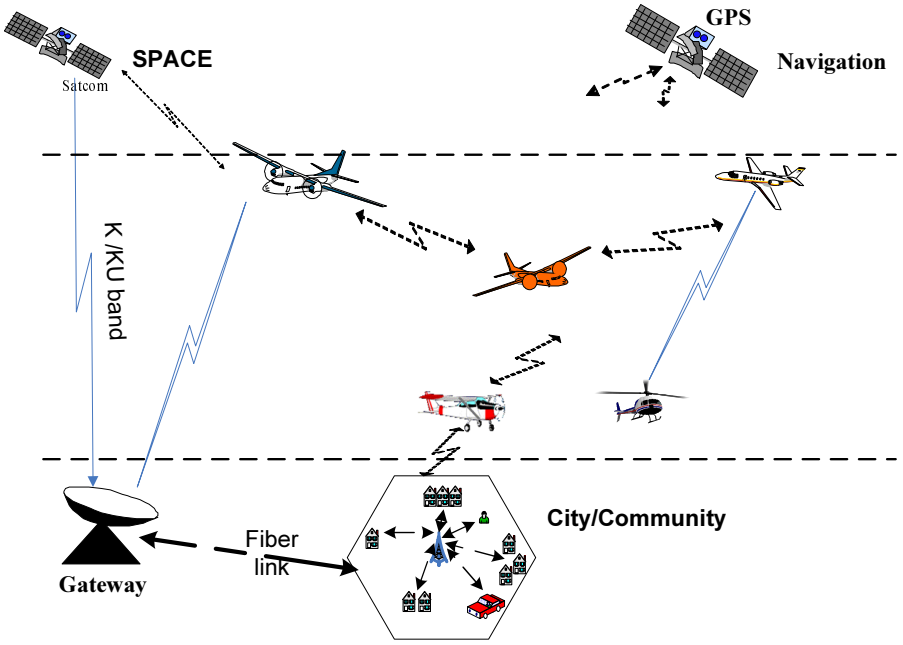

Figure 6.1 Aeronautical Data Network.

radios to alleviate communication interoperability problems. Finally, with the work by J. Mitola [115], there is now a growing interest in reconfigurable terminals.

The increase in air traffic is resulting in the desire for high speed commercial airborne communication [116]. Aircell and AeroSat have developed ground based hardware and now offer in flight Internet services. Aircell uses a concept of an air-to-ground link and provides the in-flight Internet service called 'GOGO' on aircraft [117]. GOGO service works off cellular phone base stations in the continental US, which act as access points for en route flights. On a recent flight taken from Tampa, Florida to Detroit, Ohio, a user using GOGO service, experienced an average upload speed of 0.27 Mbits/s and an average download speed of 0.33 Mbits/s with the latency of 233ms. These ground based services are limited to flights over land only. For oceanic flights, satellite based connectivity is required. AeroSat developed satellite communication (SATCOM) Ku band for commercial airliners [118]. This offers broad connectivity; however, the cost and data throughput of satellite based service is not conducive to user demand.

The growth in Software Defined Radio (SDR) has been enabled by advances in the semiconductor, which has led to the development of the programmable multi-core General Purpose Processor (GPP), Digital Signal Processor (DSP), Field Programmable Gate Array (FPGA) and high speed Analog to Digital Converter (ADC). GPP, DSPs and FPGAs provide the programmability and processing capability to realize such systems. Hence, the processing chain starting from digital Intermediate Frequency (IF) down to demodulation can be implemented in digital signal processing [119, 120]. Another key enabler is the high speed ADC that bridges the analog and digital world [121, 122]. Advanced algorithms that require intense processing can now be implemented in moderate size, weight and power processing engines. FPGAs, with their ability to parallelize, can be used to implement intense processing algorithms on programmable hardware that may be difficult to implement on a DSP or GPP. Therefore, the maturity of SDR algorithms, high bandwidth processing engines, development of tunable antenna and the availability of high speed ADC makes the implementation of CASDR a possibility. The global mobility of an aeronautical platform

is the ideal implementation of a CASDR concept. A CASDR will learn and configure itself in order to provide multi standard/service modems as it traverses continents, countries and cities [123].

6.4 Aeronautical System

The scope of the CASDR system would be to provide an intelligent configurable radio system, and connectivity for the changing geographical, political and regulatory environments that an aircraft experiences. Such a system will take advantage of opportunistic services available today and planned in the future. The communication design is beginning to converge on standard building blocks, or systems, which form the basic building blocks of communication systems, such as Read Solomon, Turbo Encoder, Modulations, and Viterbi. Whether a communication link is being developed for short range, long range, line of sight or non line of sight the basic building blocks of communication systems are the same. If available in software, they can be stitched together to build a radio transceiver. Aeronautical Networks (AN) could be an important application of such systems, since different regions or countries assign different frequency bands based on their needs and spectrum allocation policies.

Aeronautical network geometric relations are observed between an aircraft station (AS) or an aircraft's altitude (h1) with a Ground Station (GS). The LOS communication distance, without considering Fresnel and other parameters, from AS to GS can be calculated using the Pythagoras' theorem, as follows:

$$d_1 = (h_1 \cdot (2R + h_1))^{0.5} \cong (2Rh_1)^{0.5}, \tag{6.1}$$

where R is the radius of the Earth (which varies from 6336 km to 6399 km, but assumed to be 6370 km, for the purpose of calculations). For distances between the two nodes above sea level, the above formula needs additional steps for calculating the communication dis-

tance. The formula is calibrated by a statistically measured parameter by the International Telecommunication Union (ITU), i.e., 'k'.

$$d_1 \cong (2Rh_1)^{0.5} \tag{6.2}$$

Figure 6.2 shows the maximum communication distances that can be achieved between AS and AS/GS for LOS communication. The jump in the first 2 km altitudes for GS communications can be considered a very low orbit AS, which can reach a communication distance of $D = 120$ km. Commercial planes flying at the altitude of 9 km can potentially create communication zones about $D = 250$ km with a conservative approach with k =0.5 factor. On the other hand, considering the communication distance between two ASs, it can be inferred that it could reach up to $D = 480$ km, with k=1/2.

Figure 6.3 shows that ASs could be used as a back haul or relay for wireless infrastructures, since they have the capability of communicating long distances as compared to

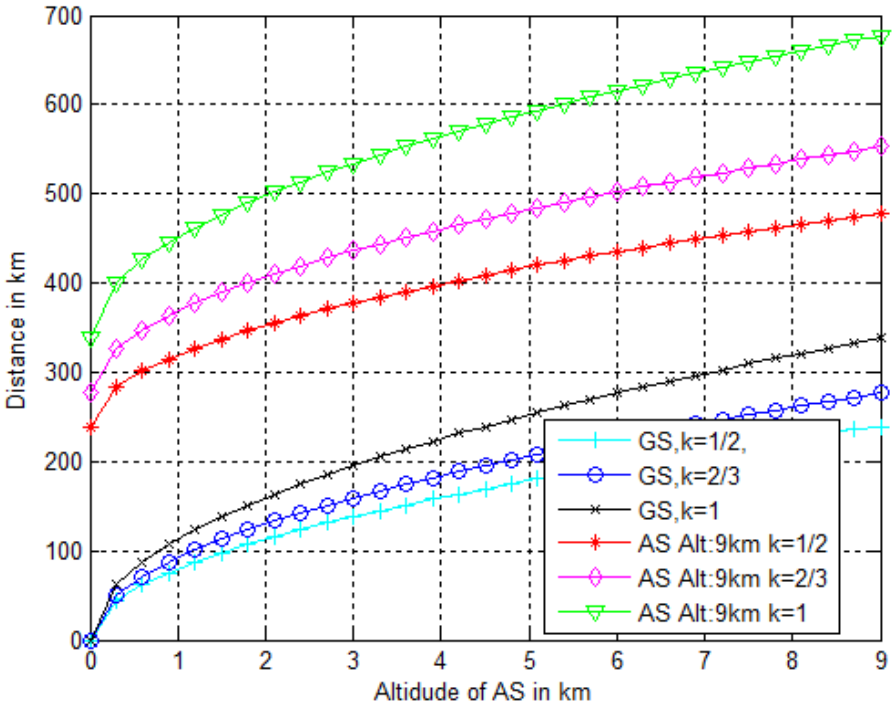

Figure 6.2 Communication Distances for AS.

wireless ground back hauls. Aeronautical Network (AN) will have a substantial lower round trip delay, which will allow for a low delay telephone and voice over IP services.

6.4.1 Aeronautical Network Scenarios and Data Access

Aeronautical networks can provide critical services for various situations, such as public safety communications, Denial of Service (DoS), disaster situations, and in-flight Internet, as well as mobile communication on the ground, and providing services for highways, trains, etc. The network structure proposed in this chapter is as follows: given a particular region to be covered, initially Service Gateway Ground Stations (SGGS) could be built according to the communication distance. Assuming that a GS can communicate to an AS within the distance of 200 km, roughly 8 SGGS will be able to provide service for an area of 1600 km by 800 km.

Data access in an AN can be defined as follows: when a GS or AS has data to send, the flow of the data should be from SGGS, so the connection with other networks such as the Public Switched Telephone Network (PSTN), cellular networks and Internet Protocol (IP) could be established. To provide in-flight services, a centralized configured network should be considered. SGGSs acts like Base Stations (BS), covering a particular region where Subscriber Stations (SS) are simply ASs. Scheduling is done by the SGGS and in this

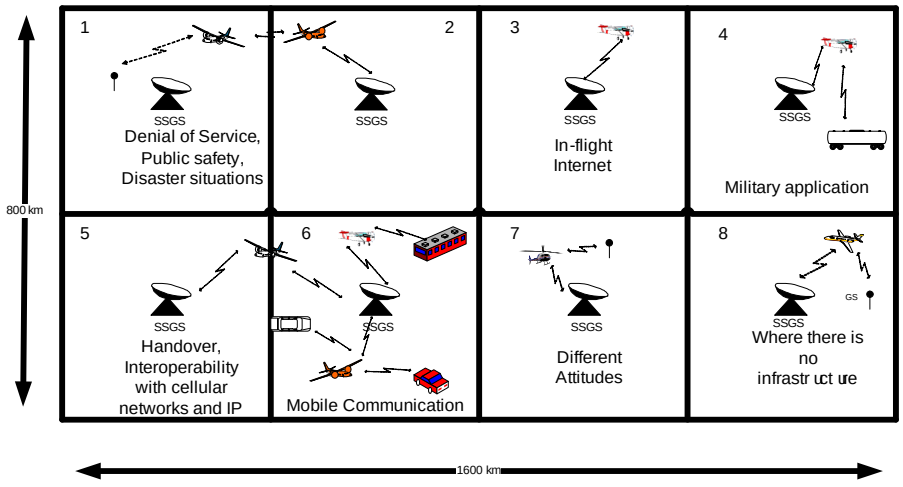

Figure 6.3 Aeronautical Network Scenarios.

structure, ASs are not communicating with each other, except with SSGSs. However, if an AS is not able to register to a SGGS, which could be the case with oceanic flights, then data of that particular AS should be routed to an AS which is already registered to a SGGS with ad-hoc networking strategies. For an aeronautical network, the use of AS as a base station used for cellular network is also discussed. In this case, SSs are the GSs, which can be fixed or mobile. When a GS has data to send, it sends its data to an AS. This can be considered as a relay, reflecting the data to its associated SGGS to finalize the establishment. This structure is feasible to provide public safety services in disaster scenarios, provide a backhaul option for terrestrial networks, and military communication applications. Moreover, in this structure, since both ASs and GSs are not fixed, the handover of a GS between multiple AS is also another challenging issue. It is important to note that the handover process in this structure is somehow different, since GSs are doing handovers not only because of their own mobility, but also due to the mobility of ASs. One of the main issues in ANs is the topology estimation. Since there are many mobile stations, in terms of GS and AS, the scheduling and routing of data would differentiate from time to time. In these cases the topology estimation of the network should be done properly, so that the data can be routed and scheduled in mesh and centralized network strategies, respectively.

The focus of this dissertation is on enabling the physical layer for the aeronautical environment. Therefore, the higher layers' design and analysis is left for system designers and future researchers.

6.5 Physical Layer

An aeronautical environment poses a daunting task to cover a huge area for any system designer. Global channel characteristics need to be understood to establish regional specific model parameters. Generally this leans toward statistical average and results in system parameters to accommodate different environments. The desire is to have the capability to fine tune parameters based on the environment, especially in the case of aeronautical channel environments. The current system based on the 'GOGO' service, uses a ground

based link and provides limited data rates. A data connectivity sample was taken, when I flew Delta flight from Tampa, Florida to Detroit, Ohio, using 'Speed test' [124]. Different global servers were pinged periodically during the flight to measure download, upload and latency. Figures 6.4 and 6.5 are the global data rates and the latency experienced during the flight. The data rates peaked at 0.7 Mbits/s, with an average of 0.3 Mbits/s. The latency averaged around 300 ms, peaking at 800 ms for distant locations.

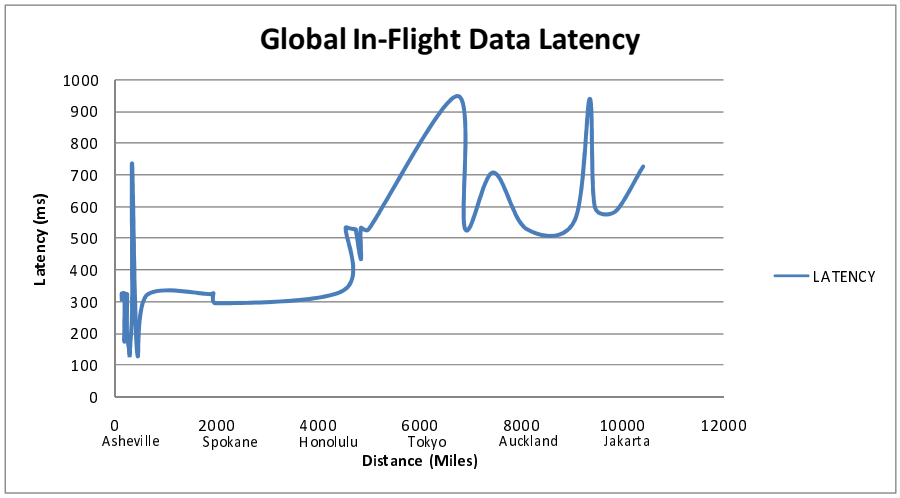

Figure 6.4 Global In-Flight Latency.

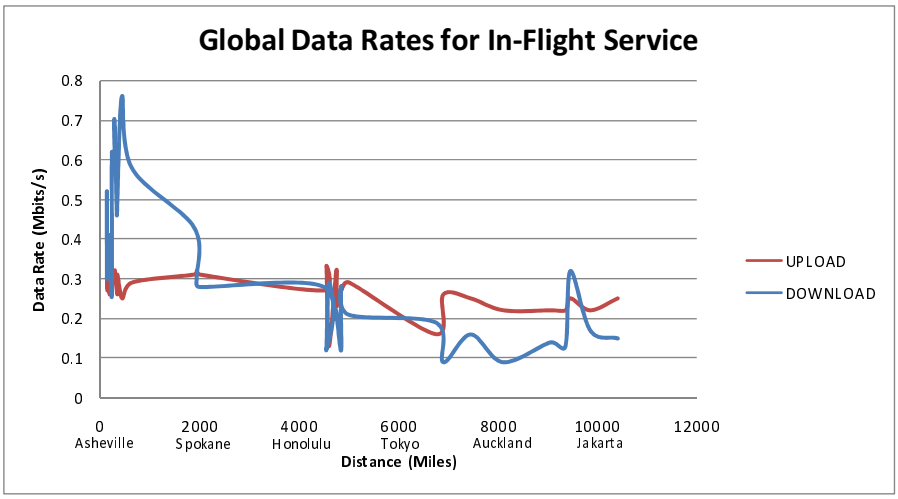

Figure 6.5 Global In-Flight Data Rates.

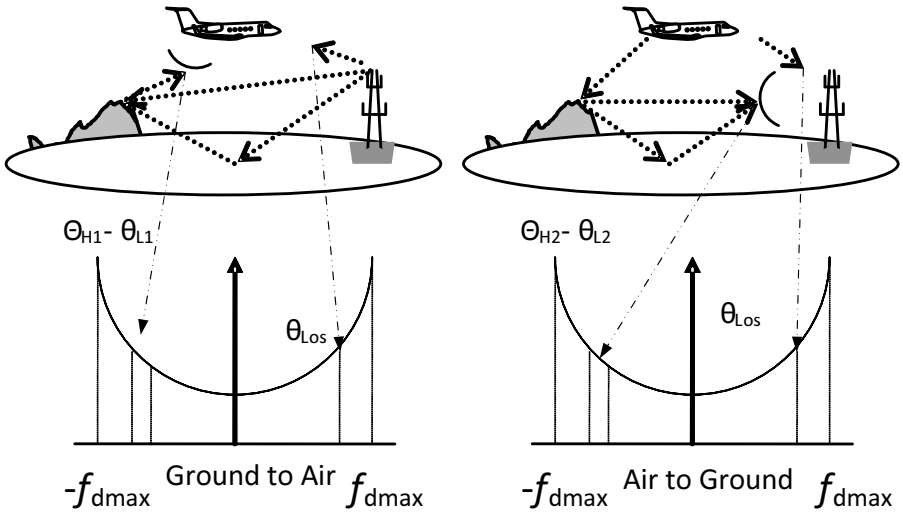

Figure 6.6 Aeronautical Doppler Spread.

Most of the current system assumes a LOS channel condition and uses it as a basis for radio design parameters. This is also the case for the aeronautical platform connectivity modeling. However, an intelligent CASDR will allow for the ability to configure the system and learn the channel conditions over the flight route and establish a history, hence establish accurate channel parameters for a given location, altitude and speed. Since aircraft traverse pre-planned routes, over time these channel parameters will provide accurate characteristics [125]. This will allow higher order spectral efficient modulations and a multi-carrier system to be used and provide higher data throughput. Details of this cognitive channel sensing behavior are discussed later in this chapter.

Figure 6.6 shows air-to-ground and ground-to-air aeronautical communications in an en route scenario and their corresponding Doppler spectrum. The arrival/take off, taxi and parking scenarios depict different multipath and received angle spreads [126]. These different scenarios have different channel parameters. Therefore, in a cognitive system, a cognitive channel system is needed to dynamically learn the channel and tune the radio parameters accordingly.

6.5.1 Cognitive Route Based Physical Layer Estimates

The aircraft routes driven by the FAA for various segments are ideal to establish a history of wireless channel conditions for a route. Once a route is traversed, its history of channel impairments is stored with associated coordinates and aircraft altitude information. This data is downloaded to a central database to be shared with another aircraft. For new routes, the cognitive channel estimator will try to understand the channel condition. Over time, the channel history collected from different aircraft will create a channel map for each route. This data collected by each airline can be stored and shared in a centralized location. The CASDR for each aircraft will then be able to download this data prior to a flight and adjust the physical layer parameters for the route. For a mobile platform that has a predetermined route, such as AN, the channel estimation is broken down to static and dynamic components. The static components affecting the channel would be large objects such as, mountains and buildings. The averaging over multiple routes will provide stable static channel estimates. The dynamic components will be due to time varying objects.

6.6 Aeronautical Software Defined Radio

The advances in components and signal processing techniques are the leading enabler for a configurable hardware and intelligent software. Software defined radio emerges from the desire of single radio hardware that molds its feature to different radio schemes [122]. The artificial intelligence needed for the smarts of such configurable hardware is emerging into what is known as cognitive radio [127].

Cognitive algorithms combined with configurable hardware can take full advantage of the varying location of an aircraft and take advantage of the opportunistic spectrum for network connectivity. A system with the ability to morph itself to accommodate for aeronautical changing environments, and channel conditions across domestic and international boundaries, is required. Cognitive Aeronautical Software Defined Radio (CASDR) platform will also allow the flexibility to comply with countries' regulations governing the spectrum usage and interference.

6.6.1 Spectrum Coverage

The large spectrum use and frequency band allocation for different systems is one of the challenges to overcome for truly building a CASDR, capable of accommodating itself for different regions. The bigger the band, a CASDR will require wider front end filters and high bandwidth A/Ds. For a given region or country, the standard may be the same, but the frequency band may be different. For example, the 802.16 specification applies across a wide range of radio frequency spectrum. WiMAX could function on any various frequency, e.g., 2.5 GHz is predominantly being used in the U.S., 2.3 GHz is used in Asia, and some countries are using 3.5 GHz. The Analog TV band (700 MHz) may become available for WiMAX usage, but currently it is being used for digital TV. Different countries might choose to use the spectrum that best suits their needs. Table 6.1 lists opportunistic frequency data networks available for CASDR [128]. Therefore, the dynamic availability and spectrum allocation in different countries can be taken advantage of by a CASDR system to provide optimum data connectivity.

Table 6.1 Standard's Frequency Bands.

Band (GHz)	BW (MHz)	Standard	Region	Service
2.4	20	802.11b/g	US	Wi-Fi
5	20	802.11a	US	Wi-Fi
2.5	20	802.16	US	Fixed WiMAX
3.5,2.5	20	802.16a	Can	Fixed WiMAX
2.3	20	802.16e	Aus	Fixed WiMAX
1.616 -1.6265	10.5	Custom	Global	Iridium Down Link
19.4 -19.6	20	Custom	Global	Iridium Up Link
2,4		Sirius/XM	US	QPSK, OFDM
1.9, 0.85	1.23, 5	W/CDMA	US	3G Cellular
1.8, 0.9	1.23, 5	W/CDMA	EU	3G Cellular
0.5 - 0.8	n/a	n/a		Analog TV

Another feature that will be necessary in a CASDR application is a tunable RF front end. Frequencies and bandwidth allocations for future wireless communication studies for aeronautical communications are managed at the World Radio communication Conference (WRC). This international body maintains and agrees to abide by the use of spectrum

by international treaty. Aeronautical Mobile (Route) Service (AM(R)S) communication is defined as a safety system requiring high reliability and rapid response. Safety and security applications with Air Traffic Control (ATC) and Air Traffic Management (ATM) communications are considered to be AM(R)S. To accommodate the future growth of aeronautical communication, new band allocations are being made in AM(R)S rather than the VHF band currently used, and L band (960-1164 MHz) and C band (5091-5150 MHz) allocations are now discussed in the meeting. L band is suggested as a suitable band for future aeronautical communication studies. C band is considered to be used in airport surface network systems, since it is thought to be useful for short range, high data throughput.

6.6.2 Critical System Parameters

A cognitive radio system will require optimization of system performance. Algorithms capable of real time optimizing system performance, as well as pre/post flight, will create pre-flight configuration (see Table 6.2). These parameters will be stored for different flight segments and serve as a means to configure the CASDR. The CASDR system will update these parameters as necessary. Over time these parameters will converge to a statistical mean and provide robust radio parameters that a CASDR will configure itself to, while it flies through a particular route.

6.7 Aeronautical Cognitive Radio

The term cognitive comes from psychology meaning "brains," the ability to learn and understand. The aeronautical environment is an ideal application for an intelligent radio which is capable of learning the environment for various locations, routes and altitudes. Over time, each aircraft flying over a certain route will store the data on board storage devices. This data will contain the route the aircraft traversed, the opportunist wireless links available, frequency band, bandwidth, data rate, wireless standard, signal quality for their routes, etc. Upon arrival at the destination, data is then downloaded to a centralized flight communication data bank. This data is then available for flights heading on the

Table 6.2 CASDR Optimization Parameters.

Aeronautical Optimization Parameters
Customer Usage
D_Q: Quantity of data transferred at various flight segments.
D_T: Duration of data transfer per segmented route
T_C: Traffic classes: multi-media, navigation, system health and safety
BER: Required bit error rate per traffic classes
Network and Data Access Layer
Protocol selection, Routing configuration, Forward error selection given the customer driven BER, Available to provide relay service, Packet error rate
Physical Layer
T_M: Multipath delay spread: Characterizes channel smearing due to arrival of multi-signal reflection arrivals
f_{DS}: Doppler spread or Doppler bandwidth
f_d: Doppler shift
A: Attenuation: power loss, function of frequency and distance
L: Impulse Response Length: length, in signal elements, of CIR
Band: Carrier frequency Band
BW: Available bandwidth
SWP: Standard waveform performance

same route. Flights heading on these routes will have a priori knowledge of performance parameters and services available.

6.7.1 Cognitive Intelligence

The brain of the aeronautical cognitive would be to work off its constant awareness of aircraft geographical location, routes and RF channel. It will sense weather conditions that may affect the radio transmission and the services available. Figure 6.7 shows the cognitive decision engine and process. This is a high level algorithm that will manage data gathering based on aircraft sensors, measure channel characteristics, check regulations and optimize radio parameters. Figure 6.8 shows the cognitive decision engine interfaced to CASDR subsystems.

6.7.2 Awareness

The aircraft navigation and radar systems will provide the sensing stimulation to the cognitive engine. The Inertial Measurement Unit (IMU) used for flight navigation will

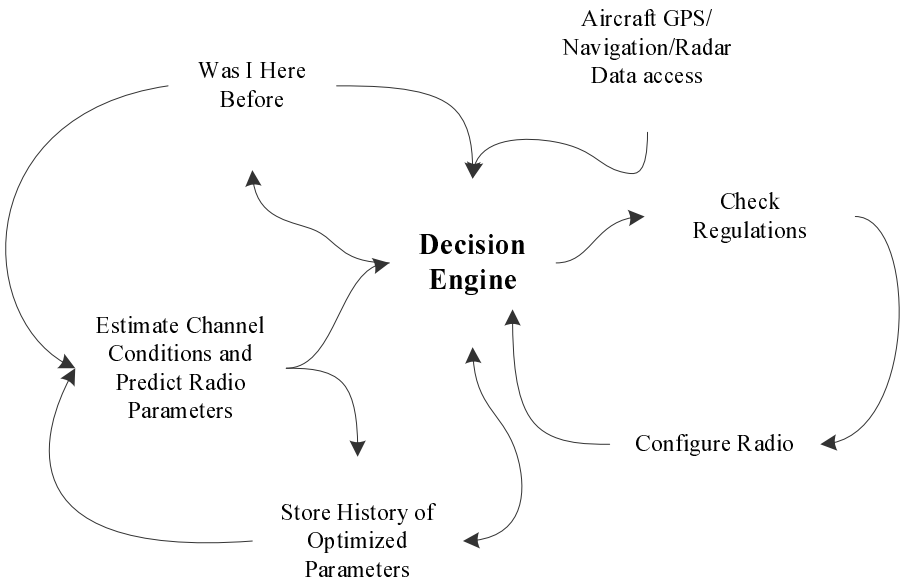

Figure 6.7 Cognitive Decision Engine.

provide aircraft speed, acceleration, altitude and attitude. This information can also be used to estimate CASDR parameters, e.g., Doppler shift. Advanced forward looking radar will provide the weather conditions that may affect the radio transmission performance. A Global Positioning System (GPS) will provide the location of the aircraft with respect to global geography. Furthermore, the awareness engine will have the ability to estimate the data requirements based on past data usage and flight profile, before accessing the spectrum for services. Hence, awareness being aware of where the CASDR system is, will be used to measure the performance and store its results for the particular route and location. This information will become available for others traveling these routes.

6.7.3 Learn

The cognitive awareness provides an opportunity for CASDR to learn the spectrum usage, data demand and system throughput based on flight route during the day or night. Such statistics will allow a constant learning and maturing of statistics profile that is stored for each route. This allows cognitive radio of other airlines that have not traveled that particular route to have a priori knowledge and schedule services accordingly. The system

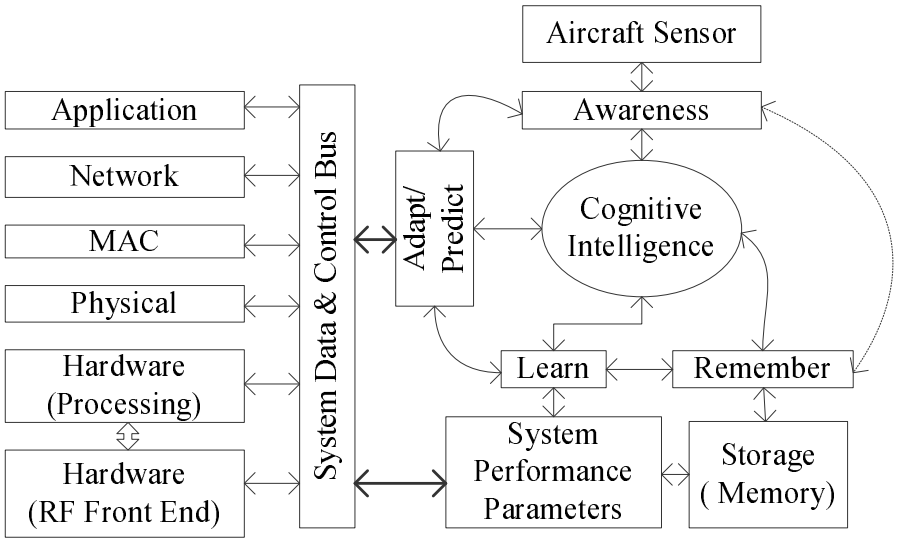

Figure 6.8 Aeronautical SDR and CE.

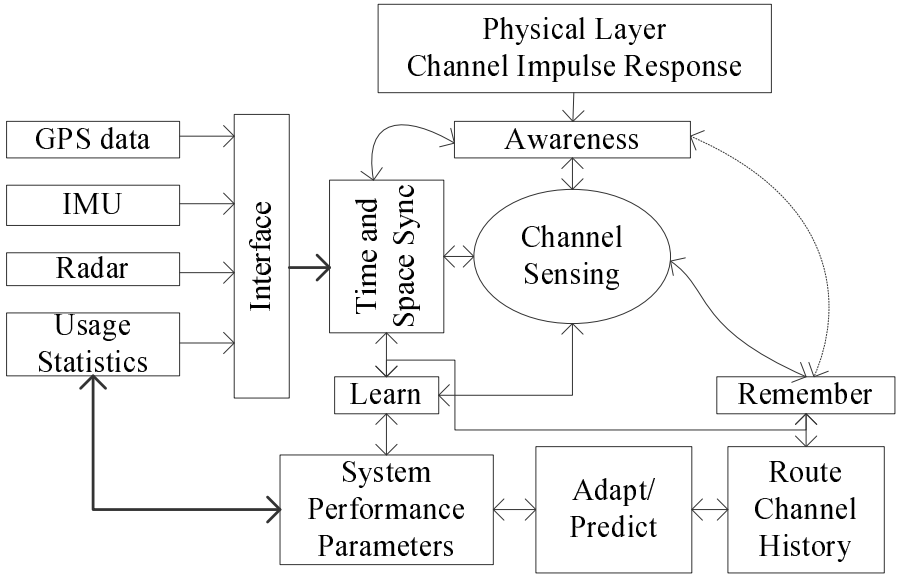

Figure 6.9 Aeronautical Channel Sensing.

parameters available for that particular location can be configured for the country or location. The channel sensing and estimation for flight routes will serve to establish channel statistics, as shown in Figure 6.9. The CASDR cognitive channel awareness can configure the system to measure channel impairments for the flight route not traveled by any aircraft. Thus, the very first flight might not provide the optimum connectivity.

6.7.4 Remember

System performance data gathered for different flight routes through different airlines will serve as a means to remember the flight parameters, exchanged through a centralized data archive. Such data will grow in time and averaging over time will provide a reliable statistic for configuring the CASDR radio parameters.

6.7.5 Adapt and Predict

The cognitive engine learning and sensing ability, tied to an aircraft system will allow CASDR the ability to predict system configuration parameters and adapt them based on a priori configurations recorded by other traveled aircraft.

6.8 Aeronautical Configurable Hardware

The key to a configurable system for an aeronautical system is to design hardware with the minimum analog front-end, access to different antenna systems, high speed ADC and a programmable processing architecture. Figure 6.10, Aeronautical Software Defined Radio, presents such a system. The RF front-end will support multiple bands with varying gain amplifiers [129]. Closely coupled A/D boards with FPGAs are required for high speed data connectivity and processing. A technique such as under sampling for demodulations is used to reduce the front-end components. The advances in ADC devices as well as the non-compliance feature of the Nyquist sampling theory is an enabler for an ASDR application. Violation of the Nyquist theory will create signals aliased at an integer multiple of the sampling frequency ($N * fs$) [130]. This puts the challenge on the front-end processing system. The advances in programmable Digital Signal Processing (DSP) and Field Programmable Gate Array (FPGA) are ideal for such processing [131]. FPGA offers the ability to parallelize processing and allow a high-end processing throughput. The Virtex-6 FPGA family of Xilinx provides up to 2,016 DSP48 slices that deliver up to 1000 Giga MAC/s of DSP processing performance. Xilinx offers solutions for evolving standards such as WCDMA, WiMAX, TD SCDMA and LTE. Texas Instrument DSP products are now offering six DSP

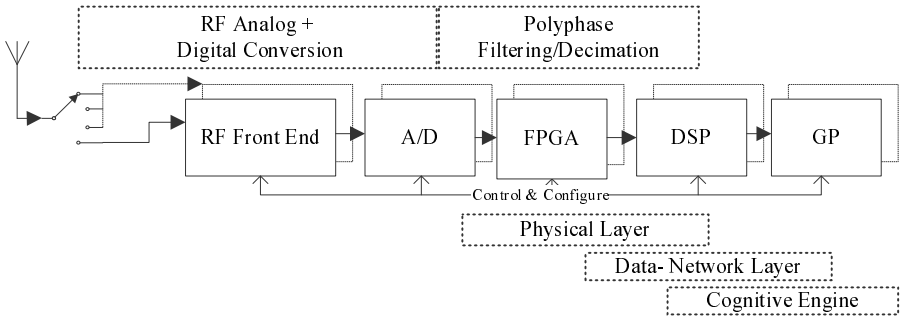

Figure 6.10 Aeronautical Software Defined Radio.

processors in a single package, with processing capability of 4000 million MACS (16-Bits) at 500 MHz [132].

6.9 Conclusion

The advances in component technology, evolution of communication services, and an increase in data demand and aircraft mobility creates an ideal application for CASDR to support the aeronautical system. Current deployed systems are beginning to take shape, e.g., GOGO, however they are adding another hardware box to provide connectivity. Since the system is hardwired for a particular modem, the evolution will require hardware modification to keep up with growth in the telecommunication market. As an example, when the aircraft is at the terminal, WLAN modulation and protocol can be hosted on the CASDR. When the aircraft is in en route, the CASDR re-configures itself to the OFDM based system using beam forming compensation, as described in Chapter 4 and 5. The novel cognitive channel measurement and estimation for each route will increase spectrum efficiency and in return provide high data throughput. An optimum combination of bandwidth, subcarrier bandwidth, acceptable Doppler frequency and multipath resilient system can be developed for the ADN. This will result in an efficient use of the spectrum and provide a high data rate for global connectivity.

CHAPTER 7

CONCLUSION AND FUTURE WORK

In this dissertation, the challenge of dual Doppler shifts with varying relative delays for an aeronautical channel condition was identified. The impact of these dual Doppler shifts on OFDM systems was analyzed and a mathematical analysis was presented. Parametric spectrum estimation was identified as a means to accurately estimate the dual Doppler shifts. MATLAB simulations using parametric algorithms, i.e., MUSIC, EV and Minimum Norm, were evaluated and their performances show a less than one percent MSE error in estimating the Doppler frequency. The parametric methods of Doppler shift estimations exploit the harmonic nature of the transmitted OFDM pilot tone or multiple tones. Parametric methods estimate the process and thus can provide better performance compared to the non-parametric method on a shorter set of data samples.

In an aeronautical channel condition, among other impairments, the transmitted signal experiences two different Doppler shifts that are detrimental to OFDM performance. The receiver then receives these two combined signals. This condition completely degrades the OFDM performance. The aeronautical large geometric area, where the angles of arrival of the two shifted signals are different, can be taken advantage of by using a smart antenna processing to separate the signals. In this dissertation, a beam forming method was proposed and its simulation results were presented. The analysis and simulations showed this method to be a viable solution. This method constitutes of first separating the signals, then Doppler shifts for individual signals are corrected. The two separated signals can then be added using diversity techniques, and thus increase performance. Simulation results show an increase in performance with diversity combining. The application of beam forming based signal

separation for the aeronautical environment is a novel technique. This technique not only resolves the problem, but takes advantage of aeronautical channel to improve performance.

The global movement of aircraft changing RF conditions and available connectivity was identified as an opportunity to develop a CASDR system. The cognitive aspect of the system learns channel conditions, connectivity and available services for different routes and regions. The software defined radio architecture will allow the data developed and analyzed for optimum performance to configure the hardware for a particular route and region. This dissertation provides a novel signal separation method to allow the use of spectrum efficient OFDM in an aeronautical system. Furthermore, a novel notional CASDR system will allow radios on the aircraft to provide optimum connectivity, wherever a potential network is available.

Certain parts of the dissertation are published or have been submitted to internationally recognized conferences, journals and books [40–44]. In the remainder of this section, the specific contributions of each publication are summarized and possible future work is discussed.

7.1 List of Specific Publications

- Paper title, "Challenges of aeronautical data networks."

  This paper focuses on current and future prospects of the aeronautical data network and the cross interoperability with a terrestrial backbone. The results of notional network capacity analyses are presented. Channel models specific to an aeronautical platform for a wide band system is discussed. Connectivity and robustness of an aeronautical based network, both as a relay for terrestrial networks, and as an in-flight Internet connectivity, are discussed.

- Paper title, "Doppler estimation for OFDM based Aeronautical Data communication".

High mobility platforms, such as trains and aircraft offer a challenging environment for increasing the spectral efficiency of the physical layer. This paper discusses the potential development of an Aeronautical Data Network (ADN) and its channel issues, particularly the high mobility and the effects of using an OFDM communication system. OFDM ICI and frequency shift caused by the high mobility of the platform is investigated and potential methods are proposed.

- Paper title, "Cognitive Aeronautical Communication System."

  The paper explores the system and architecture requirements for a cognitive driven reconfigurable hardware for an aeronautical platform, such as commercial aircraft or high altitude platforms. This paper proposes a system for an intelligent self-configurable software and hardware solution for an aeronautical system.

- Paper title, "ICI Analysis and Parametric Doppler Estimation in Aeronautical OFDM."

  In this paper, the aeronautical broadband wireless access scheme, based on OFDM in order to achieve higher data rates, is investigated. However, due to the significant speed of the aeronautical platform, Doppler shifts have a major impact on OFDM based systems. Moreover, the Doppler frequency spread depicts different characteristics compared to terrestrial networks, i.e., dual Doppler shifts in the channel. The parametric spectrum estimation methods for estimating the Doppler shifts are investigated. In particular, the MUltiple Signal Classification (MUSIC), Eigenvector (EV) and Minimum norm methods are evaluated. MATLAB modeling and its performance results are published.

- Paper title, "Aeronautical OFDM Challenges and Mitigation Using Beam Forming."

  In this paper, the issues involved with using OFDM in the aeronautical channel are investigated and a novel solution is proposed. In this environment, Doppler spread depicts different characteristics compared to the terrestrial channel. Besides the speed of the high mobility platform, i.e., aircraft, aeronautical environments have large distances, which results in a wide angle of arrivals and associated delays. OFDM is

sensitive to Doppler shifts, which results in intercarrier interference (ICI). The ICI analysis of OFDM is derived analytically and the impact of aeronautical two ray channel is presented. The parametric eigenvector decomposition spectrum methods are investigated for estimating the Doppler shifts. The ICI caused by two arriving signals with significant different Doppler shifts completely corrupts the received OFDM signal. A beam forming method is proposed to separate the signals with different Doppler shifts. This results in multiple received signals that can be taken advantage of to improve the performance.

- Book chapter, "Aeronautical Data Networks."

  The advances in component technology, evolution of communication services, increase in data demand and aircraft mobility creates an ideal application for CASDR to support the aeronautical system. Current deployed systems are beginning to form shape, e.g., GOGO, however, they are adding another hardware box to provide connectivity. Since the system is hardwired for a particular modem, the evolution will require hardware modification to keep up with growth in the telecommunication market. Accurate measurements of channel characteristics, such as Doppler shifts, will allow spectral efficient modulation to be used for higher data rates. Advanced algorithms, along with processing capabilities, can resolve the impact of Doppler shifts. The novel cognitive channel measurement and estimation for each route will increase spectrum efficiency and in return provide high data throughput. An optimum combination of bandwidth, subcarrier bandwidth, acceptable Doppler frequency and multipath immunity can be developed for ADN. This will result in an efficient use of the spectrum and provide a high data rate for global connectivity.

- Intellectual Property (IP) disclosure, "A system of beam forming to separate multi-Doppler shifted received OFDM signal."

  The novel solution in to this dissertation was disclosed for a potential patent award. The patent consisted of the use of novel beam forming technique to separate the multi-

Doppler shifted received OFDM signal. Therefore, highly spectral efficient modulation can be used to increase the data rates in the physical layer.

- Intellectual Property (IP) disclosure, "A Doppler Spread based Maximum Ratio combining of received multi-Doppler shifted OFDM signal."

  This novel solution in to this dissertation was disclosed for a potential patent award. The patent consisted of the novel use of Doppler spread coming off the separated OFDM signals in an aeronautical channel. The separated two rays now can be added to improve the BER performance. However, the reflected path may or may not have Doppler spread due to multipath. Thus, by estimating the Doppler spread, appropriate combining weights can be calculated to maximize BER performance.

7.2 Final Comments and Future Work

This dissertation identified dual Doppler shifts as a cause of OFDM performance degradation. A novel beam forming based solution offers a viable improvement in performance. Further research in the following areas can improve the performance and offers opportunity for future work.

- Parametric modeling error.

  Since parametric Doppler estimation is sensitive to model order, without knowing the number of Doppler shifts in the channel, an estimation error could potentially result. Therefore, techniques to estimate the number of Doppler shifts in the channel needs to be investigated. Algorithms such as for the number of echoes for transmitted tones can be considered, where an accurate estimation of the echoes can be used to estimate the model order. Further research in the area of exploiting the parametric methodology of learning the process of signals to estimate the Doppler shifts can be expanded to create transmitted signals with a process that is fine tuned to the parametric algorithm at the receiver. This would increase the performance and allow accurate estimation in a shorter sample size.

- Doppler spread estimation for aeronautical environments.

  The two separated signals may or may not experience Doppler spread. Based on the literature, the line of sight will have negligible Doppler spread, while the reflected signal will be prone to Doppler spread. Algorithm needs to be researched to estimate this Doppler spread for the aeronautical channel. A further inclusion of Doppler spread estimation for each received signal path could be used to derive the MRC algorithm to mitigate the impact of performance loss due to the spread. This can be done by putting less weight on the signal experiencing the Doppler spread.

- Aeronautical environments and signal interference.

  There are multiple RF transmissions and receptions taking place in an aircraft, e.g., DME, VOR, TCAS, and the other frequency bands shown in Table 1.1. These frequency bands are critical to flight operation and safety. Any frequency band chosen for a ground link has to be evaluated for potential interference with these critical flight operations bands, such as the L band. Then there are issues of wireless PDA devices; their frequency of operation, transmission of power, spectrum and their potential interference with the different frequencies being used. Therefore, there is a need to study the potential interference issues and how modern techniques can be applied to reduce such possible interference.

REFERENCES

[1] E. Haas, "Aeronautical channel modeling," *IEEE Trans. on Veh. Tech.*, vol. 51, no. 2, pp. 254–264, March 2002.

[2] "Boeing," Boeing Report on Commercial aircraft development, 2010, 100 North Riverside Chicago, Illinois 60606. [Online]. Available: http://www.boeing.com/commercial/cmo

[3] Continental Airline Route Map, 2011, 77 W. Wacker Drive Chicago, IL 60601. [Online]. Available: http://www.continental.com/web/en-US/content/travel/routes/co-world_201007.pdf

[4] FlightAware, Eight Greenway Plaza, Suite 1300 Houston, Texas 77046, 2011. [Online]. Available: http://www.flightAware.com/

[5] Flight Statistics: Sivil Havacilik Genel Mudurlugu, 2009. [Online]. Available: http://www.shgm.gov.tr/index2.html/

[6] E. Sakhaee and A. Jamalipour, "The global in-flight internet," *Selected Areas in Communications, IEEE Journal on*, vol. 24, no. 9, pp. 1748 –1757, sept. 2006.

[7] D. Soldani and S. Dixit, "Wireless relays for broadband access [radio communications series]," *Communications Magazine, IEEE*, vol. 46, no. 3, pp. 58 –66, march 2008.

[8] D. Medina, F. Hoffman, S. Ayaz, and C. H. Rokitansky, "Feasibilty of an Aeronautical Mobile Ad-Hoc Network Over the North Atlantic Corridor," in *Proc. IEEE Sensor, Mesh and Ad Hoc Commun. and Net. (SECON)*, 2008.

[9] J. Lai, "Broadband wireless communication systems provided by commercial airplanes," *US. Patents*, 1998.

[10] P. Bello, "Aeronautical channel characterization," *Communications, IEEE Transactions on*, vol. 21, no. 5, pp. 548 – 563, May 1973.

[11] S. Elnoubi, "A simplified stochastic model for the aeronautical mobile radio channel," in *Vehicular Technology Conference, 1992, IEEE 42nd*, vol. 2, May 1992, pp. 960–963.

[12] K. Birman, "The next-generation internet: unsafe at any speed?" *Computer*, vol. 33, no. 8, pp. 54–60, Aug. 2000.

[13] C. Livadas, J. Lygeros, and N. Lynch, "High-level modeling and analysis of the traffic alert and collision avoidance system (tcas)," *Proceedings of the IEEE*, vol. 88, no. 7, pp. 926–948, July 2000.

[14] A. Palatnick, "Wide-aperture digital vor," *Aerospace and Electronic Systems, IEEE Transactions on*, vol. AES-14, no. 6, pp. 853–865, Nov. 1978.

[15] D. Gebre-Egziabher, J. Powell, and P. Enge, "A dme based area navigation system for gps/waas interference mitigation in general aviation applications," in *Position Location and Navigation Symposium, IEEE 2000*, 2000, pp. 74–81.

[16] P. Misra, B. Burke, and M. Pratt, "Gps performance in navigation," *Proceedings of the IEEE*, vol. 87, no. 1, pp. 65–85, Jan. 1999.

[17] B. Strauss, M. Morgan, J. Apt, and D. Stancil, "Unsafe at any airspeed?" *Spectrum, IEEE*, vol. 43, no. 3, pp. 44–49, March 2006.

[18] T. Nguyen, S. Koppen, L. Smith, R. Williams and M. Salud, "Third generation wireless phone threat assessment for aircraft communication and navigation radios," *NASA/TP-2005-213537*, 2005.

[19] E. J. Jafri Madiha and V. Lindad, "Graphical and statistical analysis of airplane passenger cabin rf coupling paths to avionics," *NASA-2003-22dasc*, 2003.

[20] F. van der Wijk, A. Kegel, and R. Prasad, "Assessment of a pico-cellular system using propagation measurements at 1.9 ghz for indoor wireless communications," *Vehicular Technology, IEEE Transactions on*, vol. 44, no. 1, pp. 155–162, Feb. 1995.

[21] H. Zeino and M. Misson, "A simulation architecture for a pico-cellular hybrid network," in *Local Computer Networks, 1995., Proceedings. 20th Conference on*, Oct. 1995, pp. 219–226.

[22] C. Niebla, "Coverage and capacity planning for aircraft in-cabin wireless heterogeneous networks," in *Vehicular Technology Conference, 2003. VTC 2003-Fall. 2003 IEEE 58th*, vol. 3, Oct. 2003, pp. 1658–1662.

[23] T. Le and M. Nakhai, "Possible power-saving gains by dividing a cell into tiers of smaller cells," *Electronics Letters*, vol. 46, no. 16, pp. 1163–1165, May 2010.

[24] "Inmarsat, the mobile satellite company," Inmarsat Satellite service provider for the Onboard cell service, 99 City Road London, EC1Y 1AX United Kingdom, 2011. [Online]. Available: http://www.inmarsat.com/Services/Aeronautical/default.aspx

[25] P. Bacon, "Introduction to globalstartm [satellite communication system]," in *Communication Opportunities Offered by Advanced Satellite Systems - Day 1 (Ref. No. 1998/484), IEE Colloquium on*, Oct. 1998, pp. 3/1–3/8.

[26] R. Hendrickson, "Globalstar for the military," in *Military Communications Conference, 1998. MILCOM 98. Proceedings., IEEE*, vol. 3, Oct. 1998, pp. 808–813.

[27] P. Lemme, S. Glenister, and A. Miller, "Iridium(r) aeronautical satellite communications," in *Digital Avionics Systems Conference, 1998. Proceedings., 17th DASC. The AIAA/IEEE/SAE*, vol. 2, Oct. 1998, pp. H11/1–H11/9.

[28] H. Keller and H. Salzwedel, "Link strategy for the mobile satellite system iridium," in *Vehicular Technology Conference, 1996. 'Mobile Technology for the Human Race'., IEEE 46th*, vol. 2, Apr. 1996, pp. 1220–1224.

[29] "Airvana," Airvana Network Solutions, 19 Alpha Road Chelmsford, MA 01824, 2011. [Online]. Available: http://www.airvananetworksolutions.com/

[30] C. Eklund, R. Marks, K. Stanwood, and S. Wang, "Ieee standard 802.16: a technical overview of the wirelessmantm air interface for broadband wireless access," *Communications Magazine, IEEE*, vol. 40, no. 6, pp. 98–107, Jun. 2002.

[31] B. Krenik, "4g wireless technology: When will it happen? what does it offer?" in *Solid-State Circuits Conference, 2008. A-SSCC '08. IEEE Asian*, Nov. 2008, pp. 141–144.

[32] "Airbus," Airbus Traffic Forecast, 1, Rond Point Maurice Bellonte 31707 Blagnac Cedex France, 2011. [Online]. Available: http://www.airbus.com/

[33] "Federal Aviation Administration," FAA Long Range Aerospace Forecasts, 800 Independence Avenue, SW Washington, DC 20591, 2011. [Online]. Available: http://www.faa.gov

[34] "Federal Aviation Administration," Final Report of the Working Group on Oceanic and Sparse Area Communications, of the FAA REDAC Air Traffic Services Subcommittee, Paul Drouilhet, 800 Independence Avenue, SW Washington, DC 20591, 2009. [Online]. Available: http://www.faa.gov

[35] "Federal Aviation Administration," Next Generation Air Transportation System (NextGen), 800 Independence Avenue, SW Washington, DC 20591, 2011. [Online]. Available: http://www.faa.gov/nextgen/

[36] R. Kerczewski, I. Greenfeld, and B. Welch, "Communications, navigation and surveillance for improved oceanic air traffic operations," in *Aerospace Conference, 2005 IEEE*, March 2005, pp. 1799–1805.

[37] "Mathworks," MATLAB - The Language Of Technical Computing, 2011, 3 Apple Hill Drive Natick, MA 01760-2098. [Online]. Available: http://www.mathworks.com/products/matlab/index.html

[38] "The Product Development Company," Mathcad: Solve and document your most complex engineering calculations, 2011, 140 Kendrick Street Needham, MA 02494. [Online]. Available: http://www.ptc.com/products/mathcad/

[39] "Synopsys," Synopsys Signal Processing Workshop, 377 Simarano Drive Marlborough, MA 01752. [Online]. Available: http://www.synopsys.com/systems/blockdesign/digitalsignalprocessing/pages/signal-processing.aspx

[40] M. Erturk, J. Haque, and H. Arslan, "Challenges of aeronautical data networks," in *Aerospace Conference, 2010 IEEE*, March 2010, pp. 1–7.

[41] J. Haque, M. Erturk, and H. Arslan, "Doppler estimation for ofdm based aeronautical data communication," in *Wireless Telecommunications Symposium (WTS), 2010*, April 2010, pp. 1–6.

[42] J. Haque and M. C. Erturk and H. Arslan, "Aeronautical ici analysis and doppler estimation," *Communications Letters, IEEE*, vol. 15, no. 9, pp. 906–909, September 2011.

[43] J. Haque, M. Erturk, H. Arslan, and W. Moreno, "Cognitive aeronautical communication system," *International Journal of Interdisciplinary Telecommunications and Networking*, pp. 20–35, Oct. 2011.

[44] Erturk, M.C. and Haque, J. and Arslan, H. and Moreno, W., *Aeronautics*. InTech book edited by: Professor Max Mulder, Technical University Delft, Netherlands, 2011.

[45] T. S. Rappaport, *Wireless Communications: Principles and Practice*, 2nd ed. NJ: Prentice Hall, 2003.

[46] A. Neskovic, N. Neskovic, and G. Paunovic, "Modern approaches in modeling of mobile radio systems propagation environment," *Communications Surveys Tutorials, IEEE*, vol. 3, no. 3, pp. 2–12, Oct. 2000.

[47] S. Cummer, "Modeling electromagnetic propagation in the earth-ionosphere waveguide," *Antennas and Propagation, IEEE Transactions on*, vol. 48, no. 9, pp. 1420–1429, Sep. 2000.

[48] K. C. Yeh and C.-H. Liu, "Radio wave scintillations in the ionosphere," *Proceedings of the IEEE*, vol. 70, no. 4, pp. 324–360, April 1982.

[49] M. Weiner, "Use of the longley-rice and johnson-gierhart tropospheric radio propagation programs:0.02-20 ghz," *Selected Areas in Communications, IEEE Journal on*, vol. 4, no. 2, pp. 297–307, Mar. 1986.

[50] L. Ames and T. Rogers, "Available bandwidth in 200-mile vhf tropospheric propagation," *Antennas and Propagation, IRE Transactions on*, vol. 3, no. 4, pp. 217–218, Oct. 1955.

[51] P. F. M. Smulders, "Statistical characterization of 60-ghz indoor radio channels," *IEEE Transactions on Antennas and Propagation*, 2009.

[52] A. P. Ron Schroer and J. L. Smith, "A Systems View of Future Air Traffic Management (ATM) Operations and Equipments," in *IEEE Proceeding*, 2002.

[53] G. Janssen, P. Stigter, and R. Prasad, "Wideband indoor channel measurements and ber analysis of frequency selective multipath channels at 2.4, 4.75, and 11.5 ghz," *Communications, IEEE Transactions on*, vol. 44, no. 10, pp. 1272–1288, Oct. 1996.

[54] M. A. Do and S. Sun, "Statistical modeling of broadband wireless lan channels at 18 ghz using directive antennas," *International Journal of Wireless Information Networks.*, vol. 4, no. 1, 1997.

[55] K. Siwiak, *Radiowave Propagation and Antennas for Personal Communication.* Artech House, 1995.

[56] R. Crane, "Prediction of attenuation by rain," *Communications, IEEE Transactions on*, vol. 28, no. 9, pp. 1717–1733, Sep. 1980.

[57] M. Odedina and T. Afullo, "Rain attenuation prediction along terrestrial paths in south africa using existing attenuation models," in *AFRICON 2007*, Sept. 2007, pp. 1–7.

[58] B. Glance and L. Greenstein, "Frequency-selective fading effects in digital mobile radio with diversity combining," *Communications, IEEE Transactions on*, vol. 31, no. 9, pp. 1085–1094, Sep. 1983.

[59] M. Rice, A. Davis, and C. Bettweiser, "Wideband channel model for aeronautical telemetry," *Aerospace and Electronic Systems, IEEE Transactions on*, vol. 40, no. 1, pp. 57–69, Jan. 2004.

[60] M. Rice, R. Dye, and K. Welling, "Narrowband channel model for aeronautical telemetry," *Aerospace and Electronic Systems, IEEE Transactions on*, vol. 36, no. 4, pp. 1371–1376, Oct. 2000.

[61] W. Braun and U. Dersch, "A physical mobile radio channel model," *Vehicular Technology, IEEE Transactions on*, vol. 40, no. 2, pp. 472–482, May 1991.

[62] S. Jayaweera and H. Poor, "On the capacity of multiple-antenna systems in rician fading," *Wireless Communications, IEEE Transactions on*, vol. 4, no. 3, pp. 1102–1111, May 2005.

[63] Q. Zhang and D. Liu, "A simple capacity formula for correlated diversity rician fading channels," *Communications Letters, IEEE*, vol. 6, no. 11, pp. 481–483, Nov. 2002.

[64] G. Raleigh, S. Diggavi, A. Naguib, and A. Paulraj, "Characterization of fast fading vector channels for multi-antenna communication systems," in *Signals, Systems and Computers, 1994. 1994 Conference Record of the Twenty-Eighth Asilomar Conference on*, vol. 2, Oct. 1994, pp. 853–857.

[65] W. C. Y. Lee, *Mobile Cellular Telecommunications Systems.* McGraw-Hill, 1989.

[66] E. Biglieri, J. Proakis, and S. Shamai, "Fading channels: information-theoretic and communications aspects," *IEEE Trans. Inf. Theory*, vol. 44, no. 6, pp. 2619–2692, Oct. 1998.

[67] J. G. Proakis, *Digital Communications*, 4th ed. New York: McGraw-Hill, 2001.

[68] E. W.C. Jakes, *Microwave Mobile Communications.* New York Wiley, 1974.

[69] P. Moose, "A technique for orthogonal frequency division multiplexing frequency offset correction," *IEEE Trans. on Commun.*, vol. 45, pp. 2908–2914, Oct. 1994.

[70] P. Robertson and S. Kaiser, "Analysis of the loss of orthogonality through doppler spread in OFDM systems," *Global Telecommun. Conf. (GLOBECOM)*, vol. 1B, pp. 701–706, 1999.

[71] P. A. Bello, "Selective fading limitations of the kathryn modem and some system design considerations," *IEEE Trans. Comm.*, vol. 27, no. 13, Sept. 1965.

[72] R. W. Chang, "Synthesis of band-limited orthogonal signals for multichannel data transmission," *Bell Syst. Tech. J.*, vol. 45, no. 5, Dec. 1966.

[73] R. W. Chang, "Orthogonal frequency division multiplexing," *U. S. Patent 3 488 445*, Jan. 1970.

[74] B. Saltzberg, "Performance of an efficient parallel data transmission system," *Communication Technology, IEEE Transactions on*, vol. 15, no. 6, pp. 805–811, Dec. 1967.

[75] M. Doelz, E. Heald, and D. Martin, "Binary data transmission techniques for linear systems," *Proceedings of the IRE*, vol. 45, no. 5, pp. 656–661, May 1957.

[76] L. J. Cimini, "Analysis and simulation of a digital mobile channel using orthogonal frequency division multiplexing," *IEEE Trans. Comm.*, vol. 7, no. 33, July 1985.

[77] *Digital Audio Broadcasting (DAB) to Mobile, Portable, and Fixed Receivers*, Ets300 401 ed., European Telecommunications Standards Institute, Sophia Antipolis, France, May 1997.

[78] *Digital Video Broadcasting Framing Structure, Channel Coding, and Modulation for Digital Terrestrial Television*, Draft en300 744 v1.2.1 ed., European Broadcasting Union, Geneva, Switzerland, Jan. 1999.

[79] *Part 11:Wireless LAN Medium Access Control (MAC) and Physical Layer(PHY) Specifications: High-Speed Physical Layer in the 5 GHz Band*, IEEE Std. 802.11-1999, Aug. 1999.

[80] *Local and Metropolitan Area Networks Part 16, Air Interface for Fixed Broadband Wireless Access Systems*, IEEE Std. 802.16a, Jan. 2003.

[81] *Draft IEEE Standard for Local and Metropolitan Area Networks, Part 16: Air Interface for Fixed and Mobile Broadband Wireless Access Systems Amendment for Physical and Medium Access Control Layers for Combined Fixed and Mobile Operation in Licensed Bands,*, IEEE Std. 802.16a, May 2005.

[82] H. Sampath, S. Talwar, J. Tellado, V. Erceg, and A. Paulraj, "A fourth-generation mimo-ofdm broadband wireless system: design, performance, and field trial results," *Communications Magazine, IEEE*, vol. 40, no. 9, pp. 143–149, Sep. 2002.

[83] K. Etemad and M. Riegel, "Topics and updates on 4g technologies [series editorial]," *Communications Magazine, IEEE*, vol. 48, no. 8, pp. 38–39, Aug. 2010.

[84] F. Davarian, "Sirius satellite radio: Radio entertainment in the sky," in *Aerospace Conference Proceedings, 2002. IEEE*, vol. 3, 2002, pp. 1031–1035.

[85] D. Layer, "Digital radio takes to the road," *Spectrum, IEEE*, vol. 38, no. 7, pp. 40–46, July 2001.

[86] D. Bodson, "Digital audio around the world," *Vehicular Technology Magazine, IEEE*, vol. 5, no. 4, pp. 24–30, Dec. 2010.

[87] Y. Li and J. Cimini, "Bounds on the interchannel interference of OFDM in time-varying impairments," *IEEE Trans. Commun.*, vol. 49, no. 3, pp. 401–404, 2001.

[88] M. Speth, S. Fechtel, G. Fock, and H. Meyr, "Optimum receiver design for wireless broad-band systems using ofdm," *Communications, IEEE Transactions on*, vol. 47, no. 11, pp. 1668–1677, Nov. 1999.

[89] T. Keller and L. Hanzo, "Adaptive multicarrier modulation: a convenient framework for time-frequency processing in wireless communications," *Proceedings of the IEEE*, vol. 88, no. 5, pp. 611–640, May 2000.

[90] Y. Li and J. Cimini, L.J., "Bounds on the interchannel interference of OFDM in time-varying impairments," *IEEE Trans. on Commun.*, vol. 49, no. 3, pp. 401–404, Mar. 2001.

[91] J. Cadzow, "Spectral estimation: An overdetermined rational model equation approach," *Proceedings of the IEEE*, vol. 70, no. 9, pp. 907–939, Sept. 1982.

[92] T. M. Schmidt and D. C. Cox, "Robust frequency and timing synchronization for OFDM," *IEEE Trans. on Commun.*, vol. 45, pp. 1613–1621, Dec. 1997.

[93] M. J.J. Van De Beek and P. Borjesson, "Ml estimation of the time and frequency offset in OFDM system," *IEEE Trans. on Sig. Process.*, vol. 45, pp. 1800–1805, July 1997.

[94] H. Liu and U. Tureli, "A high efficiency carrier estimator for OFDM communications," *IEEE Commun. Lett.*, vol. 2, pp. 104–106, April 1998.

[95] "The 5 ghz airport surface area channel: Part II, measurement and modeling results for small airports," Ohio State University Electrical Engineering Dept.

[96] M. Russell and G. Stuber, "Interchannel interference analysis of ofdm in a mobile environment," *IEEE Trans. Veh. Tech.*, vol. 2, pp. 820–824, July 2002.

[97] S. Chen and T. Yao, "Intercarrier interference suppression and channel estimation for OFDM systems in time-varying frequency-selective fading channels," *IEEE Trans. on Consum. Electron.*, vol. 50, no. 2, pp. 429–435, 2004.

[98] V. F. Pisarenko, "The retrieval of harmonics from a covariance function," *Geophysics J. Roy. Astron. Soc.,*, vol. 33, no. 4, pp. 347–366, Apr. 1973.

[99] R. Schmidt, "Multiple emitter location and signal parameter estimation," *in Proc. RADC Spect. Est. Workshop*, pp. 243–258, 1979.

[100] I. Rezek and S. Roberts, "Parametric model order estimation: a brief review," *Model Based Digital Signal Processing Techniques in the Analysis of Biomedical Signals (Digest No. 1997/009), IEE Colloquium on the Use of Biomedical Signals (Ref. No.1997/009)*, pp. 3/1–3/6, 1997.

[101] M. Vanderveen, A. J. Van der Veen, and A. Paulraj, "Estimation of multipath parameters in wireless communications," *Signal Processing, IEEE Transactions on*, vol. 46, no. 3, pp. 682–690, Mar. 1998.

[102] M. Vanderveen, C. Papadias, and A. Paulraj, "Joint angle and delay estimation (jade) for multipath signals arriving at an antenna array," *Communications Letters, IEEE*, vol. 1, no. 1, pp. 12–14, Jan. 1997.

[103] B. D. V. Veen and K. M. Buckley., "Beamforming: A versatile approach to spatial filtering," *IEEE ASSP Magazine*, April 1998.

[104] C. Zhang, H. Han, and H. Yu, "Nc-osdm transmission for ici cancelation in high speed mobile systems," in *Cognitive Radio and Advanced Spectrum Management, 2009. CogART 2009. Second International Workshop on*, May 2009, pp. 50–53.

[105] J. An, Y. Wu, and G. Liu, "Delay and doppler shift joint tracking method for ofdm based aeronautical communication systems," in *Wireless Communications, Networking and Mobile Computing, 2008. WiCOM '08. 4th International Conference on*, Oct. 2008, pp. 1–4.

[106] L. Godara, "Application of antenna arrays to mobile communications. ii. beamforming and direction-of-arrival considerations," *Proceedings of the IEEE*, vol. 85, no. 8, pp. 1195–1245, Aug. 1997.

[107] A. Shah and A. M. Haimovich., "Performance analysis of maximal ratio combining and comparison with optimum combining for mobile radio communications with cochannel interference," *IEEE Trans. on Veh. Tech.*, vol. 49, no. 4, July 2000.

[108] N. Kong and L. Milstein, "Average SNR of a generalized diversity selection combining scheme," in *Proc. IEEE Int. Conf. on Commun. (ICC)*, 1998, pp. 1556–1558.

[109] A. Shah and A. Haimovich, "Performance analysis of maximum ratio combining and comparison with optimum combining for mobile radio communications with cochannel interference," *IEEE Trans. on Veh. Tech.*, vol. 49, pp. 1454–1463, 2000.

[110] J. R. Wertz and W. J. Larson, *Space Mission Analysis and Design*, 3rd ed. NJ: Prentice Hall, 2003.

[111] EE Times Signal Processing Design. [Online]. Available: http://www.eetimes.com/design/signal-processing-dsp

[112] "RITA," Research and Innovative Technology Administration (RITA). U.S. Department of Transportation, U.S. Department of Transportation 1200 New Jersey Avenue, SE Washington, DC 20590, 2011. [Online]. Available: www.bts.gov/programs/airline_information

[113] R. Lackey and D. Upmal, "Speakeasy: The military software radio," *IEEE Communications Magazine*, vol. 33, pp. 56–61, May 1995.

[114] "JPEOJTRS," Joint Tactical Radio System (JTRS), JPEO JTRS 33000 Nixie Way San Diego, CA 92147-5110, 2011. [Online]. Available: http://jpeojtrs.mil

[115] J. Mitola, "The software radio architecture," *IEEE Communications Magazine*, vol. 33, pp. 26–38, May 1995.

[116] "Eurocontrol," Eurocontrol, Air Traffic Statistics and Forecasts, EUROCONTROL - STATFOR 96 Rue de la Fuse 1130 Brussels BELGIUM, 2011. [Online]. Available: http://www.eurocontrol.int/statfor/public/subsite_homepage/homepage.html

[117] "Aircell in AIR and ON," J. Blumenstein. Aircell: Inflight Wi-Fi Built for the Airline Business, 2011. [Online]. Available: http://www.aircell.com/resource-center/white-papers

[118] "AeroSat Corporation," AeroSat Corporation. About Airborne SatCom, 62 Route 101A, Suite 2B Amherst, NH 03031, 2011. [Online]. Available: www.aerosat.com/about/about_airborne_satcom.asp

[119] R. Srikanteswara, R. C. Palat, J. H. Reed, and P. Athanas., "An overview of configurable computing machines for software radio handsets," *Communications Magazine IEEE*, vol. 41, no. 07, pp. 134–141, July 2003.

[120] R. M. M. D. B. Mohebbi E. C. Filho and F. J. Kurdahi, "A case study of mapping a software-defined radio (sdr) application on a reconfigurable dsp core," *IEEE/ACM/IFIP International Conference*, pp. 103 –108, October 2003.

[121] A. H. Zanikopoulos and H. van Roermund., "A. programmable/reconfigurable adcs for multi-standard wireless terminals," *IEEE Conferences in Communications, Circuits and Systems Proceedings*, vol. 2, pp. 1337–1341, 2006.

[122] H. N. Salkintzis, A.K. and Mathiopoulos., "Adc and dsp challenges in the development of software radio base stations," *IEEE Personal Communications*, vol. 6, no. 2, pp. 47–55, Aug. 1999.

[123] M. Cummings and S. Haruyama, "Fpga in the software radio," *IEEE Communications Magazine*, vol. 37, no. 2, pp. 108–112, February 1999.

[124] "Ookla," Speed Test, 538 5th Ave. E. Kalispell, MT 59901-4929 USA, 2011. [Online]. Available: www.speedtest.net

[125] IATA (International Air Transport Association) Schedule Reference Service(SRS), 800 Place Victoria PO Box 113 Montreal - H4Z 1M1 Quebec - Canada. [Online]. Available: http://www.iata.org/ps/publications/srs/

[126] P. Hoeher and E. Haas, "Aeronautical channel modeling at vhf-band," in *Vehicular Technology Conference, 1999. VTC 1999 - Fall. IEEE VTS 50th*, vol. 4, 1999, pp. 1961–1966.

[127] J. Mitola and G. Q. Maguire, "Cognitive radio: Making software radios more personal," *IEEE Personal Communications*, vol. 6, no. 2, pp. 13–18, August 1999.

[128] Y. Zhang and N. Ansari, "Wireless telemedicine service over integrated ieee802.11/wlan and 802.16/wimax," *IEEE Wireless Communications*, February 2010.

[129] D. Pilgrim, "Defense electronics," Simplifying RF front-end design in Multiband Handsets, 2008. [Online]. Available: http://rfdesign.com/microwave_millimeter_tech/rf_front_end_mmic/radio_simplifying_rf_frontend/index1.html

[130] H. Susaki, "A fast algorithm for high-accuracy frequency measurement: Application to ultrasonic doppler sonar," *IEEE journal of oceanic engineering*, vol. 27, no. 1, January 2002.

[131] "Xilinx," Xilinx DSP Design, Xilinx, Inc. 2100 Logic Drive San Jose, CA 95124-340, 2011. [Online]. Available: http://www.xilinx.com/products/technology/dsp/index.htm

[132] "Texas Instruments Corporation," Fixed Point Digital Signal Processing, 12500 TI Boulevard, Dallas, Texas 75243, 2011. [Online]. Available: http://focus.ti.com/docs/prod/folders/print/tms320c6472.html

APPENDICES

Appendix A Two Ray Autocorrelation

For sake of simplicity, let us assume a single tone is received as compared to two tones, hence eq. (4.5) from Chapter 4 can be written as:

$$\begin{aligned} y(n) &= h_0 e^{\frac{j2\pi n(\epsilon_0+\rho)}{N}} + w(n) \\ &= h_0 e^{jn\omega_0} + w(n). \end{aligned} \tag{A.1}$$

where h_0 is complex amplitude, $w(n)$ is white noise ω_0 is the Doppler shifted pilot tone frequency in radians, where $\omega_i = \frac{2\pi(\epsilon_i+\rho)}{N}$. Assume uniformly distributed phase between $-\pi$ and π. Then the mean of the process will be

$$m_x(n) = E h_0 e^{jn\omega_0} = 0. \tag{A.2}$$

Then using k and l for taking the autocorrelation of $y(n)$ will be

$$\begin{aligned} r_x(k,l) &= E\left\{y(k)y(l)^*\right\} \\ &= E\left\{h_0 e^{jk\omega_0} h_0^* e^{-jl\omega_0}\right\} \\ &= E\left\{|h_0|^2 e^{j(k-l)\omega_0}\right\} \\ &= |h_0|^2 e^{j(k-l)\omega_0}. \end{aligned} \tag{A.3}$$

Since the mean of the both $x(k)$ and xl process is constant, then the autocorrelation $r_x(k,l)$ is a function of only difference between k and l.

$$r_x(k,l) = r_x(k-l,0). \tag{A.4}$$

Therefore, the mean and the autocorrelation do not change if the process is shifted in time.

$$r_y(k) = |h_0|^2 \, e^{jk\omega_0} + \sigma_\omega^2 \delta(k). \tag{A.5}$$

where $|h_0|^2$ is the complex power. Hence, a (MXM) of autocorrelation matrix for $y(n)$ is the sum of the autocorrelation matrix due to the signal and noise, $\mathbf{R}_s$ and $\mathbf{R}_n$. Therefore, the autocorrelation matrix may be written as

$$\mathbf{R}_y = \mathbf{R}_s + \mathbf{R}_n. \tag{A.6}$$

where the signal autocorrelation matrix is

$$\mathbf{R}_s = \begin{bmatrix} 1 & e^{-jw_0} & e^{-j2w_0} & \dots & e^{-j(M-1)w_0} \\ e^{jw_0} & 1 & e^{-jw_0} & \dots & e^{-j(M-2)w_0} \\ e^{j2w_0} & e^{jw_0} & 1 & \dots & e^{-j(M-3)w_0} \\ \vdots & \vdots & \vdots & & \vdots \\ e^{j(M-1)w_0} & e^{j(M-2)w_0} & e^{j(M-3)w_0} & \dots & 1 \end{bmatrix}. \tag{A.7}$$

where $\mathbf{R}_s$ has a rank of one and the noise autocorrelation matrix is diagonal,

$$\mathbf{R}_n = \sigma_w^2 \mathbf{I}. \tag{A.8}$$

The noise autocorrelation has full rank. Let us define

$$\mathbf{e}_i = [1, \; e^{j\omega_0}, \; e^{j2\omega_0}, \cdots, \; e^{j(M-1)\omega_0}]^T. \tag{A.9}$$

Then $\mathbf{R}_s$ can be written as

$$\mathbf{R}_s = h_0 \mathbf{e}_1 \mathbf{e}_1^H. \tag{A.10}$$

The rank of $\mathbf{R}_s$ is equal to one, therefore, $\mathbf{R}_s$ has only one nonzero eigenvalue. Eq. A.10 can re-written as

$$\begin{aligned} \mathbf{R}_s\mathbf{e}_1 &= h_0(\mathbf{e}_1\mathbf{e}_1^H)\mathbf{e}_1 \\ &= h_0\mathbf{e}_1(\mathbf{e}_1^H\mathbf{e}_1) \\ &= Mh_0\mathbf{e}_1. \end{aligned} \tag{A.11}$$

Therefore, the nonzero eigenvalue is equal to Mh_0 and that e_1 is the eigenvector. Since $\mathbf{R}_s$ is the hermitian, then the remaining eigenvectors, $\mathbf{v}_2, \mathbf{v}_3 \cdots, \mathbf{v}_M$, will be orthogonal to e_1, such that

$$\mathbf{e}_1^H\mathbf{v}_i = 0 \;\; ; \;\; i = 2, 3, \cdots M, \tag{A.12}$$

which is the basis of signal and noise separation. The eq. A.5 is used to formulate eq. 4.6 for multiple tones.

ABOUT THE AUTHOR

Jamal Haque received his B.S. and M.S. degrees in Electrical Engineering from the University of South Florida. He is currently pursuing his Ph.D. in Electrical Engineering at the University of South Florida, Tampa, FL. His research interests include wireless systems, OFDM based systems in high mobile platform, synchronization, channel estimation, cognitive, software defined radio and channel coding.